Optimisation of the Analysis of Alkyl Polyglycosides by MEKC-PAD

a dissertation submitted to the FB-C
of the Bergische Universität Wuppertal
in partial fulfilment of the requirements
for the degree of
Doctor of Natural Science

Nguyễn Minh Nguyệt Ánh
born in Hà Nội, Việt Nam

Wuppertal
May, 2004

Acknowledgements

I wish to express my sincere gratitude to all people who have contributed to the realisation of this thesis.

I am deeply indebted to my research advisor, Prof. Dr. Siegmar Gäb, for his countless advice, guidance and enthusiastic supervision throughout the years. His kindness and neverending support have encouraged me to overcome the difficulties not only in scientific work but also in social life.

I am also very grateful to my supervisor, PD. Dr. Oliver J. Schmitz, for his everlasting stimulating advice. His suggestions and guidance have been of immense help to me during the whole course of my work.

I would like to express my sincere thanks to Dr. Walter V. Turner for his friendliness and constant readiness to help. His specialised help in analysing the NMR data is very meaningful to me. And, I will remember him as a lively encyclopedia who knows everything not only in natural science but also in social science especially languagestic, history and literature.

Without their help and encouragement, and without their insightful comments and detailed correctness of this manuscript, I would never accomplish this thesis.

I would like to express my gratitude to PD. Dr. Detlev Belder for his acceptance to co-referee this thesis.
I would like to express my appreciation to Prof. Dr. Hans-Josef Altenbach and Prof. Dr. Walter Reineke for their kindness to be co-examiners.

My warm thanks are also directed to Dr. Hans-Willi Kling and Dr. David Melchior for suggesting the theme of the dissertation and for their useful discussion; and to Cognis Deutschland GmbH for the financial support during this work.

My distinguished thanks are also due to Jane Hübner for her assistance and co-operation in performing a part of measurements for this work, and to Ralf Radon for his ready help in solving the technical problems.
I would like to extend my thanks to all my former and current colleagues for their friendship and inspirations: Dr. Axel Boddenberg, Dr. Axel Patrick Ligon, Claus Schumann, Dr. Damian Sobotzik, Dr. David Melchior, Dr. Jan Schäper, Marc Constapel, Marc Schellenträger, Michaela Wirtz, Rahil Taheri, Silke Möschter, Simone Wiesufer, Stefan Droste, Dr. Torge Schwierz and Dr. Weiying Yan.
Especially, I would like to express my sincere appreciation to Ms. Waltraud Schiewek and her family for their great care and endless help right from the first day I came to Germany. I will never forget the afternoons we hang around together, for shopping or for ice eating. Their friendliness and kindly guidance in every aspect help me to integrate more easily to the German life.

I gratefully acknowledge the help of Mr. Axel Brakelmann and his co-workers at the workshop of faculty C in preparing the capillary-electrode holder and the eletrolyte vial.

I would also like to thank Mrs. Ilka Polanz for the NMR measurements, Mr. V. Fahrney for his help in electronic problems, Mr. Josef Luderich and Mr. Robin Brning for the preparation of the glasswares.

My sincere thanks are due to Prof. Dr. Luis A. Colón at the Department of Chemistry, University at Buffalo, for his enthusiastic guidance in the very first measurements with the CE-EC system.

My warmest thanks go to Prof. Dr. Wolfgang Schuhmann, Dr. Albert Schulte and Florin Turcu at the department of Elektroanalytik & Sensorik, Ruhr-Universität Bochum, for the fruitful discussions and collaboration in the field of electrochemistry and the for the kind hospitality each time I visited their group. Especially, my sincere

thanks are due to Florin Turcu for his help in preparing the working electrode. Without their help, it was not possible to complete the work for my thesis.

I express my gratefulness to Prof. Dr. Petr P. Boček at the institute of Analytical Chemistry, Brno, for his friendliness, patience and useful discussion on the indirect UV detection and the system peaks.

It is my pleasure to thank PD. Dr. Ute Pyell at the department of Chemistry, Philipps-Universität Marburg for her friendliness and the interesting discussion about MEKC optimisation.

And last but certainly not the least, I would like to express my deepest gratitude to my parents and my sister for their great love, care and support all through these decades. I would like to specially thank my mother, who has left her career behind to come here and share with me the most difficult period during this work.

My most sincere thanks are to my husband for his love and encouragement, for his suggestion and guidance on the electronic matters and for his help in preparation of this dissertation. To my beloved daughter, your smile has the greatest meaning to me.

Thank you very much one and all.

Table of contents

List of Figures

List of Tables

Chapter 1

Introduction and objectives

Alkyl polyglycosides (APGs), a new group of non-ionic surfactants with good dermal tolerance, low toxicity, and high biodegradability, are of increasing importance [1,2]. Because of the complexity of APG formulations (they are mixtures of substances with different fatty alcohol chain lengths and with varying polymerisation of the carbohydrate moiety), efficient methods are required for product development, product control, biodegradation and toxicity studies and environmental analysis [1, 2].

Several analytical techniques, including spectroscopy [3, 4] and separation methods, are not suitable for the selective determination of APGs. Commonly used analytical approaches include gas chromatography (GC) and liquid chromatography (LC). In GC, time-consuming and often complex derivatisation procedures are required. LC approaches with reversed phases have been widely used, but problems arise because of incomplete separation of the components, although the use of LC-MS might provide further enhancement [5–7].

In addition, before a new batch of a product is released, the quality has to be tested, preferably directly after production. This requires suitable methods for rapid, routine analysis. In the frame of a research project in collaboration with Cognis Deutschland GmbH, the objective of this research was to develop a sensitive and reproducible method for analysis of APGs by means of capillary electrophoresis (CE).

This dissertation consists of two parts. The first is dedicated to theoretical aspects of APGs and methods of analysis. In Chapter 2, the history as well as the production of APGs are discussed. Chapter 3 presents a short introduction to the theory of the various methods which were used to analyse APGs in this work.

In the second part, the results of using CZE and MEKC to separate APGs are described in detail. In Chapter 4, the determination of APGs with UV detection is discussed. The rest of that chapter is dedicated to the coupling of CE with amperometric detection; the most interesting results are presented here. The main achievements of the work are discussed in brief in Chapter 5. Finally, in Chapter 6, the experimental details are described.

Chapter 2

Alkyl polyglycosides

2.1 Overview of alkyl polyglycosides

Alkyl glucosides (AGs) and alkyl polyglycosides (APGs) are a new generation of highly effective carbohydrate-derived surfactants that are low in toxicity, ecologically safe and made from renewable resources at low cost [1]. They offer a broad range of applications owing to their special properties, including their compatibility and synergistic effects when they are combined with many other surfactants and ingredients of surfactant-based formulations. With a worldwide production capacity recently increased to about 60,000 metric tons/year, APGs are by far the most important sugar-based surfactants [2].

The first alkyl glucoside was synthesised and identified by Emil Fischer more than 100 years ago. However, it was not until 1934 that their potential as surface-active agents was appreciated (cf. patent grant to H. Th. Böhme AG of Chemnitz, Germany [1]). Thereafter, another 40 to 50 years went by before research groups in various companies redirected their attention to AGs and developed technical processes for the production of APGs on the basis of Fischer's synthesis.

In the course of this development, Fischer's early work, which involved the reaction of glucose with hydrophilic alcohols such as methanol, ethanol, glycerol, etc.,

was applied to hydrophobic alcohols with alkyl chains ranging from octyl (C_8) up to octadecyl (C_{18}) - the typical fatty alcohols. Fortunately, with regard to their application properties, not pure alkyl mono-glucosides, but a complex mixture of alkyl mono-, di-, tri-, and oligoglycosides, are produced in the industrial processes. The industrial products thus are called alkyl polyglycosides [1]. The products are characterised by the length of the alkyl chain and the average number of glucose units linked to it - the "degree of polymerisation" (**Figure 2.1**).

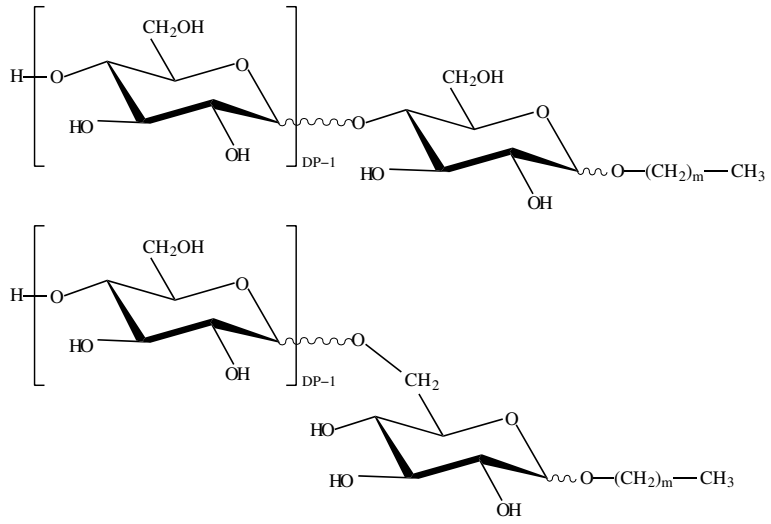

DP = degree of polymerisation
(average number of glucose units/alkyl chain)
m = 7–17

Figure 2.1: Structural formula of alkyl polyglycosides

Three types of isomerism determine the very complex product spectrum of APGs: stereoisomerism with α- and β-anomers; positional isomerism, where 1,6- and 1,4-interglycosidic linkages are preferred; and ring isomerism with pyranoside and furanoside forms. Accordingly, even the alkyl monoglucoside consists of four isomeric forms. There are 64 diglucoside isomers, 1024 triglucoside isomers, etc. When branched oligosaccharide groups may be formulated in the head-group, further isomers must also be considered [2].

The water-soluble APGs are C_8-, C_{10}-, C_{12}- and C_{14}-polyglycosides, while those with more than 16 carbon atoms in the alkyl chain are insoluble in water.

2.2 Production of alkyl polyglycosides

There are several preparative methods for AG or APG mixtures. The various syntheses range from stereospecific synthesis routes involving protective groups, which give defined compounds with high selectivity, to non-selective processes that lead to complex isomer and oligomer mixtures [1, 2].

A fundamental approach, known as the *"Fischer glycosidation"*, is an acid-catalysed reaction of glucose with ethanol to produce ethyl glucoside, with water as a by-product (**Figure 2.2**). The reaction mechanism is discussed and described in detail in an overview by Capon [8]. In fact, Fischer glycosidation products are complex. Mostly, they are equilibrium mixtures of $\alpha-/\beta-$ anomers and pyranoside/furanoside isomers and also include randomly linked glycoside oligomers [8].

Treating D-glucose with methanol in the presence of 1 % hydrochloric acid at 35°C yields a mixture of methyl α-D-glucofuranoside (0.6 %), methyl β-D-glucofuranoside (0.9 %), methyl α-D-glucopyranoside (65.8 %) and methyl β-D-glucopyranoside (32.7 %) [9, 10].

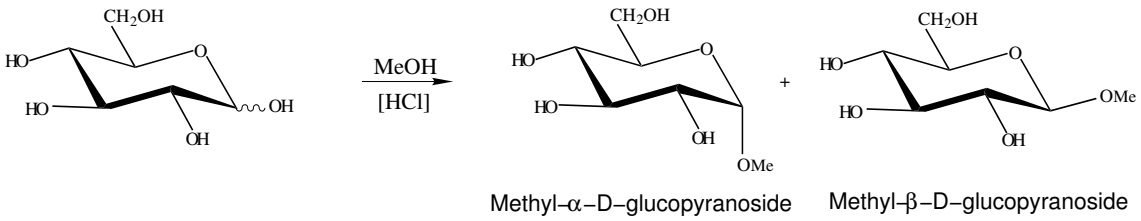

Figure 2.2: Synthesis of glycosides according to Fischer [1]

Synthesising glucosides of defined structure is a complex matter [11, 12]. Particular problems with selective synthesis generally occur in the control of the anomeric

configurations of the saccharide units and the bonding sites of the intersaccharidic glycosidic linkage. To solve these problems, multistep syntheses are often required. These include the use of special reagents to activate the anomeric center and protect the hydroxyl groups that should not enter into glycosidic bonds, by means of suitable blocking groups [2].

There are a number of other methods for APG synthesis, such as the Koenigs-Knorr method [13–19], the Lewis-acid method [19–21], the Schmidt method [12,22], the synthesis of APG through base-catalysed alkylation [23–25], and enzymatically catalysed synthesis [26–28]. So far as the industrial production of APG is concerned, processes based on the Fischer synthesis have been successfully adopted. Modern production plants on the basis of the Fischer synthesis are the embodiment of low-waste, virtually emission-free technology. Another advantage of the Fischer synthesis is that the average degree of polymerisation of the products can be precisely controlled over a wide range. Relevant performance properties, such as hydrophilicity and water solubility, can thus be adapted to end-use requirements [29–31].

2.2.1 Raw materials

Fatty alcohols

Fatty alcohols can be obtained either from petrochemical sources (synthetic fatty alcohols) or from renewable resources such as fats and oils (natural fatty alcohols). Fatty alcohol blends are used in the APG synthesis to build up the hydrophobic part of the molecule. The natural fatty alcohols are obtained after transesterification and fractionation of fats and oils (triglycerides) to produce the corresponding fatty acid methyl esters and subsequent hydrogenation. In accordance with the desired alkyl chain length of the fatty alcohol, the main feedstocks are the following oils and fats: coconut or palm-kernel oil for the $C_{12/14}$ range and tallow, palm or rapeseed oil for the $C_{16/18}$ fatty alcohols [1].

Carbohydrate source

The hydrophilic moiety of the APG molecule is derived from a carbohydrate. Both polymeric and monomeric carbohydrates are suitable as raw materials for the production of APG. Polymeric carbohydrates include, for example, starch (from corn, wheat or potatoes) or glucose syrups with low degradation levels, while monomeric carbohydrates can be any of the various forms in which glucose is available, for example water-free glucose, glucose monohydrate (dextrose) or even highly degraded glucose syrup. Raw-material choice influences not only raw-material costs, but also production costs [1, 2]. Generally speaking, raw material costs increase in the order starch, glucose syrup, glucose monohydrate, water-free glucose, while plant equipment requirements and hence production costs decrease in the same order (**Figure 2.3**) [1].

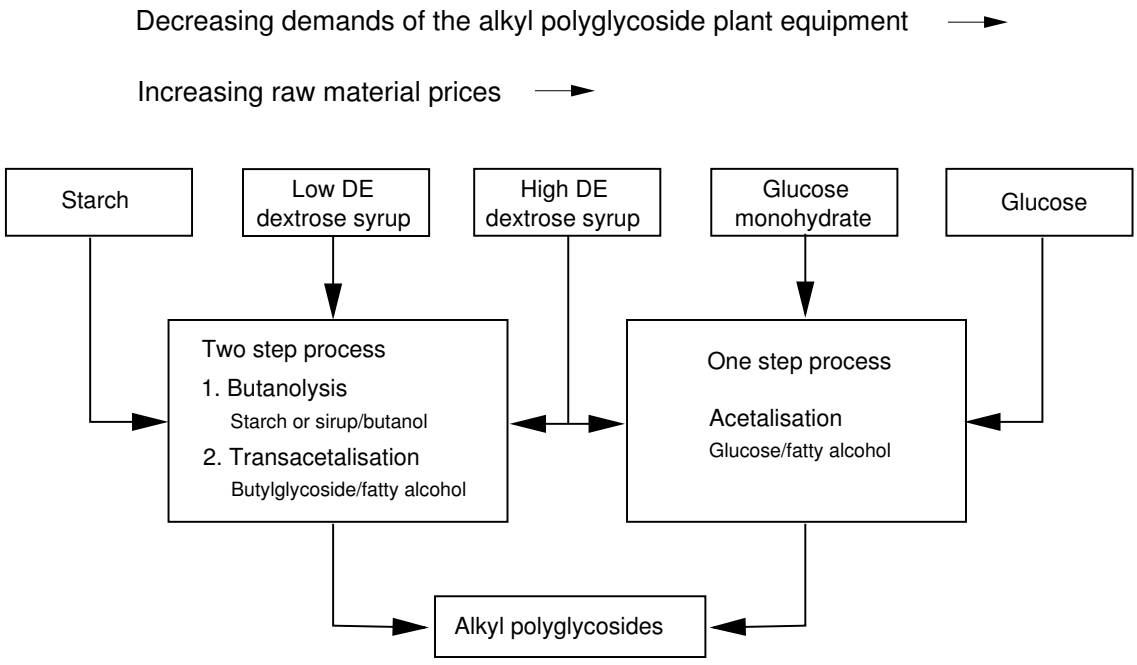

Figure 2.3: Carbohydrate sources for industrial-scale alkyl polyglycoside synthesis [1]

(DE = dextrose equivalent)

Starch is a potential raw material because of its practically ubiquitous occurrence in nature and its low price compared with D-glucose, but alcoholysis of starch into alkyl glucosides demands much more drastic conditions than glycosidations of D-glucose or the transglycosidation of simple alkyl glucosides [32, 33]. Therefore, the use of D-glucose appears more favorable than starch and has been increasingly desribed and given preference in the patent literature.

2.2.2 Degree of polymerisation

The polyfunctionality of the carbohydrate partner means that the conditions of the acid-catalysed Fischer reaction yield an oligomer mixture in which on average there is more than one glycose unit per molecule. The average number of glycose units linked to an alcohol group is described as the (average) degree of polymerisation (DP) [1]. In this mixture, the concentration of the individual oligomers (mono-, di-, tri-, ...-, glycoside) is largely dependent on the molecular ratio of glucose to alcohol in the reaction mixture. The greater the molar excess of the alcohol employed, the smaller the DP of the products [2]. The average DP is an important determinant of the physical chemistry and the applications of APG. In an equilibrium distribution, the DP—for a given alkyl chain length—correlates well with basic product properties such as polarity and solubility [2]. In principle, this oligomer distribution can be described by a mathematical model. The content of individual species in the mixture decreases with increasing degree of polymerisation. In simple terms, the DP of APG mixtures can be calculated from the mole percent p_i of the respective oligomeric species i in the glycoside mixture [34]

$$DP = \frac{p_1}{100} \times 1 + \frac{p_2}{100} \times 2 + \cdots = \sum_{i=1}^{\infty} \frac{p_i}{100} \times i.$$

2.2.3 Synthesis procedures

Basically, all processes for the conversion of carbohydrates to APG by the Fischer synthesis can be assigned to one of two process variants, namely direct synthesis and

transacetalisation. In either case, the reaction can be carried out either in batches or continuously [1].

Direct synthesis is simpler from the equipment point of view. In this case, the carbohydrate reacts directly with the fatty alcohol to form the required long-chain APG [35–37]. The carbohydrate used is often dried before the actual reaction (for example to remove the crystal-water in case of glucose monohydrate = dextrose). This drying step minimises side reactions and shifts the reaction equilibrium toward the desired products [2]. Monomeric solid glucose, used as fine particles, has to be thoroughly suspended in the alcohol, since the reaction is heterogeneous [38]. For highly degraded glucose syrup (DE> 96; DE = dextrose equivalent), the use of a second solvent and/or emulsifiers (for example an initial concentration of APG itself) is necessary to provide a stable fine-droplet dispersion between alcohol and glucose syrup [2]. The dextrose equivalent is defined as a measure of the total reducing sugars in a syrup calculated as dextrose and expressed as a percentage of the total dry substance in solution.

The two-stage transacetalisation process involves more equipment than the direct synthesis. In the first stage, the carbohydrate reacts with a short-chain alcohol (such as n-butanol or propylene glycol) and optionally depolymerises. In the second stage, the short-chain alkyl glycoside is transacetalised with a long-chain alcohol ($C_{12/14}$-OH) to form the required APG [39–41]. If the molar concentrations of carbohydrate and alcohol are identical, the oligomer distribution obtained in the transacetalisation process is basically the same as in the direct synthesis [2].
The transacetalisation process is applied when oligo- and polyglycoses (for example starch or syrups with a low DE value) are used. The necessary depolymerisation of these starting materials requires a temperature higher than 140°C. If a lower alcohol is being used, this can create high pressures that impose more stringent demands on equipment and can lead to higher plant cost.
Besides the two reaction stages, additional storage facilities and, optionally, work-up facilities for the short-chain alcohol have to be provided. APG has to be refined on account of specific impurities in the starch (such as protein) [2].

In **Figure 2.4** both synthesis routes for APG are shown.

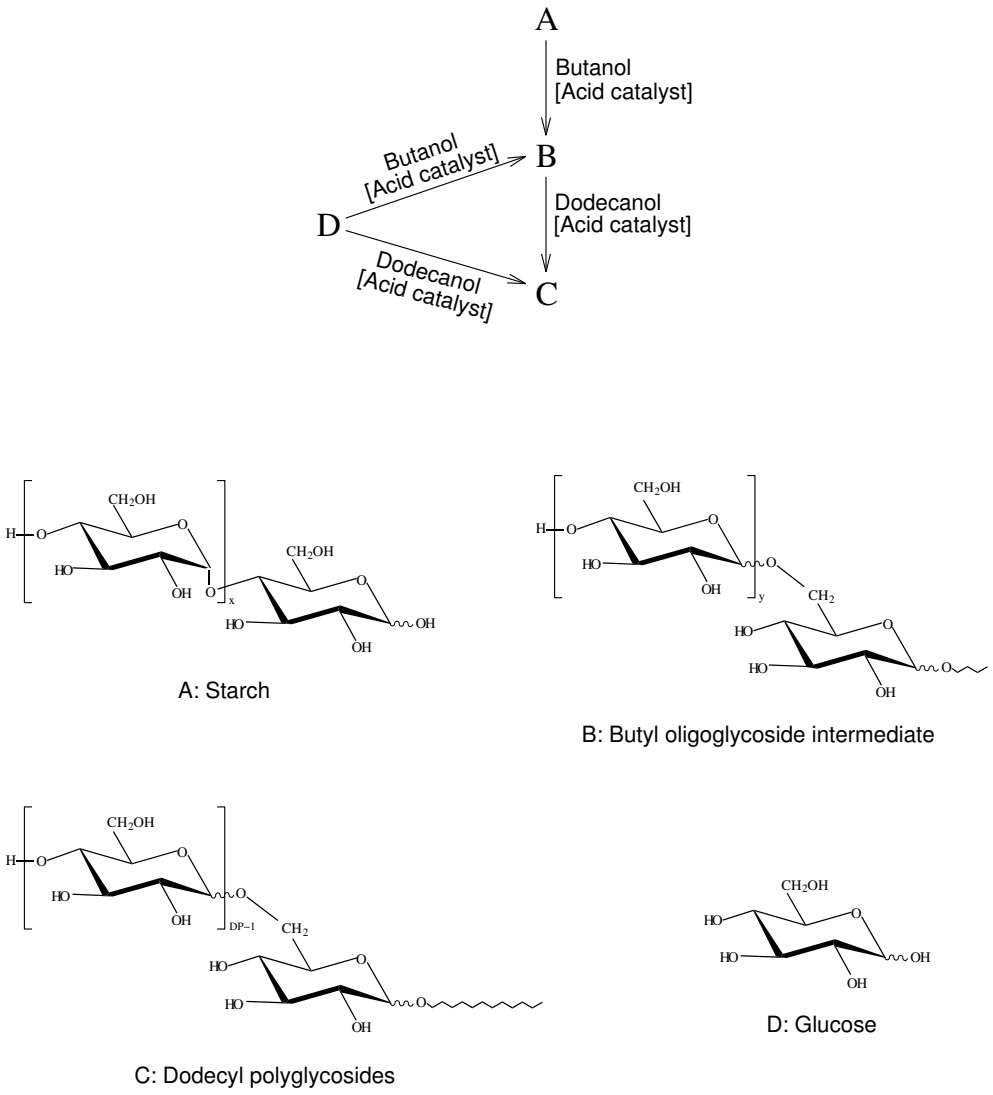

Figure 2.4: Alkyl polyglycoside synthesis pathways

2.3 Derivatives of alkyl polyglycosides

APGs are available today in sufficient quantities and at competitive costs [42], so that their use as a raw material for the development of new specialty surfactants is arousing considerable interest. Thus, the surfactant properties of APGs, for example foaming and wetting, could be modified as required by chemical transformation. The derivatisation of APGs is currently being pursued with great commitment [43]. The resulting derivatives may be non-ionic, anionic or cationic surfactants **(Figure 2.5)**.

AGs and APGs have primary and secondary alcoholic hydroxyl functions that offer themselves to derivatisation. These hydroxyl functions often behave chemically like those of monofunctional alcohols. The primary hydroxyl function of the saccharide is most reactive and is preferentially derivatised. However, the differences in reactivity of the hydroxyl groups are often too slight for targeted derivatisation, so that most reactions also take place simultaneously at the secondary hydroxyl groups. In this process, mixtures are obtained with different distributions of the substituents at the saccharide rings. Typical derivatisation reactions offered by those alcohols are oxidation, esterification and ether formation [44].

Derivatisations at the alkyl residues by substitution of hydrogen atoms appear less practicable, but APG derivatives may be obtained by the use of derivatives of long-chain alcohols for glucoside synthesis. Keana et al. [45] and Holme and Hall [46] have synthesised alkenyl glucosides with unsaturated hydrocarbon residues. Furthermore, there are also a few examples of the substitution of oxygen by other heteroatoms such as sulfur or halogen [47, 48].

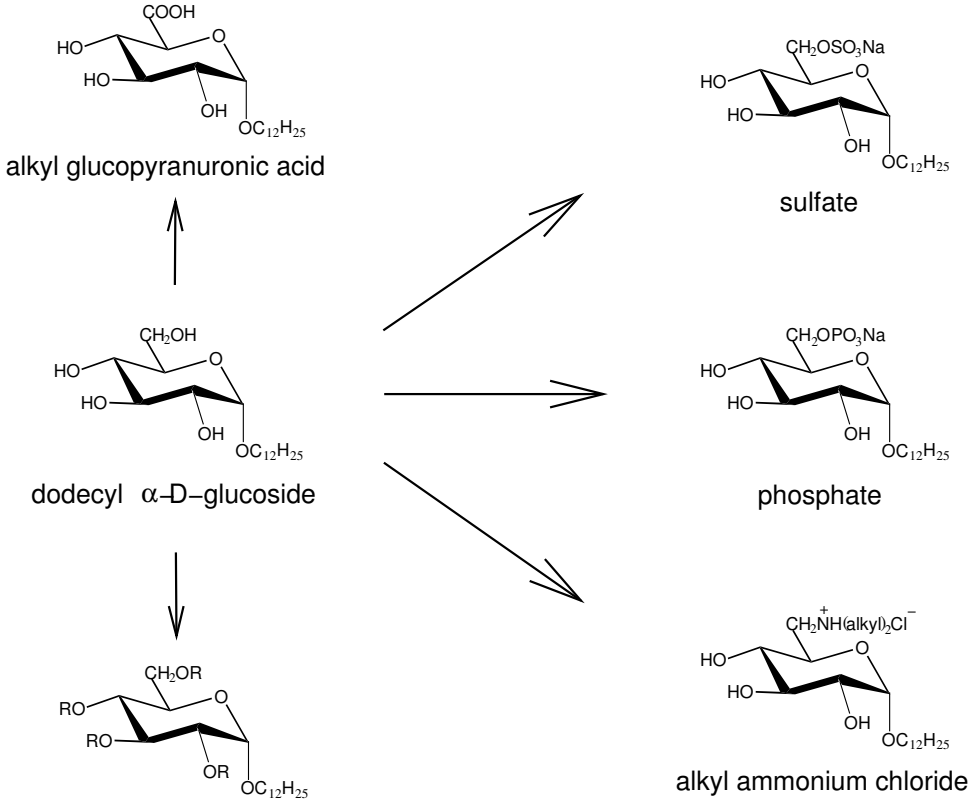

Figure 2.5: Alkyl polyglycoside derivatives [1, 2]

Chapter 3

Methods of analysis

3.1 Capillary electrophoresis

3.1.1 Introduction

Capillary electrophoresis (CE) is a modern analytical technique that separates species rapidly and efficiently by the application of voltage across buffer-filled capillaries. The technique is most often used for separating charged species [49].

Under the influence of an electric field, particles with different charges (q) and/or molecular mass (w) migrate with different velocities. A particle with a larger charge to mass ratio ($\frac{q}{w}$) moves faster than one with a smaller ratio [50]. This is the basic principle of all electrophoretic separation methods [51]. Neutral solutes are not influenced by the electric field and are conveyed through the capillary by the electroosmotic flow (EOF) (explained below).

Capillary electrophoresis, then, is a collection of a range of separation techniques that involve the application of high voltages (typically 10 - 100 kV) across narrow-bore capillaries (normally from 5 to 200 μm in internal diameter) to achieve separation [52]. The separation based on mass and charge differences between analytes

is termed Capillary Zone Electrophoresis (CZE). In Micellar Electrokinetic Chromatograph (MEKC), neutral compounds are separated by surfactant micelles. The sieving of solutes through a gel network is defined as Capillary Gel Electrophoresis (CGE). Capillary Isoelectric Focusing (cIEF) separates zwitterionic solutes within a pH gradient. The separation of ions in a discontinuous buffer system consisting of a leading and a terminating electrolyte is termed Capillary Isotachophoresis (CITP), and a combined electrokinetic and chromatographic separation technique which involves applying voltages across a capillary filled with silica-gel stationary phases is called Capillary Electrochromatography (CEC) [50, 51, 53].

Many of the CE separation techniques rely on the presence of an electrically induced flow of solution (electroosmotic flow, EOF). In contact with a high-pH electrolyte solution, the wall of a fused-silica capillary is negatively charged by the dissociation of the silanol groups. To preserve electroneutrality, positively charged ions tend to be adsorbed onto the silica wall electrostatically. In the model proposed by Stern, a rigid layer of adsorbed ions is superposed by a diffuse layer. When a voltage is applied, the ions of this diffuse layer migrate towards the cathode. The flow of these ions is called the EOF. The speed of the EOF can be adjusted by changing the pH and the concentration of the buffer, adding organic modifier, or changing the diameter of the capillary or the voltage applied. The EOF effectively pumps solutes along the capillary, generally towards the detector at the cathodic end. It can significantly reduce analysis times or force an anion to overcome its migration tendency towards the anode [50].

Since its inception in the early 1980s [54–56], CE has become established as a routine technique within many fields of analysis. Indeed, it has been available in the form of integrated and automated commercial systems for most of the past decade. Generally, CE is carried out with aqueous electrolytes, but the use of non-aqueous solvents in CE is growing [57].

3.1.2 Instrumentation

The instrumentation required for CE is remarkable simple in design, as **Figure 3.1** illustrates [58].

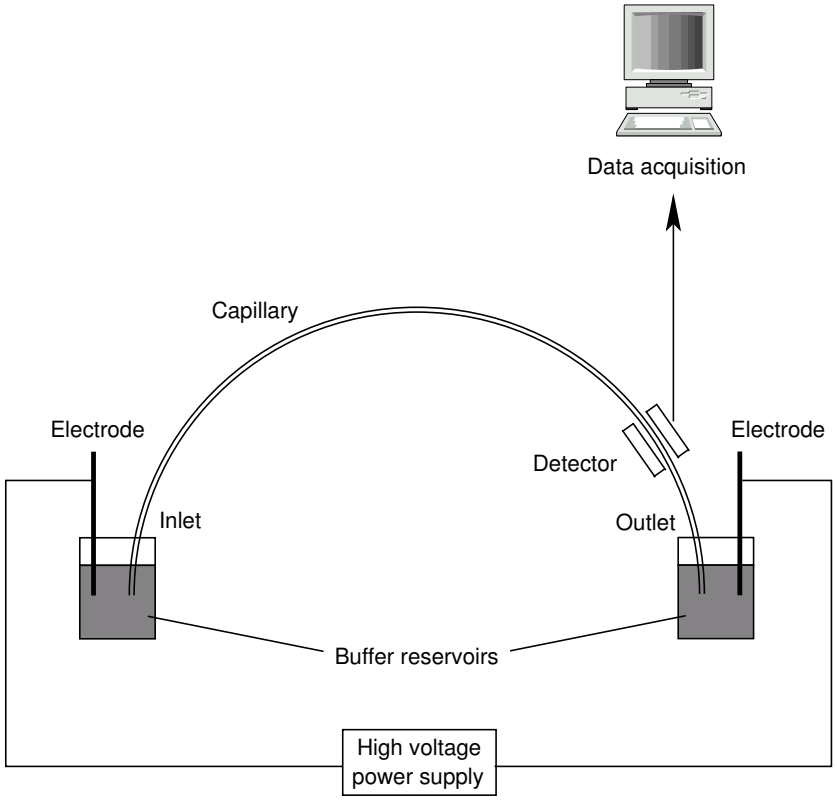

Figure 3.1: A schematic representation of the main components of a typical CE system [58]

The capillary is filled with electrolyte solution which conducts the current. The ends of the capillary are placed in buffer reservoirs that are also filled with the electrolyte. Electrodes made of an inert material such as platinum are inserted into the electrolyte reservoirs to complete the electrical circuit. These electrodes are connected to a high-voltage power supply capable of delivering up to 30 kV. To inject a small volume of sample into one end of the capillary, one of the buffer

reservoirs (normally at the anode) is temporarily replaced with a sample reservoir, and either an electric potential or external pressure is applied for a few seconds. After the buffer reservoir is replaced, an electric potential is applied across the capillary, and the separation is carried out. Optical (UV/visible or fluorometric) detection of the separated analytes can be achieved directly through the capillary wall near the opposite end (normally the cathodic end). The plot of detector response against time that is generated is termed an electropherogram. The solutes are seen as peaks as they pass through the detector, and the area of each peak is proportional to their concentration, which allows quantitative determination [51].

Basic features of a CE instrument include an autosampler, a detection module, a high-voltage power supply, the capillary and a computer to control everything [51–53].

3.2 Micellar electrokinetic chromatography

MEKC, initially developed by Terabe et al., is a powerful analytical method that enables excellent separation of electrically neutral species by capillary electrophoresis [59, 60]. The separation is based on the distribution of solutes between a pseudo-stationary micellar phase and an aqueous mobile phase. MEKC is therefore not only an electrophoretic but also a chromatographic technique. It can be applied to the separation of both uncharged and charged species. With charged species, the electrophoretic mobility leads to an additional selectivity of the system. In this case, they will be separated according to their different electrophoretic mobility as well as different interaction with the micelles [61–63].

Micelles are molecular aggregates of surfactants that have amphiphilic properties, i.e., they contain both hydrophilic and hydrophobic regions in their structure. Hence, surfactants can be recognised by the charge of the polar head group (as non-ionic, anionic, cationic and zwitterionic surfactants) or by the variations in the nature of the hydrophobic moiety (as hydrocarbon, bile salts and fluorocarbon surfactants) [64]. Above the critical micellar concentration (CMC), surfactants aggregate

to form spherical micelles in which the hydrophilic head groups form an outer shell and the hydrophobic tail groups form a nonpolar core into which solutes can partition. The diameter of typical micelles lies in the range of $30 - 50$ Å. Micelles have a dynamic structure that results from the rapid exchange of surfactants in the aggregated and monomeric forms. The number of monomer surfactants in the aggregate form (called aggregation number) and the size of micelles are dependent upon the kind of surfactant and the surrounding solution [51].

Micelles of ionic surfactants migrate electrophoretically according to their surface charge, e.g. negative sodium dodecyl sulphate (SDS) micelles to the anode and positive cetyl trimethyl ammonium bromide (CTAB) micelles toward the cathode. Because in most cases the electroosmotic velocity is higher than the electrophoretic velocity of the micelles, the net velocity even of negatively charged micelles is toward the cathode [51]. Uncharged solutes are then separated via their differential migration in the two phases, or, in other words, according to their differential interaction with the micelles. They elute in a time interval given by the retention time t_{EOF} of a solute that does not interact with the micelles (a very polar solute that arrives at the detector with the EOF) and the retention time t_{mc} of a solute that is completely solubilised in the micelles (very hydrophobic solutes). This time interval is referred as the *"migration time window"* [65].

Schematic representation of the principle of MEKC for anionic micelles is illustrated in **Figure 3.2** [66].

A main advantage of MEKC is the possibility of changing the composition of the electrolyte system in order to optimise selectivity and efficiency [64, 67].

3.3 CE with indirect UV detection

Initial developments of indirect detection modes for use with UV-absorbance detectors in capillary electrophoresis have been done by Hjertén et al. [68]. Indirect detection schemes are universal and can be used for compounds which do not possess the

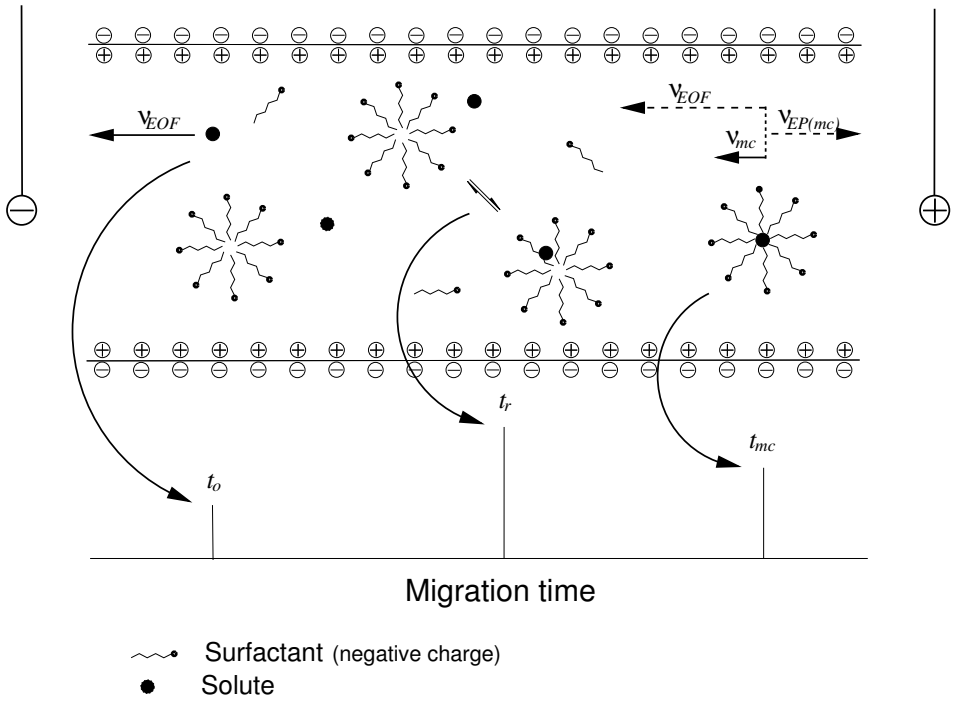

Figure 3.2: Schematic of the separation principle of MEKC [66]

necessary physical properties for direct detection, i.e. chromophores or fluorophores. Indirect detection modes eliminate the need for pre- or post-column derivatisation to convert the analyte of interest into a species that yields an acceptable detector response [52, 53].

In indirect UV detection, an ionic compound with a high UV absorptivity is used as co-ion, one of the constituents of the background electrolyte. The mechanism of indirect detection is explained as the displacement of one co-ion by one analyte ion of the same charge, in accordance with the electroneutrality principle. A general scheme illustrating the principles of indirect detection is shown in **Figure 3.3** [69].

As can be seen in **Figure 3.3A**, the detectable co-ion provides a constant background signal; when the analyte zone, which is deficient in this absorbing co-ion, passes through the detector, there is a decrease in the background signal (**Figure 3.3B**). When the analyte has completely passed through the detection point, the detector

response returns to the original baseline (**Figure 3.3C**). Thus, the resulting negative signal is derived from the detectable background co-ion rather than from the analyte itself [69], as illustrated in **Figure 3.4**.

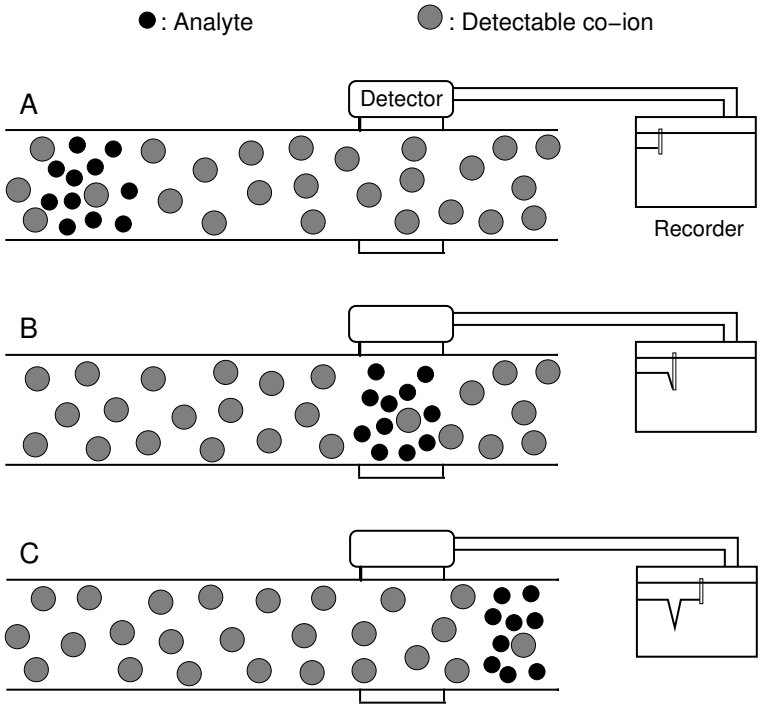

Figure 3.3: Illustration of the displacement mechanism for indirect detection [69]

There is a guideline for successful indirect UV detection [51]:

- Choose the absorbance of the visualising co-ion to be close to the upper limit of detector linearity (≈ 0.1 absorbance unit).
- The mobility of the co-ion should be close to that of the pair of substances in the sample which are most difficult to separate. The reason is that, if the concentration of analyte exceeds 0.01 times the concentration of the co-ion, the analyte has a higher mobility than the co-ion resulting in a fronting peak, while a tailing peak is observed with the one having lower mobility than the co-ion.

- The concentration of the background electrolyte should be as low as possible.
- Select a counterion of low mobility in order to minimise Joule heating.
- The co-ion should provide a broad UV absorbance, so that a detection wavelength can be chosen where all sample components possess a very low absorptivity.

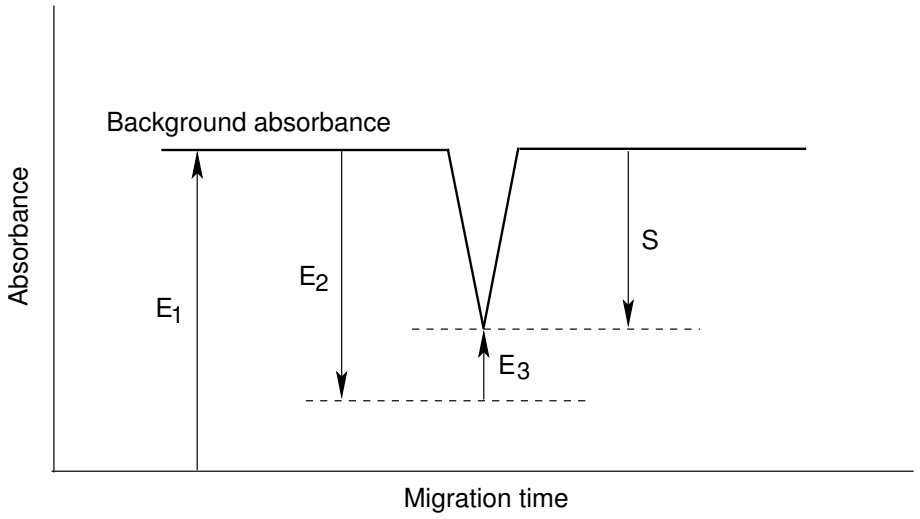

E_1: Absorbance of the background electrolyte (BGE)

E_2: Reduction of the background absorbance on replacement of the BGE by the analyte

E_3: Absorbance of the analyte itself

S : Resulting negative signal

Figure 3.4: Formation of the negative signal in indirect detection

3.4 CE with pulsed amperometric detection

3.4.1 Electrochemical detection

The use of electrochemical detection (ED) in conjunction with CE (CE-ED) has grown steadily since the first report of such a system by Wallingford and Ewing in 1987 [70]. The high-efficiency CE separation has proven to be a good match with the high sensitivity of the ED. In addition, ED is well suited to CE because the detection cell can be miniaturised with little or no loss in sensitivity.

Electrochemical detectors can be classified into three categories: amperometric, conductometric, and potentiometric. For each type, the measured response is dependent on the concentration of analyte in solution. Traditionally, when the term "electrochemical detection" was used, only amperometric detection was meant. However, the term refers to all three detection methods [71].

Amperometric detection is based on the measurement of the current resulting from oxidation or reduction (electrolysis) of analytes at the surface of an electrode in a flow-through cell.

Conductometric detection is based on the measurement of the conductivity between two inert electrodes. The presence of analyte in the background electrolyte causes a detectable change in the conducted current. No oxidation or reduction reactions take place. This method is particularly useful for the detection of small ions that have no chromophores.

Potentiometric detection is based on the measurement of the potential difference that develops between the internal filling solution of the sensor and the sample solution when an analyte is selectively transfered from solution into a membrane.

An excellent review of the use of CE coupling with conductometric and potentiometric detection was published by Harber [72].

3.4.2 Amperometric detection (AD)

Different types of amperometric detection

Three approaches for AD have been reported, namely amperometric detection at constant potential (ADCP), pulsed amperometric detection (PAD) and integrated pulsed amperometric detection (IPAD).

With ADCP, a constant potential is applied to the working electrode, and the resulting current is measured [71, 73, 74].

To avoid poisoning the working electrode through oxidation of analytes at its surface in the ADCP mode, the PAD or IPAD technique has been used. These techniques are especially useful for analytes such as carbohydrates and amines that tend to foul the electrode surface.

With PAD, the applied potential is accompanied by pulsed steps at extreme positive and negative potentials to activate the surface and clean the electrode [75–78].

IPAD incorporates scanning voltammetry, using a potential scan in the detection step along with pulsed steps for cleaning and surface activation [78, 79].

Applications of CE-AD

AD is tunably selective through proper control of the applied potential. The major applications are the detection of amines [78–99], carbohydrates [78,81,84,86,98,100–103], sulfur compounds [78, 79, 82, 99] and a variety of nonbiological compounds, including hydroquinone [83,89,95], hydrazine [104] and ferrocene [105]. One important application of CE-AD is the determination of inorganic ions [106].

Background electrolyte of the CE

Most CE-AD applications involve CZE. Zwitterionic buffers are preferred, as they give the lowest separation current and, therefore, the smallest amount of background

at the detector [70, 80]. Dynamic modifiers such as cetyl trimethyl ammonium bromide (CTAB), which reverse the direction of the electroosmotic flow, have also been used in conjunction with CE-AD [81, 100]. Furthermore, some applications of CE-AD with nonaqueous background electrolytes have been reported [106–111].

MEKC has been used in coupling with AD [82, 105]. There are indications that the surfactants generally reduce the sensitivity of CE-AD through electrode fouling or reduced access of the analyte to the electrode surface [112].

Amperometric cell

An amperometric cell is a miniature flow-through, three-electrode cell with a working electrode, a reference electrode and an auxiliary electrode. Electrolysis of analytes is accomplished by applying a potential between the working and the reference electrodes.

Working electrodes used for CE-AD have been fabricated from a number of materials, including carbon [85, 87, 90, 92, 94, 95, 113, 114]; noble metals such as Pt [81, 96, 105, 106, 115, 116] and Au [78, 79, 81, 83, 84, 115]; and transition metals like Cu [80, 81, 86, 97, 100], Ni [86, 98, 102], Co [117, 118] and Ru [119]. In addition, chemically modified electrodes, which have been altered through the addition of a catalyst or a redox mediator, extend the applicability of CE-AD to compounds that could otherwise not be detected electrochemically (or only at high potential) [81, 82, 99, 103, 104].

The reference electrode is chosen such that the potential difference between it and the solution is fixed by an electrochemical redox couple. The most commonly used reference electrode is a silver/silver chloride electrode. Any changes in the potential applied between the working and reference electrode will be developed entirely between the working electrode and the solution [71].

To maintain a constant potential difference between the reference electrode and the solution, the cell current must be prevented from flowing through the reference

electrode. A section of the detector's electronic circuit (the potentiostat) causes the cell current to flow instead through the auxiliary electrode. The potentiostat automatically compensates for the solution resistance between the reference and the auxiliary electrodes [71].

Different types of amperometric cell

Three types of flow-through amperometric cells are in common use [71, 120]. They are the in-capillary, wall-jet, and on-capillary cells as shown in **Figure 3.5**.

- **The in-capillary cell** is formed by partially inserting the electrode into the capillary opening [77, 84, 121], which is sometimes chemically etched to create a wider gap that can accommodate larger electrodes [121].
- **The wall-jet cell** uses a flat, disk-shaped electrode in place of a cylindrically shaped wire or fiber. Here, the electrode is simply pushed up against the capillary outlet so that the existing solution impinges directly onto it and then flows radially across its surface [81, 86, 98, 100, 122, 123].
- **The on-capillary cell** has both the capillary and the electrode incorporated into a single unit [81, 83, 124].

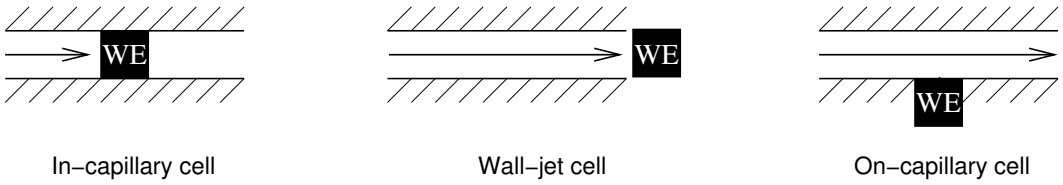

Figure 3.5: Flow-through amperometric cells

(WE = working electrode)

Problem of coupling CE with AD

The major drawbacks in combining CE and AD are the need to isolate the electrochemical detector from the potential used in the separation and the difficulty encountered in aligning the working electrode with the end of the capillary.

Two approaches can be used to isolate the separation current from the detection current. The first method is incorporation of a fracture into the capillary prior to the AD, through which the separation current is grounded. In the second, the detection electrode is placed outside of the capillary orifice in such a way that most of the potential field drops at the end of the capillary before reaching the working electrode.

In most CE-AD applications, decoupling is accomplished by making a fracture in the CE capillary a few centimeters before the working electrode. The fracture is placed in solution maintained at ground, and analytes are transported over the fracture to the detector by the bulk flow generated by the separation capillary. Therefore, the distance between the fracture and the detector must be small (ca. 1.5-2 cm) to avoid band broadening. The simplest decoupler of this design is the bare fracture [80, 87, 125]. This fracture is sometimes coated with a thin layer of conductive polymer to stabilise the joint and minimise analyte leakage, while still permitting the current to drop across the decoupler. Decouplers of this type use Nafion or cellulose acetate applied directly to the fracture [79,83,91,98,101,104,105,126], fitted tightly over the fracture in the form of a tube [78, 79] or cast as an open tubular extension of the CE capillary [88, 89, 92, 94, 113]. Alternatively, a porous glass joint has been fabricated by etching the capillary with hydrofluoric acid [70, 95, 112, 127]. Another form of decoupler that utilises a palladium union to join the CE capillary to a second "detection" capillary was introduced in 1995 [99].

The second approach to isolating the AD from the separation current is called end-column detection. The electrode is placed at the end of the capillary, outside the potential field [81,85,86,90,93,96,97,100,102,106,114,115]. This approach is attractive because it eliminates the need to create a fracture in the often fragile separation

capillaries. To reduce the separation current, capillaries of very small diameter or a low field strength and/or low conductivity buffers for the background electrolyte can be used.

The alignment of the electrode with the CE capillary is critical for reproducible operation of the system. Normally, it is achieved with the aid of micropositioner and a light microscope [74,76,100]. Fermier et al. have introduced the use of a holder that automatically aligns the capillary and the electrode in a wall-jet configuration upon insertion and precludes the need for a micropositioner [86,96,98]. Another approach that avoids the use of micropositioners is affixing the electrode permanently to the end of the CE capillary [83].

3.5 Alkyl polyglycoside analysis - The state of the art

3.5.1 Methods for the determination of alkyl polyglycosides

Detailed analysis of APG mixtures is a difficult task because of the varying alkyl chain lengths and the very large number of isomers presented: stereoisomers, ring isomers and position of the interglycosidic linkage for diglucosides and higher oligomers.

For a qualitative determination of APG in raw products as well as in formulated products, thin-layer chromatography (TLC) together with a specific staining can be recommended because sufficient sensitivity and separation power are achieved. Analysis by this method yields information about the alkyl chain length distribution (TLC on a nonpolar phase such as RP-8 or RP-18) [5, 128–132] or a rough estimate of the degree of polymerisation (DP) (TLC on unmodified or aminopropyl-modified silica) [3, 5, 131].
For the determination of alkyl chain length, high performance liquid chromatography (HPLC) performs as well as TLC. Gas chromatography (GC) requires a silylation of the sample, but has no advantage over other methods for this analytical task [133]. High temperature gas chromatography (HTGC) after silylation [3, 128, 134] is the

only method that can be recommended for an exact determination of the DP. In fact, GC yields the most information about the sample and is the method of choice if a very detailed analysis is required.

A quantitative determination of APG in raw products can be done by each chromatographic technique: HPLC [3, 128, 135–138], TLC or GC. Which method is chosen depends on the instruments available and on the required analysis time, the accuracy and the need for automation.

Non-chromatographic methods could also be used for quantifying the active matter in raw products. The first of these is based on a derivatisation of the hydroxyl groups in a nonaqueous solvent and subsequent titration [139]. The second method is to hydrolyse the APG to the fatty alcohol and glucose and subsequently make a photometric determination of the glucose [130, 140]. The third method is an enzymatic hydrolysis of the AG and a subsequent determination of the glucose with an enzyme electrode [141, 142].

For environmental samples, which usually require sample cleanup and preconcentration by solid-phase extraction [128, 143], HPLC or GC are suitable methods for both qualitative and quantitative determination.

For purposes of process control and quality assurance, i.e., if numerous samples of a similar composition have to be analysed or if an on-line analysis is required, the powerful method of IR spectroscopy should be considered [144–147]. It allows very fast and simple analysis, but requires a lot of work for calibration by chemometric techniques [144].

With the use of nuclear magnetic resonance (NMR) spectroscopy, integrating the intensities of the signals allows calculation of the relative concentrations of the alkyl chain and the glucose groups and of the ratio between various isomers [3]. Thus, the approximate DP can be estimated, but this method is not accurate enough because the signals are too broad. Moreover, if the sample contains residual fatty alcohol and/or unreacted glucose, both components interfere with this method and lead to inaccurate results.

3.5.2 Detection methods for alkyl polyglycosides in CE

Until now, there is no publication about the analysis of APGs by CE. In general, all of the detection methods used for the determination of APGs by HPLC could also be applied to CE. Since APGs do not possess either chromophoric or fluorophoric groups, application of direct UV or fluorescence detectors is impossible. Instead, the use of the following detectors after separation by HPLC has been described in the literature: UV detector after post-column derivatisation [135], refractive index (RI) detector [3, 128], evaporative light scattering detector (ELSD) [136, 137], electrochemical detector (ED) in the pulse amperometric mode [128,137], mass spectrometer (MS) (both LC-MS and LC-MS/MS) [5–7] and nuclear magnetic resonance (NMR) spectrometer [3, 6].

Chapter 4

Results and discussion

The APGs lack chromophores in their structures, a condition that hinders their direct detection with spectroscopic methods. To circumvent this impediment, several detection strategies could be applied, including indirect UV and fluorescence detection, electrochemical detection, and derivatisation with a suitable chromophore and/or fluorophore.

In addition, APGs possess no charged functional groups which would allow different electromigration and thus separation. The separation of neutral analyte by CE has often required the aid of micelles in the electrolyte or the *in situ* conversion into charged species via the formation of complexes with other ions such as borate [148, 149] or metal cations [150]. Furthermore, because of the ionisation of the hydroxyl groups of the carbohydrates at extremely high pH, highly alkaline electrolyte solutions are also useful for the electrophoresis of APGs [151].

At the beginning of this work, all analyses were carried out only with the Cognis samples, as summarised in **Table 4.1**. Some samples are mixtures of underivatised APGs which differ mainly in the degree of polymerisation and in the length of the alkyl chains. Others contain both underivatised and derivatised APGs; the former are neutral and will be transported through the capillary together with the EOF, while the latter are carboxymethyl derivatives (CM) of APGs with electrophoretic mobility to the anodic end of the capillary.

APG samples	Alkyl chain length	Remark
APG 220 UP	C_8 and C_{10} (α, β)	> 60% monoglucoside, DP=1.5
APG 600 UP	C_{12} and C_{14} (α, β)	> 60% monoglucoside, DP=1.4
APG 1200 UP	C_{12} and C_{14} (α, β)	> 98.5% mono-, di-, triglucoside, DP=1.4
7407-26-1	C_{12}	only monoglucoside
7953-43	C_{12}	CM of 7407-26-1
6501-166	C_{12}	mono-, di-, triglucoside, DP=1.2
7706-109	C_{12}	CM of 6501-166
7706-1	C_{12} and C_{14}	mixture of APGs and their CM
7484-150	C_8, C_{10}, C_{12} and C_{14}	mixture of APGs and their CM
7484-152	C_{12} and C_{14}	mixture of APGs and their CM
7484-166	C_{12} and C_{14}	mixture of APGs and their CM
7484-174	C_{12} and C_{14}	mixture of APGs and their CM

DP: degree of polymerisation

CM: carboxymethyl derivatives

Table 4.1: The Cognis samples

4.1 Indirect UV detection

Indirect detection methods are often useful for compounds lacking a chromophore. Ensuring adequate detection limits requires as carrier for the neutral analyte a further electrolyte anion with a high molar absorptivity and an effective electrophoretic mobility close to the mobilities of the analytes.

4.1.1 MEKC

One potential means of resolving the uncharged APGs is micellar electrokinetic chromatography (MEKC).

A number of electrolyte systems, consisting of both background chromophores (to enable indirect-UV detection) and negatively charged surfactants (to form the micelles needed for separation) were tested, as described in **Table 4.2**.

Background electrolyte	Micelles	Chromophore	Detection wavelength
10 mM borate pH 9.3	20 mM OBS		214 nm
	20 mM DBS		214 nm
	50 mM SDS	2 mM AMP	254 nm
10 mM phosphate pH 9	20 mM OBS		214 nm
	20 mM DBS		214 nm
	50 mM SDS		195 nm
	50 mM SDS	2 mM AMP	254 nm
		2 mM GBETS	195 nm
		5 mM EAB	190 nm
		0.3 mM fluorescein	488 nm
10 mM phosphate pH 9 + 10% MeOH	50 mM SDS	2 mM CLA	214 nm
100 mM TRIS pH 9	50 mM cholate		254 nm

borate: sodium borate
phosphate: sodium phosphate
MeOH: methanol
OBS: 4-octylbenzenesulfonic acid, sodium salt
DBS: dodecylbenzenesulfonic acid, sodium salt
SDS: sodium dodecyl sulphate
AMP: (-)-adenosine 5'-monophosphate monohydrate
GBETS: glycine benzyl ester, toluene-4-sulfonic acid salt
fluorescein: fluorescein, sodium salt
EAB: ethyl-p-aminobenzoate
CLA: conjugated linoleic acid
cholate: cholic acid, sodium salt
TRIS: tris(hydroxymethyl)aminomethane

Table 4.2: Electrolyte systems for MEKC separation and indirect UV detection

The chromophores examined were chosen to represent a wide range of mobilities so as to find one with mobility most similar to that of APGs in micelles.

However, the baseline was unstable in all the MEKC systems studied, and some

additional peaks were presented by a number of by-products which could also be indirectly detected. Moreover, the separation was insufficient, i.e., the interaction of APGs with the micelles was not ideal. MEKC was thus deemed unpromising, and attention was turned to electrolytes containing cyclodextrin.

4.1.2 Cyclodextrin electrokinetic chromatography (CDEKC)

To improve the separation, cyclodextrins (CDs) might be useful complexing agents. With their hydrophobic internal cavity, CDs are able to form complexes with aromatic or alkyl groups. Although CDs are themselves neutral, they can alter the electrophoretic mobility of a charged analyte, since the complexed and the free species have different molecular masses. Thus, the electrophoretic mobility is influenced by the complex formation constant. Substantial differences in the complex formation constant may be found even for structurally similar compounds like enantiomers because CDs are enantiomerically pure.

As underivatised APGs are uncharged, obtaining migration in an electrical field required the use of CDs modified so as to be charged. Two electrolyte systems were tried, both containing 2 mM (-)-adenosine 5'-monophosphate monohydrate (AMP) as chromophoric co-ion and 50 mM carboxymethyl β-CD. One had 6 mM sorbate pH 12 as background electrolyte, while the other had 10 mM borate pH 9.3.

Neither system was able to separate the components, perhaps because the big cavity of β-CD was not selective for the APG molecules.

4.1.3 Analyses with high-pH electrolyte

The different electromigration of carbohydrates in highly alkaline solution is due to the ionisation of the hydroxyl groups [151]. The ionisation constants for carbohydrates are in the range of 10^{-12} to 10^{-14} mol/l, i.e., $pK_a = 12 - 14$.

Sorbate as both electrolyte and chromophore for indirect UV detection of underivatised carbohydrates was first introduced in 1992 by Bonn and co-workers

[152,153]. At pH 12-12.2 and sorbate concentrations ranging from 6-10 mM, several signals were observed with Cognis sample 7706-1 (a mixture of C_{12} and C_{14} APGs and their carboxymethyl derivatives, see **Table 4.1**). The separation of this sample was even better if 2 mM AMP was added to the sorbate electrolyte (**Figure 4.1**). The peak at 2.4 minutes shows the EOF signal. The peaks between 2.9 and 4.7 minutes are probably belong to APGs and their carboxymethyl derivatives; they resolved very well from each other. The three peaks between 6.7 and 8.9 minutes are corresponding to the system peaks since they are presented permanently irrespective of water, buffer or any sample to be injected.

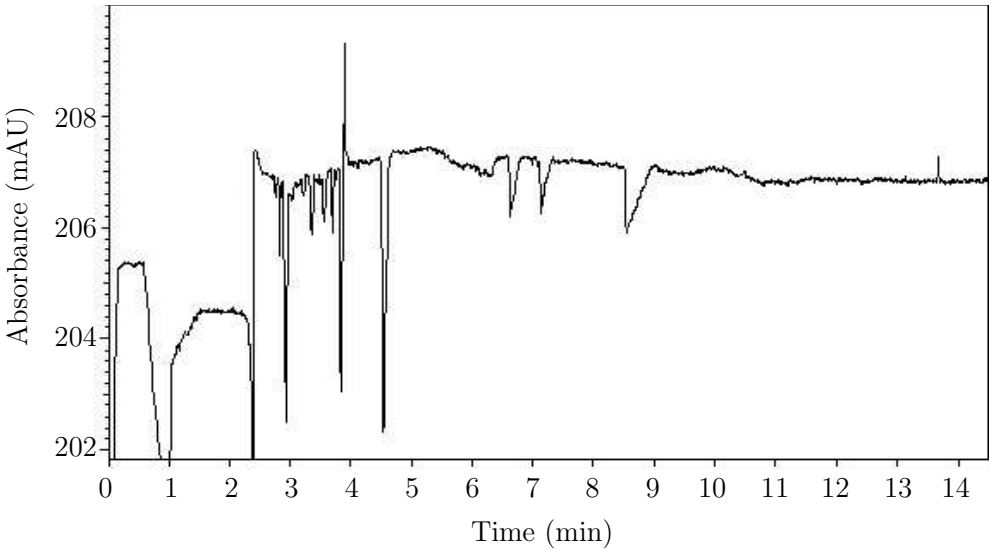

Figure 4.1: Analysis of Cognis sample (10 mM, 7706-1); electrolyte: 1.5 mM AMP in 6 mM sorbate, pH 12

However, apart from the EOF and the system signals, there was no additional signal when samples of APG 220 or APG 600 were injected, meaning that the pH was not high enough for dissociation of the APGs and the signals observed with sample 7706-1 were, in fact, just from the derivatised APG components.

In the next step, the pH was increased to enhance the ionisation of the APGs, but

this gave rise to high current and poor separation. It was in accordance with the observation reported by Xu et al. [154] that the use of high pH background electrolyte resulted in a rapid increase of the low-frequency noise and baseline instability. This was found to be related to joule heating and insufficient thermostating of the capillary. In addition, the increasing concentration of sodium ions in the background electrolyte with rising pH probably increased the thickness of the diffusion double layer at the inner capillary wall [155], so that the electroosmotic flow gradually decreased. Depend on the magnitude of the electrophoretic mobility of analyte, the analysis time might increase. Moreover, increasing the pH rapidly decreased the sensitivity as a result of increasing competition of hydroxide ions in the displacement of the chromophore [154].

The buffer with both 10 mM phosphate pH 12.6 and 6 mM sorbic acid was tested further. With normal carbohydrates like glucose and fructose, excellent signals were obtained, as shown in **Figure 4.2**.

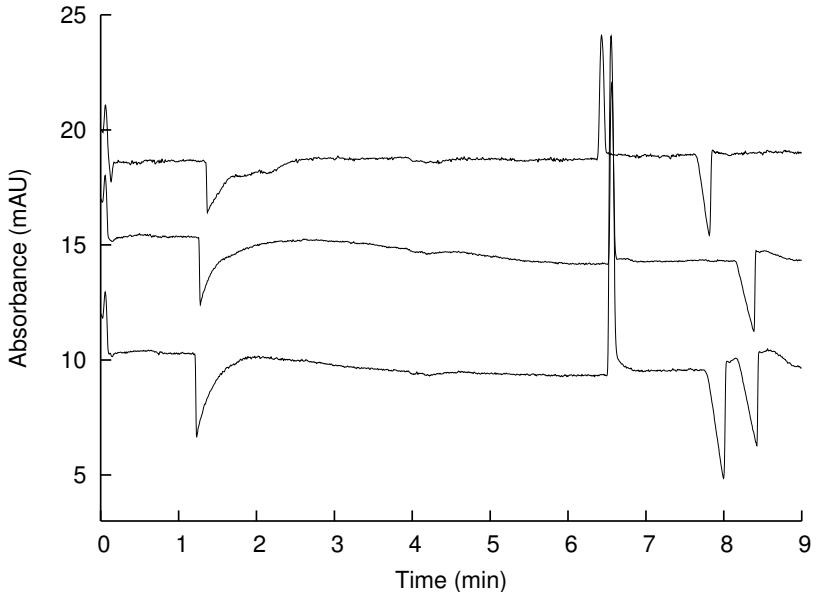

Figure 4.2: Analysis of glucose (top), fructose (centre) and a mixture of the two; electrolyte: 6 mM sorbic acid in 10 mM phosphate, pH 12.6

However, no signal or satisfactory separation could be seen when various Cognis samples were injected. Apparently, the ionisation of these substances is more difficult than that of the simple carbohydrates.

In summary, the indirect detection approach turned out not to be selective and may suffer from the interference of the matrix. It was therefore decided to examine direct UV detection of APGs after complexation with borate.

4.2 Direct UV detection as borate complexes

Polyhydroxyl compounds, including carbohydrates, can reversibly form anionic complexes with borate [148]. Borate complexation of native carbohydrates allows direct UV detection between 195 nm and 205 nm, since the UV absorbance of the complexes is 2- to 50-fold that of the uncomplexed carbohydrates [149]. Furthermore, owing to the negative charge of this complex, the underivatised APGs should now be separated from the neutral components. In addition, borate complexation enhances steric differences in the solutes, leading to an improved electrophoretic resolution of the solutes with an otherwise identical charge-to-mass ratio [156]. The formation of the borate complex is illustrated in **Equation 4.1**.

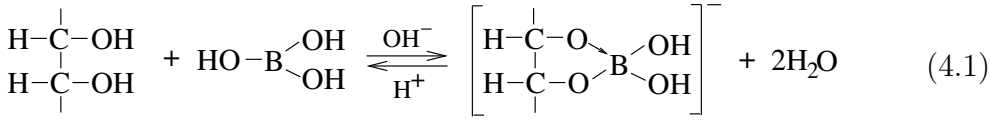

(4.1)

Given a constant concentration of carbohydrates, the complex component increases with borate concentration, according to the law of mass action, as well as with increasing pH, as a result of the higher concentration of tetrahydroxyborate in alkaline solution [149]. The complex stability depends on the configuration of the carbohydrate molecule, the number of hydroxyl groups and the presence of substituents. Hofstetter-Kuhn et al. have reported that elevated temperature shortens the analysis time, improves the peak shape and increases the sensitivity [149].

Attempts were made to separate mannose, galactose, glucose and xylose (each 10 mM in water) with 50 mM sodium borate pH 9.3 as background electrolyte and 60°C as both sample storage and separation temperature (**Figure 4.3**). Even though some signals were observed, the separation was not good, and the baseline was very unstable as the result of the elevated temperature. This effect prevented sensitive detection with this approach. With 200 mM boric acid adjusted to pH 10 with 1 M KOH solution, the separation was not improved. **Figures 4.4** and **4.5** illustrate the separation under the latter set of conditions when water or 5 mM APG 220 was injected, with a temperature of 25°C in both sample storage and separation capillary.

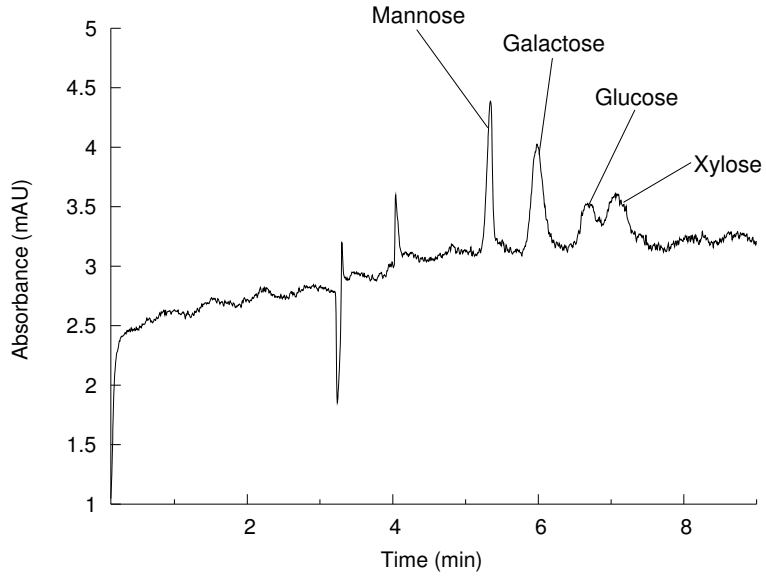

Figure 4.3: Analysis of mannose, galactose, glucose and xylose; electrolyte: 50 mM sodium borate, pH 9.3, both sample storage and separation temperatures were 60°C

Poor separation was obtained with sample APG 220. It could be explained by the fact that the carbohydrate-borate complex formation is greatly influenced by the very presence of substituents in the polyhydroxyl molecule, as well as by their charges, locations, and anomeric linkages [157]. Therefore, the derivatised groups, including the alkyl chains in APGs, might obstruct the complex formation.

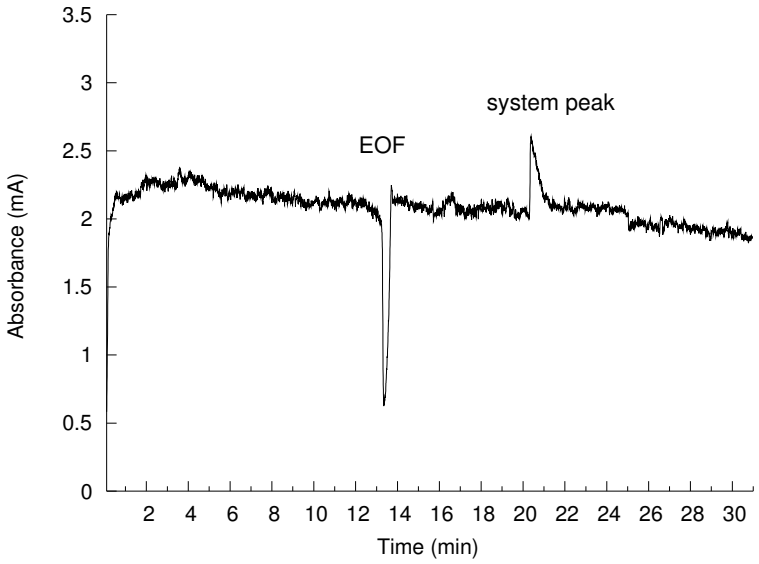

Figure 4.4: Control run with water as blank; electrolyte: 200 mM boric acid adjusted to pH 10 with 1 M KOH solution; both sample storage and separation temperatures were 25°C

On the other hand, with the carboxymethyl derivatives of APGs, the presence of charged substituents in the polyhydroxyl molecule may decrease the stability of borate ester, as a result of coulombic repulsion between a negatively charged substituent and $B(OR)_4^-$ [157].

In the next set of experiments, to simplify the optimisation of the analysis, oleyl alcohol and its glucosides were chosen. These substances have nearly the same structure as the APGs, but possess a UV absorbance. Thus, the electrolyte system suitable for this new sample could also be useful for efficiently separating the APGs.

4.3 New sample - Oleyl alcohol and its glucoside

The new sample (7669-168-4) contains 65.2 % oleyl alcohol, 24.2 % oleyl monoglucoside, 5.1 % oleyl diglucoside, 3.9 % oleyl triglucoside, 1.2 % oleyl tetraglucoside

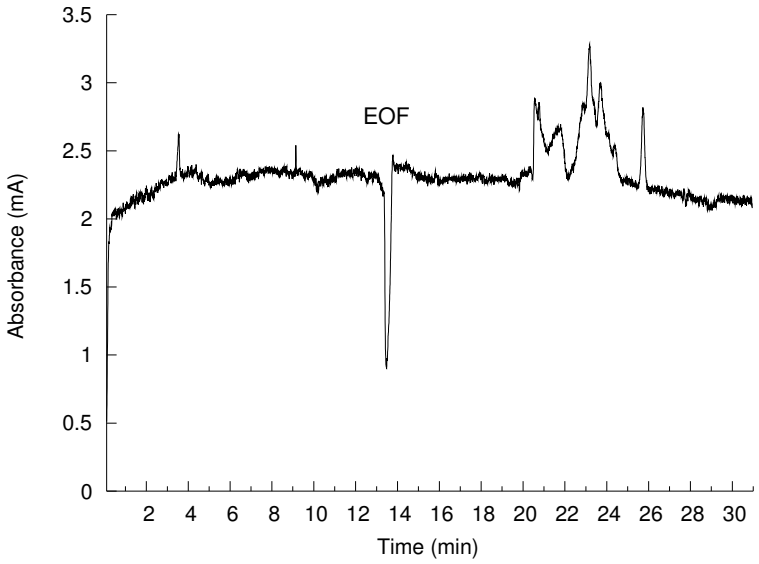

Figure 4.5: Analysis of 5 mM APG 220; electrolyte: 200 mM boric acid adjusted to pH 10 with 1 M KOH solution; both sample storage and separation temperatures were 25°C

and 0.3 % oleyl pentaglucoside. Possessing a double bond, these analytes have UV absorbance at 195 nm, but have no charged functional group. Furthermore, oleyl alcohol is not a polyhydroxyl compound, so it can not be converted into a charged complex with other ions such as borate or metal cations. Therefore, the separation can only be performed by means of MEKC or CDEKC.

The micelles increase the hydrophobicity of the electrolyte, which in turn reduces the problem of low solubility of analytes in aqueous solution. As a result, the mixture of oleyl alcohol and its glucoside dissolved much more readily in buffer than in water, where it forms an emulsion. This effect is particularly clear in **Figure 4.6**, although that is treated in **Section 4.3.1**.

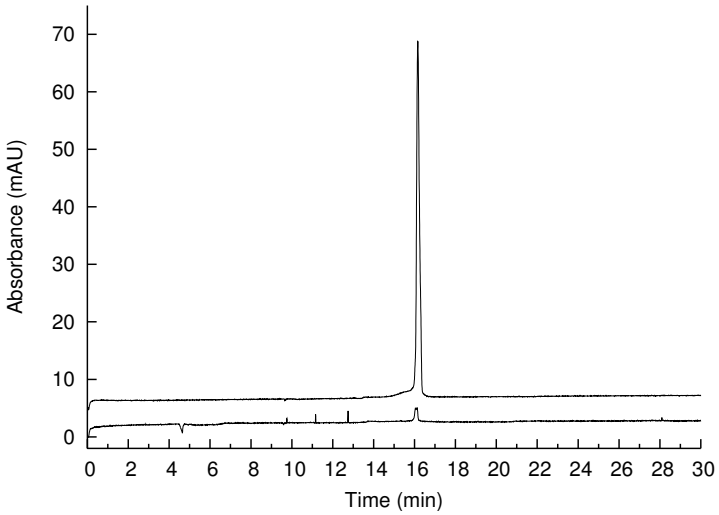

Figure 4.6: Analysis of Cognis sample (10mM, 7669-168-4) dissolved in water (bottom) and in buffer (top); electrolyte: 10 mM sodium phosphate, pH 9 and 50 mM SDS

4.3.1 MEKC

In a set of experiments, the effect of 20 mM phosphate buffer containing 50 mM SDS and 10 mM borate buffer with different concentrations of SDS (15, 20, and 25 mM) was tested. No separation was observed. The result was not improved even when 5-10 % methanol (MeOH) or acetonitrile (ACN) was added to the buffer. This means that there was insufficient interaction between analytes and SDS-micelles.

Some other micelles systems (such as Brij 35, cholate, taurocholate) were applied, but the separation was not better. It could be assumed that all of the analytes remained inside the micelles to the same extent because of a similar interaction with the micelles.

It was believed that the use of mixed micelles could increase the size of the elution window; and varying the mole fraction of surfactants in their mixture could vary the retention factors of the analytes as well as the selectivity of the system. Therefore, a number of buffer systems were screened, as summarised in **Table 4.3**.

The best separation was found with electrolyte containing 10 mM borate, pH 9.3,

20 mM SDS, 100 mM cholate and 10 % ACN; this is shown in **Figure 4.7**. The peaks between 30 and 35 minutes are probably corresponding to oleyl alcohol and the isomers of its glucosides. Nevertheless, the resolution in this case was still not high enough. The experiments described next were to study the application of CDEKC on analysing APGs.

Buffer	Micelles 1	Micelles 2	Organic modifier
20 mM phosphate pH 9	20 mM SDS	50 mM Brij 35	—
10 mM borate pH 9.3	20 mM SDS	50 mM Brij 35	—
	25 mM SDS	50 mM taurocholate	—
	25 mM SDS	50 mM taurocholate 100 mM cholate	—
	25 mM SDS	100 mM cholate	—
			5% ACN
			10% ACN
			15% ACN
			10% MeOH
	0-100 mM SDS	—	10% ACN
	20 mM SDS	40-150 mM cholate	10% ACN
	0-100 mM SDS	100 mM cholate	10% ACN

Brij 35: polyoxyethylene lauryl ether

Table 4.3: Mixed-micelles systems for separation of oleyl alcohol and its glucosides

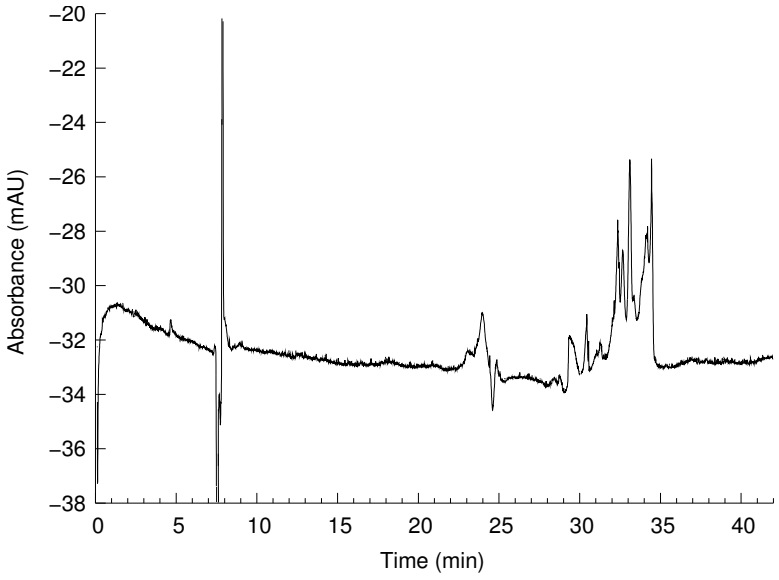

Figure 4.7: Analysis of Cognis sample (10 mM, 7669-168-4); electrolyte: 20 mM SDS and 100 mM cholate in 10 mM borate, pH 9.3 with 10% ACN

4.3.2 CDEKC

The oleyl alcohol and its glucosides could only be separated from each other by the use of charged CD or a mixture of SDS and neutral CD.

First, 2-hydroxy-3-trimethylammonoiapropyl-β-CD (CAVASOL W7 TMA) was used in 10 mM borate at pH 9.3. Screening with 10 mM borate, pH 9.3 and 10-100 mM CAVASOL was carried out to determine the optimum concentration. With this system, the baseline was unstable and there was sometimes no current at all because of the low solubility of the MeOH solution of oleyl mixture in the electrolyte.

In search of improvement, an organic modifier (such as MeOH) was added to the electrolyte. Electrolyte with 10 mM borate, pH 9.3, 40 mM CAVASOL and 10-15 % MeOH was tested, but no improvement in the separation was obtained.

Other charged-CD systems like 10 mM highly sulphated-α-cyclodextrin (HS-α-CD) or 10 mM highly sulphated-β-cyclodextrin (HS-β-CD) were tried with the 20 mM phosphate buffer, pH 9. In every case, a minimum of 30 % MeOH was required to ensure the solubility of analyte in the electrolyte; this resulted in an unstable baseline and an irreproducible migration time.

With these rather lipophilic APGs, a non-aqueous electrolyte was expected to be suitable, but the charged CD could not be dissolved in buffers with organic modifiers.

Up to this point, the study had provided no satisfactory separation of oleyl alcohol and its glucosides. The following factors were responsible for the difficulties:

- The low solubility of analytes prevented the usage of a large number of electrolyte systems or required a high proportion of organic solvent, which resulted in unstable baselines.
- Because of the low or absent UV activity, a high concentration of samples had to be injected. Hence, the MEKC system was overloaded; this likewise required a higher proportion of organic solvent, with the problems mentioned above.

In summary, the methods of direct or indirect UV detection were not suitable for both APGs and oleyl glucosides. It was necessary to find another detection method, which was able to detect APGs directly with high sensitivity and selectivity. Pulsed-amperometric detection seemed the most suitable among the choices available.

4.4 Preliminary experiments

To take part in the electrochemical reaction, the APGs should be highly dissociated to negatively charged groups. This requires the use of a strongly basic electrolyte. To make sure that the analytes did not degenerate under these conditions, the analytes were examined by nuclear magnetic resonance spectroscopy (NMR) and thin layer chromatography (TLC) before and after exposure to 1 M NaOH.

4.4.1 Nuclear magnetic resonance spectroscopy

^{1}H-spectra and ^{13}C-spectra of C_{12}-β-D-glucopyranoside were run by the Department of Organic Chemistry at the Bergische Universität Wuppertal and were analysed with the help of Dr. W. V. Turner from our group.

- From ^{1}H-spectra of the sample in neutral (**Figure 4.8**) and in basic CD_3OD (1 M NaOH) (**Figure 4.9**), it was clear that the protons of the alkyl chain (δ 0.8 to 1.7), other than those next to the oxygens, were not changed by the treatment.

  However, the protons of the hydroxyl groups (δ 3.1 to 4.3) were considerably different in the two spectra. It is likely that the observed differences were purely a matter of the differing solvents.

- The ^{13}C-spectra of the sample in neutral (**Figure A.1**, see Appendix) and in basic solution (**Figure A.2**, see Appendix) were, however, quite similar.

In each spectrum, some of the aliphatic carbons overlapped at ca. δ 30, but the pattern and the chemical shifts were nearly the same (δ 14 to 33).

The C1 carbon of the glucose moiety was essentially unchanged, falling at δ 104.3 in one spectrum and 104.9 in the other (relative to MeOH at δ 49.0).

The pattern of the carbon atoms attached to oxygen atoms was only slightly changed. In each case, these fell between δ 62 and δ 79, as expected. The very small shift ($\leq$ 0.7 ppm) in their position in the second spectrum in comparison to the first one is probably due to the different solvents.

- Conclusion: These spectra suggest strongly that the sample was stable in 1 M NaOH solution. It appears that the highly basic solution at most gave rise to the dissociation of the hydroxyl groups of the glucose moiety. However, the alkyl chain and the carbon backbone of the sugar moiety were not influenced.

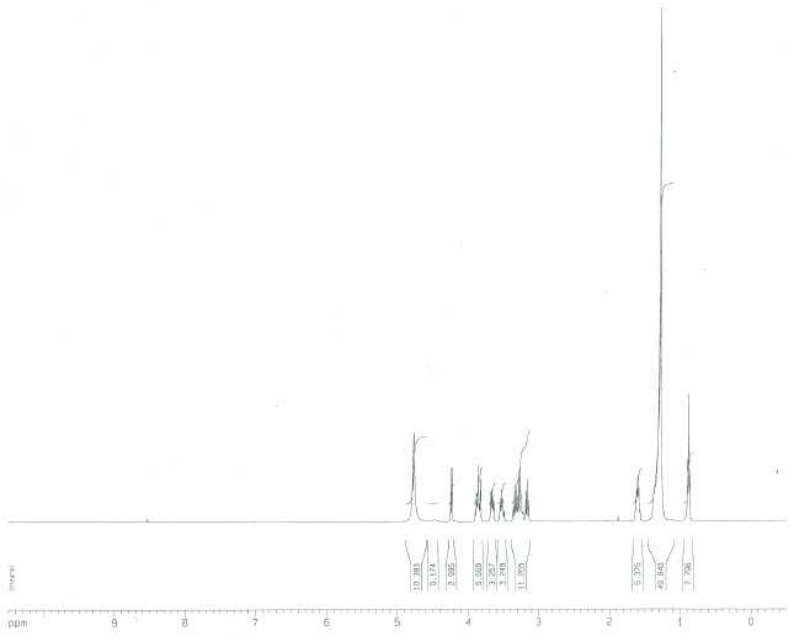

Figure 4.8: ^{1}H-NMR spectrum of C_{12}-β-D-glucopyranoside in CD_3OD

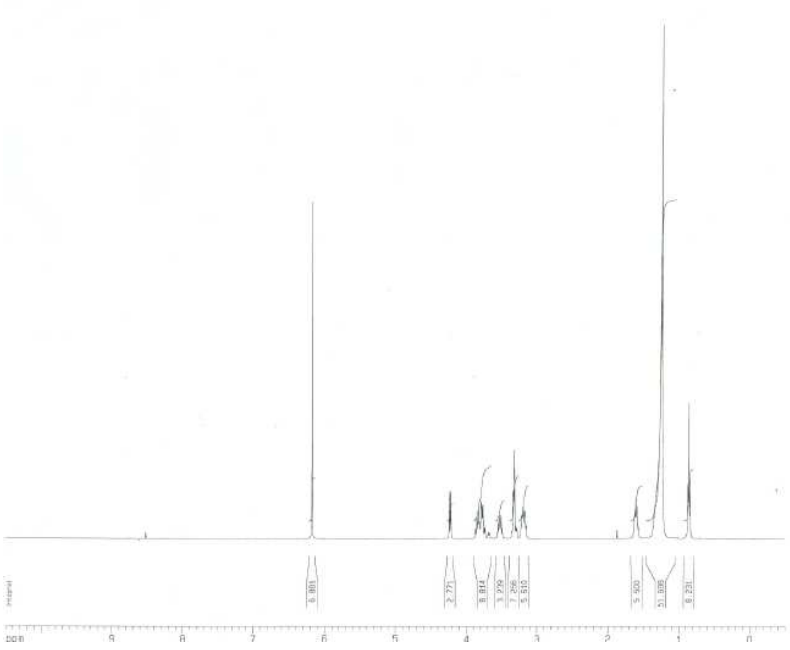

Figure 4.9: ^{1}H-NMR spectrum of C_{12}-β-D-glucopyranoside in 1 M NaOH in CD_3OD

4.4.2 Thin-layer chromatography

Three solutions of C_{12}-β-D-glucopyranoside were analysed by reversed-phase thin-layer chromatography (TLC). The first solution contained 10 mg C_{12}-β-D-glucopyranoside in 0.5 mL MeOH. The second had the same amount of analyte in 0.5 mL of 1 M NaOH in MeOH. The third sample was 10 mg C_{12}-β-D-glucopyranoside first dissolved in 0.5 mL of 1 M NaOH, then neutralised with 1 M HCl. These solutions were spotted onto an RP-18 F_{254s} TLC plate and eluted by MeOH/water (9/1, v/v). The analytes were visualised as dark spots by spraying with sulfuric acid (200 g/L) solution and subsequently warming with a heat-gun.

It was observed that the spots obtained from the first and the third sample had the same R_f values, indicating that the strong basic solution did not damage the APG.

Several APG standards and mixtures were examined by this chromatographic method. The APG type was identified by reversed-phase TLC. With an RP-18 F_{254s}

plate and a mixture of MeOH/water (9/1) as eluent, various alkyl chain lengths could be differentiated (**Figure 4.10**). While normal-phase TLC, with silica-gel 60 F_{254} plate and elution by $CHCl_3$/MeOH (8/2), separated mono- and di-glucosides (**Figure 4.11**); no separation of individual APG type according to alkyl chain lengths could be achieved by this method.

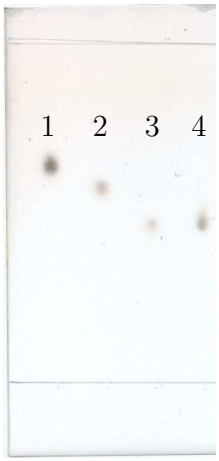

Figure 4.10: Separation of APGs with different alkyl chain lengths by TLC; RP-18 F_{254s} TLC plate, eluted by MeOH/water (9/1) and visualised by H_2SO_4 (200 g/L) . (1) C_8-β-D-glucopyranoside; (2) C_{10}-β-D-glucopyranoside; (3) C_{12}-β-D-glucopyranoside; (4) C_{12}-β-D-maltoside.

All of the samples from Cognis were applied to an RP-18 F_{254s} plate to characterise the alkyl chain length of their constituents (**Figure 4.12**). On this plate, the R_f values of C_8, C_{10}, C_{12} and C_{14} were 0.71, 0.62, 0.51 and 0.39, respectively. As expected, the compounds with the longer alkyl chains were eluted more slowly than the shorter ones. The long track at the upper part of the plate represented the by-products in Cognis samples.

With this simple chromatographic method, a general idea about the distribution of alkyl chain lengths in an APG mixture could be obtained quickly .

Figure 4.11: Separation of mono- and di-glucosides; silica-gel 60 F_{254} TLC plate, eluted by $CHCl_3$/MeOH (8/2) and visualised by H_2SO_4 (200 g/L). (1) C_{12}-β-D-glucopyranoside; (2) C_{12}-β-D-maltoside

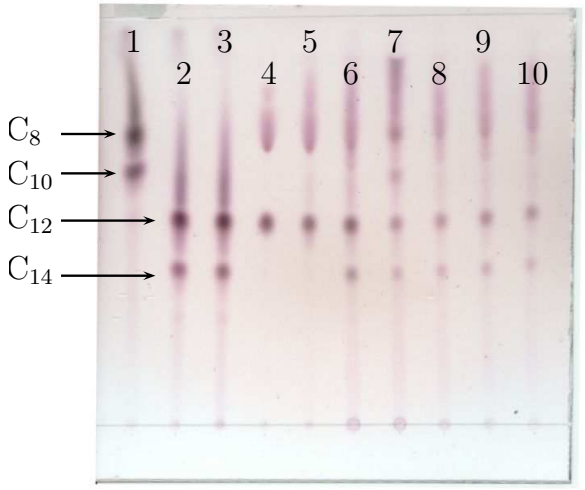

Figure 4.12: The alkyl-chain-length distribution of different APG samples; RP-18 F_{254s} TLC plate, eluted by MeOH/water (9/1) and visualised by H_2SO_4 (200 g/L). (1) APG 220 (C_8 and C_{10}); (2) APG 600 (C_{12} and C_{14}); (3) APG 1200 (C_{12} and C_{14}); (4) 7953-43 (only C_{12}); (5) 7706-109 (only C_{12}); (6) 7706-1 (C_{12} and C_{14}); (7) 7484-150 (C_8, C_{10}, C_{12} and C_{14}); (8) 7484-152 (C_{12} and C_{14}); (9) 7484-166 (C_{12} and C_{14}); (10) 7484-174 (C_{12} and C_{14}).

4.5 Pulsed amperometric detection

4.5.1 The electrodes

For the amperometric detector, a reference, an auxiliary, a ground and a working electrode are required.

For the entire work, a silver/silver chloride reference electrode and a platinum wire auxiliary electrode from BAS (Bioanalytical Systems, Inc., Warwickshire, UK) were used, as described in **Section 6.5**. The potential of this reference electrode at 25°C is + 0.196 V (*vs.* the standard hydrogen electrode).

The CE ground was used to drop the voltage in the detection cell to almost zero while high voltage was applied across the separation capillary. This is also discussed in **Section 6.5**.

As a working electrode, gold or platinum is more suitable for pulsed amperometry than either carbon or transition metals like copper, nickel, cobalt or ruthenium, because these noble metals establish equilibrium rapidly following a change in potential [71]. The sensitivity of PAD for analysing carbohydrates at gold electrodes is maximised under conditions of high alkalinity, and pH $>$ 12 is commonly recommended. These same compounds yield a PAD response at platinum electrodes at all pH values [65]. However, regardless of the more restrictive pH requirements for gold electrodes, gold is clearly more popular than platinum for the detection of carbohydrates. One reason is the reduced interference from the cathodic response of dissolved O_2 under conditions of the most commonly used PAD waveforms [65]. Gold was therefore chosen for the working electrode.

Previously, the performance of disk electrodes of different sizes in the range of μm and mm was compared by Matysik [108] and Everett [125]. The major differences in the electrodes consisted of their background electrochemical responses and equilibration times. The mm-sized electrodes required a longer equilibration time and gave a higher background current. Moreover, the mm-electrode detector introduced zone

broadening that was not found with the μm-electrode arrangement. The peak tailing observed with the larger electrode resulted mainly from diffusion of the analytes across the electrode surface after exiting the capillary.

The coulometric efficiency, i.e. the percentage of analyte that is actually converted at the working electrode, depends considerably on the size of the electrode used. Despite the fact that the absolute signals for the μm-sized electrode were much smaller than those with the larger disk electrode, the μm-electrode configuration offers comparable limits of detection. This shows that a high coulometric efficiency is not necessarily a prerequisite for sensitive electrochemical detection in capillary-based analysis [108].

Therefore, the μm-sized electrode with a diameter six times that of the I.D. of the separation capillary was chosen as the most reasonable. In our case, the capillary had an I.D. of 50 μm; therefore, the working electrode with 300 μm diameter was used. For the first experiments, the working electrode was a 300-μm gold wire insulated by a 30-μm layer of PTFE (so that the O.D. of this electrode was equal to that of the capillary).

4.5.2 Construction of the detection cell

Among different approaches for coupling CE and AD, as discussed in **Section 3.4**, the end-column detection design with capillary-electrode holder of Fermier et al. [86] was constructed first. This design facilitates the exchange of electrodes and capillaries without the need of refabricating the entire capillary-electrode setup. The system can be assembled in a very short time. This design, together with the construction of the working electrode, was gradually improved in each step of the study to get a more stable baseline, more intense signals and better peak shape.

First construction

The capillary-electrode holder was fabricated in the workshop of Faculty C at the Bergische Universität Wuppertal from two small pieces of plexi-glass with dimensions of 10 mm width × 20 mm length × 3 mm thickness. A small groove (350 μm width × 355 μm depth) was machined lengthwise at the centre of one of the pieces. A hole with a diameter of 3 mm was also machined through the centre of both plexi-glass pieces. The capillary and the working electrode were accommodated in the groove, and the two plexi-glass plates were brought together and secured in place by means of four small screws (**Figure 4.13**).

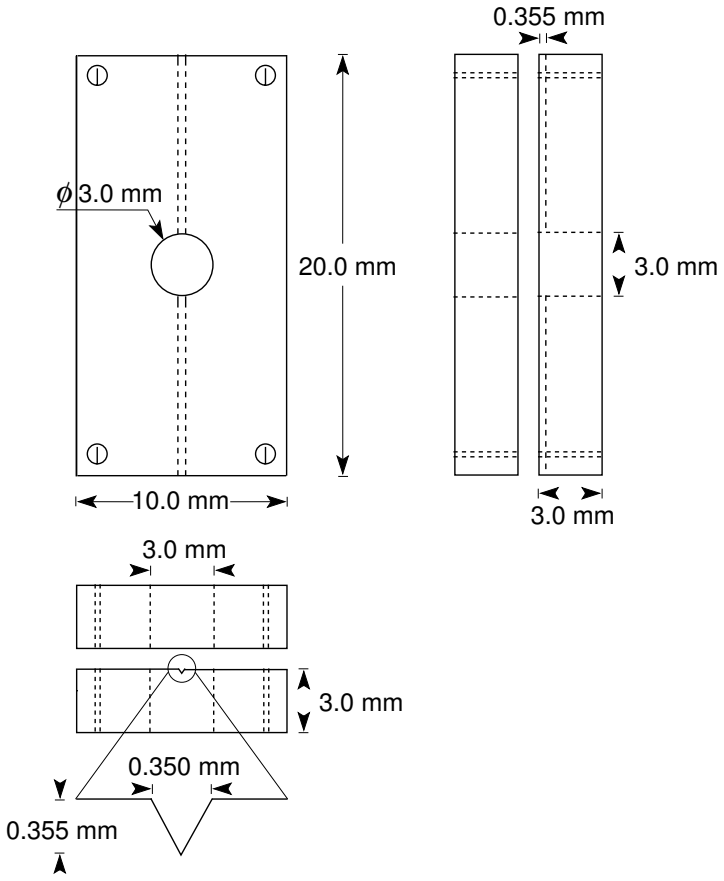

Figure 4.13: The first construction of the capillary-electrode holder

In this construction, the working electrode was placed close to the outlet of the capillary in a "wall-jet" configuration, so that the analyte was detected as it exits the capillary. The holder automatically aligned the capillary and the electrode upon insertion, precluding the need for a micropositioner. The distance between the capillary and the working electrode was adjusted under a microscope to about 10 μm. It was observed that distances above this value could result in broadening of the signal by diffusion of analyte in the electrolyte medium, while with smaller distances the separation voltage could interfere with the detection potential, giving an unstable baseline.

Once the electrode and the capillary had been secured in place, the assembly was introduced into the electrolyte solution contained in a cylindrical PVC vial (30 mm O.D. $\times$ 65 mm height) (**Figure 4.14**).

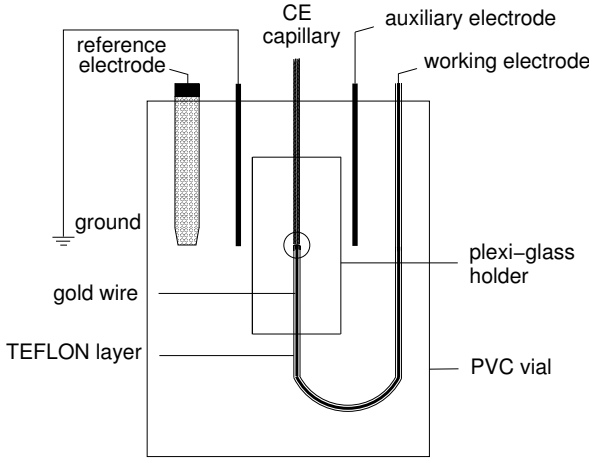

Figure 4.14: The first cell design

The top of this container was covered by a rubber septum with four small holes ($\approx$ 300 μm) for the capillary, the ground, the working and the auxiliary electrodes. The fifth hole, for the reference electrode, had a diameter of 6 mm. The electrodes were then connected to the potentiostat. The rubber septum was kept in position with the support of a PVC ring, which could be fastened to the PVC vial by turning. The cell in place in the CE instrument is pictured in **Figure 6.2**.

Second construction

In the first construction, the ground was not held very firmly, which made it difficult to control all of the potentials in the cell. This resulted in an unstable baseline even though the separation voltage was only 5 kV. Therefore, it was necessary to design another holder which would hold the ground as well as the auxiliary electrode firmly. This time, two grooves, instead of one, were machined perpendicular to each other and meeting at the centre of one of the plexi-glass plates. The capillary and the working electrode were situated in the lengthwise groove, while the ground and the auxiliary electrode were accommodated in the direction of the breadth. All of them converged at the 3.0-mm hole at the centre of the holder, as illustrated in **Figure 4.15**.

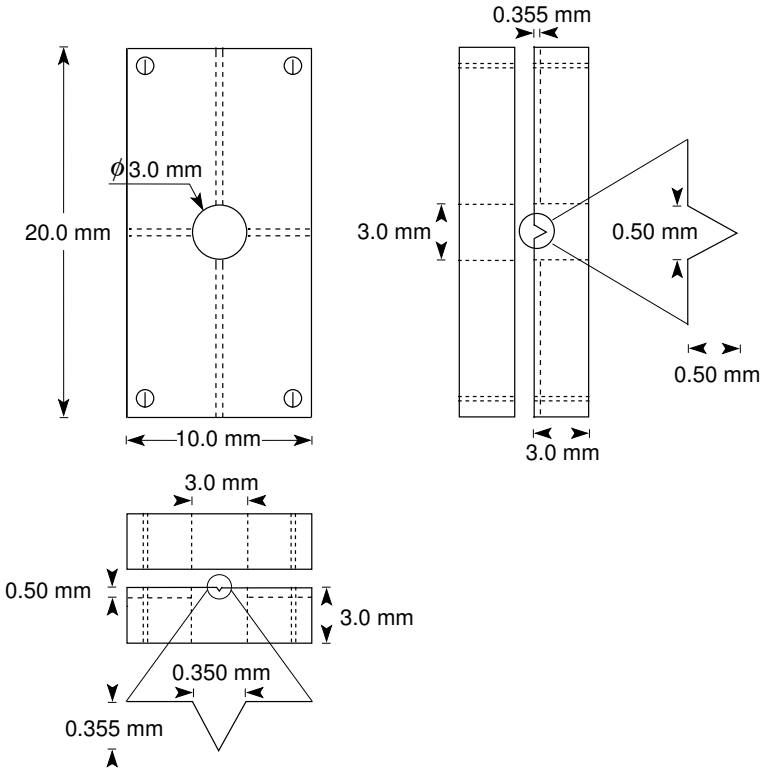

Figure 4.15: The second construction of the capillary-electrode holder

Outside the holder, the ground and the auxiliary electrode were bent into an L-shape to facilitate bringing them out the top. For stability, the capillary, the electrodes and the ground were threaded into 1 mm I.D. × 3 mm O.D. × 60 mm length PVC tubes. The rubber septum on top of the PVC vial then contained four 3-mm-diameter holes positioned in a line, through which the PVC tubes came out of the cell. The fifth hole, for the reference electrode, had a diameter of 6 mm. It was just opposite the hole for the capillary, so that the end of the reference electrode was just in front of the hole at the centre of the plexi-glass plates (**Figure 4.16**). The placement of the reference electrode close to the working electrode was to avoid any errors due to a small electric field that the separation voltage might induce near the working electrode [158].

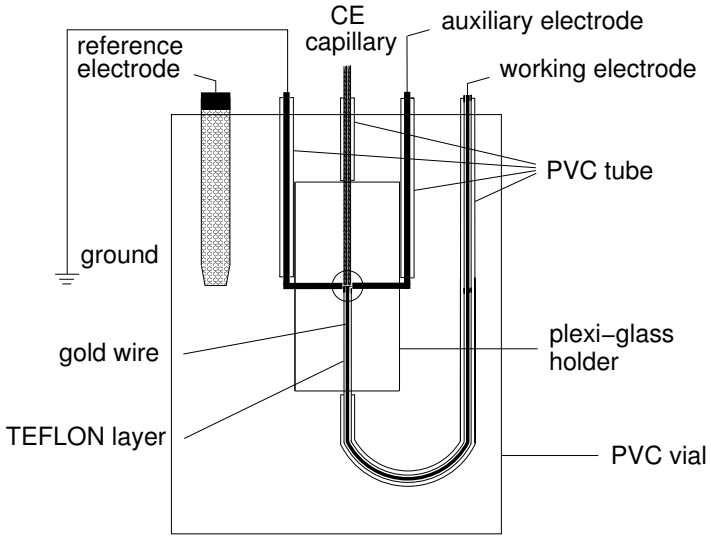

Figure 4.16: The second cell design

Third construction

The second construction still did not give a very stable baseline. It was believed that the working electrode would yield a more stable and reproducible result if it was

insulated by a glass tube; this could fix it significantly more strongly than PTFE. Therefore, a special microcylindrical working electrode was fabricated, in collaboration with the Department of Elektroanalytik & Sensorik at the Ruhr-Universität Bochum, by tightly sealing the metal wires into the tapered ends of drawn borosilicate glass tubes (O.D. 1.5 mm, I.D. 0.75 mm, length 100 mm; Hilgenberg, Malsfeld) as follow.

The upper end of the tube was vertically positioned by lateral screwing to a holder, whereas the other end was held firmly in a brass cylinder (O.D. 15 mm, height 34 mm) (**Figure 4.17a**). A constantan wire with highly electrical resistance was coiled around the lower end of the tube. A suitable current through this wire (in this case, 17 A for 3 V of applied voltage) melted the glass tube slowly and thus narrowed its diameter (except on the unfortunate occasions when it broke quickly into two shorter tubes) (**Figure 4.17b**).

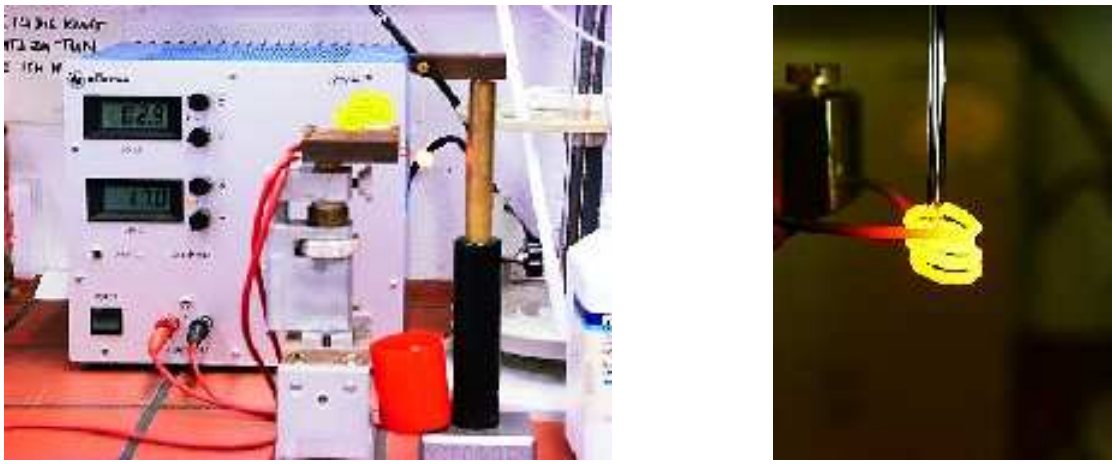

(a) (b)

Figure 4.17: The capillary puller

A 5-mm in length and 300-μm in diameter gold wire was positioned inside the tapered tip of the long tube (**Figure 4.18a**). To ensure that this piece of wire was fastened inside the pulled tip, a short exposure to the flame of a microtorch was

necessary. Establishing a tight seal around the wire required that the glass be melted again. As an additional problem, air could be accidentally entrapped as bubbles in the molten glass and lead to an improper electrode tip. To avoid this, a water-jet vacuum pump was connected to the open end of the capillary while the heat was applied. This reduced bubble formation and pressed the flowing glass towards the tip wire, thus speeding up the embedding procedure.

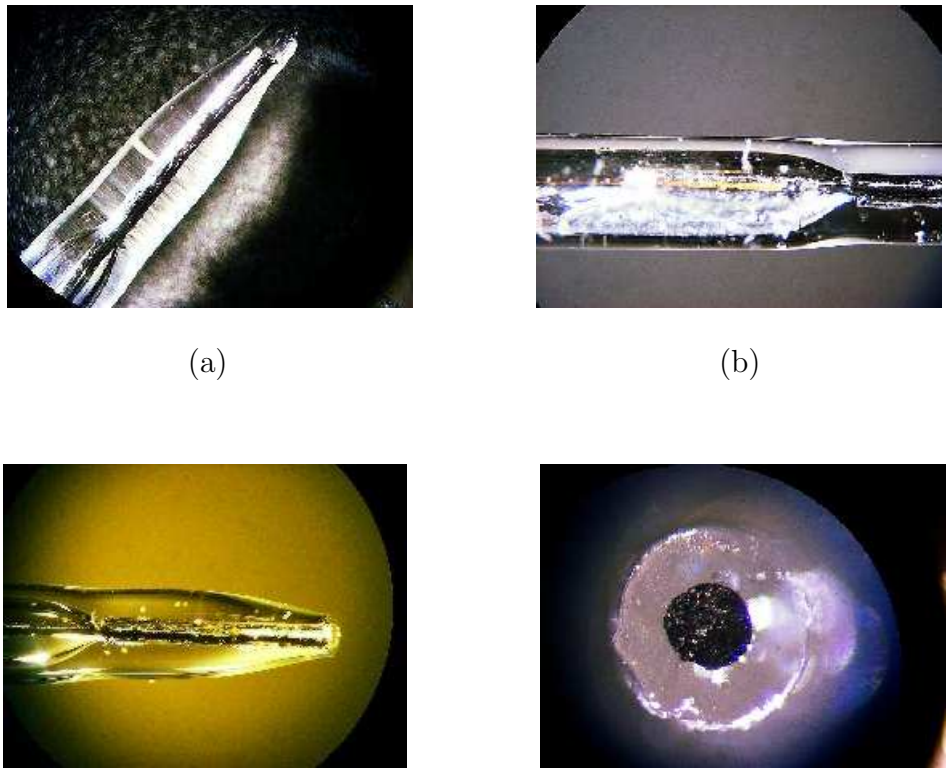

(a) (b)

(c) (d)

Figure 4.18: The production of a working electrode

To allow an electrical connection to the potentiostat, a thin copper wire was inserted into the open end of the glass tube. In contrast to classical methods, zinc and tin solder instead of silver epoxy glue or carbon paste were used to make a good and stable electrical contact between the gold and copper wires (**Figure 4.18b**).

Through its open end, the capillary was first filled with small amounts of very fine zinc powder, subsequently fully covering the internally protruding gold microwire. Next, tiny pieces of crushed tin solder were placed on top of the zinc and slowly heated to melting. The melted solder ensured a good electrical connection between the copper, the zinc powder and the gold wire.

At this stage, the gold disk at the tip of the electrode assembly was not yet exposed, but this was achieved by successively polishing the tip at 90° to the capillary with emery papers of grade 320 to 2000. A smooth, electroactive surface (**Figure 4.18c,d**) was finally established by polishing the glass-insulated gold disk with alumina or diamond paste (of diminishing particle size, from 5 μm down to 3 μm, 1 μm, 0.3 μm, 0.05 μm and 0.01 μm) on a polishing cloth. Between analyses, only 0.3-μm and 0.01-μm paste was used to re-polish the microelectrode. Afterward, the electrode was further rinsed with deionised water in an ultrasonic bath for about two minutes.

The electrodes fabricated in this way are more robust than fibre electrodes and can easily be mechanically polished, which facilitates long-term use.

An improper electrode tip with air entrapped as bubbles in the molten glass is shown in **Figure 4.19**.

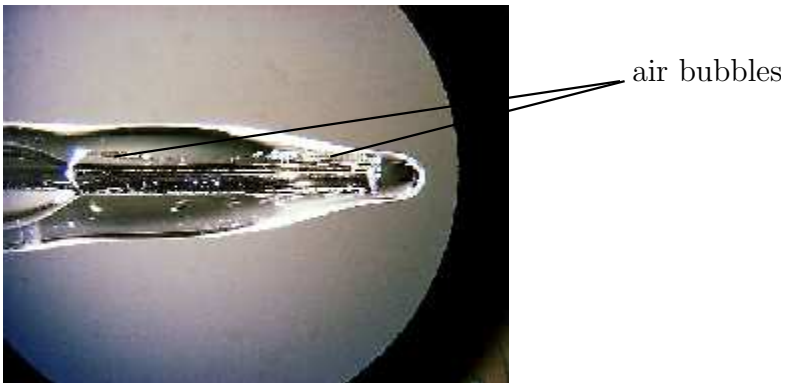

Figure 4.19: An imperfect working electrode containing air bubbles inside the channel

Since a system with electrolyte container and electrode mantle made of glass might be physically and chemically more stable than the one with PVC support, a detection

cell was constructed entirely from glass. The working electrode was bent into a U-shape (**Figure 4.20a**) before being inserted into the capillary-electrode holder (**Figure 4.20b**). However, this design was quickly obsolete, since it performed worse than the PVC-based construction.

(a) (b)

Figure 4.20: The construction of a glass cell

Now the capillary-electrode holder had to be re-fabricated. It still consisted of two small pieces of plexi-glass (10 mm × 20 mm × 3 mm) with a hole of 3 mm at the centre of both pieces. To ensure the alignment of the electrode with the CE capillary, the grooves had to be machined symmetrically on the two plexi-glass plates. The groove for the CE capillary had a diameter of 360 μm, while that for the working electrode was 1.5 mm in diameter. The grooves for the ground and the auxiliary electrode ran from side to side and had an overall diameter of 0.5 mm (**Figure 4.21**).

The PVC tubes were also used to increase the stability of the capillary, the electrodes and the ground. The whole system (**Figure 4.22**) was placed into a vial which was the same as in the previous constructions.

All of the analyses described below were carried out with this third construction.

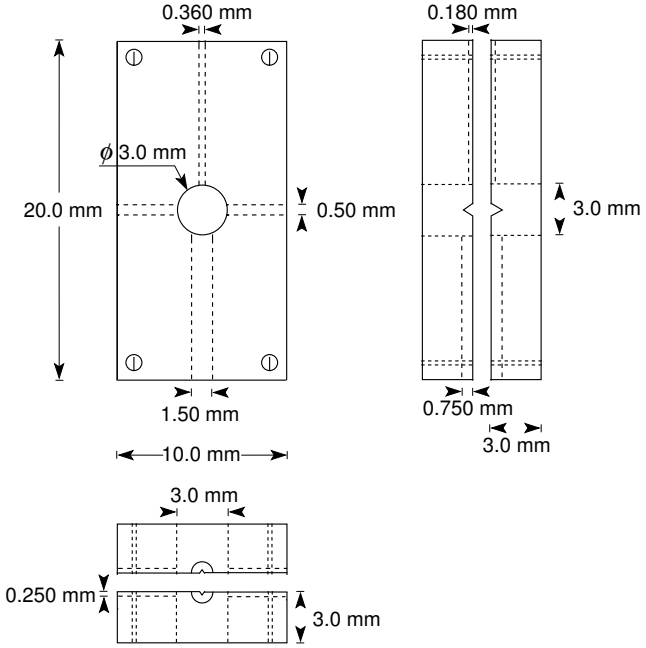

Figure 4.21: The third construction of the capillary-electrode holder

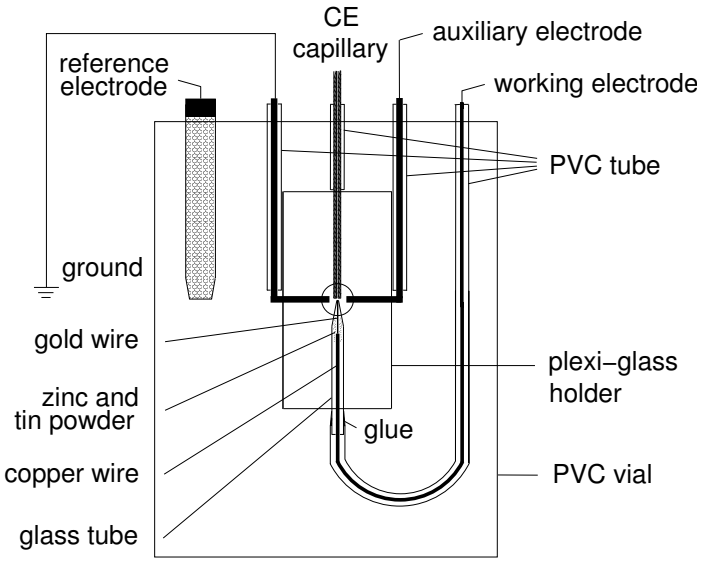

Figure 4.22: The third cell design

4.5.3 Detection conditions

Direct detection of APGs at the gold electrode with a constant potential results in electrode fouling with serious attenuation of the electrode response. However, reproducible detection can be achieved with multi-step potential-time waveforms (E vs. t) consisting of brief applications of detection potential ($E_{det},\ t_{det}$) followed by large positive and negative potential steps to achieve oxidative cleaning ($E_{oxd},\ t_{oxd}$) and reductive reactivation ($E_{red},\ t_{red}$), respectively, of the gold surface. Signal acquisition is by digital integration of electrode current during a fixed integration period (t_{int}) after a brief delay (t_{del}) following application of E_{det}, i.e. $t_{det} = t_{del} + t_{int}$. The potential applied at the working electrode was referenced to that of the Ag/AgCl electrode.

For simplicity, a typical carbohydrate waveform with a gold electrode in preliminary experiments was taken from the instructions of BAS (Bioanalytical Systems, Inc., Warwickshire, UK) for their Epsilon system for an LC-PAD measurement. The required four-step pulse is described in **Table 4.4**.

STEP	**POTENTIAL** (mV)	**DURATION** (mSec)	**FUNCTION**
1	50	400	Equilibration (Delay)
2	50	200	Integration
3	800	200	Oxidative cleaning
4	−600	200	Reductive reactivation

Table 4.4: PAD waveform for sugars

4.5.4 Separation of sugars by CZE

The detection of carbohydrates by PAD at a platinum electrode following HPLC separation was first reported in 1981 by Hughes and Johnson [159]. Since then, this approach has been developed instrumentally and characterised mechanistically,

largely by the Johnson group, and applied extensively by numerous groups to a wide variety of carbohydrate-analysis problems. In the process, PAD has also been employed at gold electrodes, which are now the electrodes of choice for this technique [120]. In recent years, electrochemical detection methods have become increasingly important for the determination of carbohydrate compounds in a variety of biological and pharmaceutical samples [120]. Therefore, before applying this system for analysis of APGs, some simple sugars were used to test whether the developed CE-PAD system worked well.

A 0.1 M NaOH solution was used as electrolyte to ensure the deprotonation of sugars, which would otherwise be uncharged and thus unsuitable for electrophoretic separation and electrochemical detection.

First, glucose was injected into the capillary, and the separation voltage of 15 kV was applied. Only one signal was observed, at around 12.5 minutes, indicating that the system functions well (**Figure 4.23**).

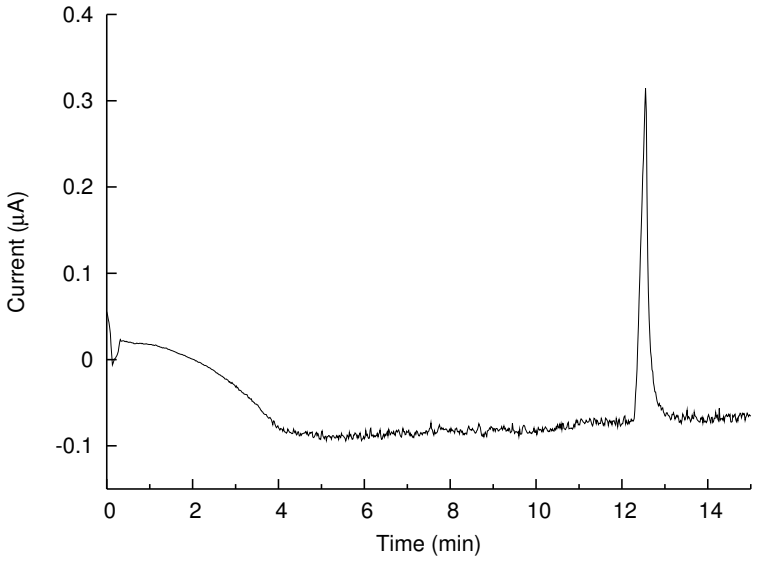

Figure 4.23: Analysis of 1.5 mM glucose; electrolyte: 0.1 M NaOH; voltage: 15 kV

Then a mixture of either glucose and lactose or of glucose and ribose was introduced into the capillary with the applied voltage of 15 kV and 10 kV, respectively. It was evident from the electropherograms (**Figures 4.24** and **B.1**, see Appendix) that these simple sugars could be separated. The higher separation voltage resulted in a less stable baseline but shorter migration times.

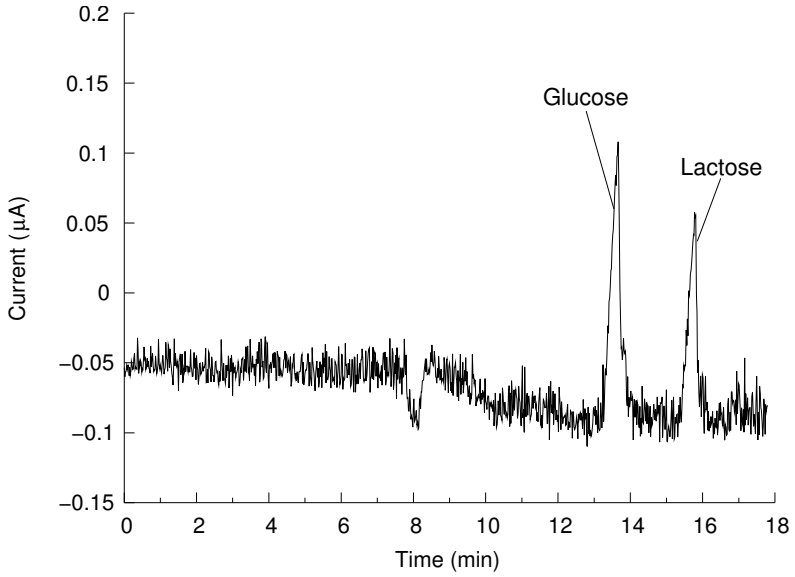

Figure 4.24: Analysis of glucose and lactose, each 1.5 mM; electrolyte: 0.1 M NaOH; voltage: 15 kV

The application of pressure and voltage simultaneously for separation was also tried. It was interesting to see that the baseline was much more stable and the shape of the signals as well as their separation were better than when only voltage was applied (**Figures 4.25** and **B.2**, see Appendix). This could be explained by the fact that the applied pressure shortened the migration time, thereby diminishing the diffusion of the sugars.

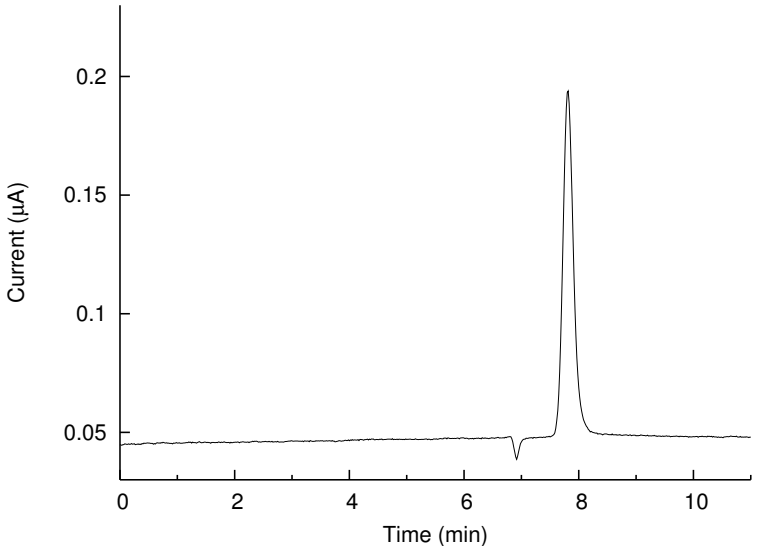

Figure 4.25: Analysis of 1.5 mM glucose; electrolyte: 0.1 M NaOH; application of both pressure and voltage: 1 psi and 5 kV

4.5.5 Separation of APGs by CZE

The same separation and detection conditions were then applied for analysis of APGs. As can be seen in **Figures 4.26** and **4.27**, both C_8-β- and C_{10}-β-D-glucopyran-oside gave quite sharp signals. However, no separation was obtained when a mixture of the two was injected.

The same result was obtained with the mixture of C_8-β- and C_{12}-β-D-glucopyranoside, and even with the sample 7706-1 from Cognis, which contains not only underivatised APGs with different degrees of polymerisation and various alkyl chain lengths (C_{12} and C_{14} APGs) but also their carboxymethyl derivatives (**Figure 4.28**).

Since only the anions can be oxidised at the gold electrode, the pH of the electrolyte was high enough for the dissociation of the hydroxyl groups of sugars and APGs; hence, these analytes could be detected electrochemically. Perhaps, under these conditions, the charge-to-mass ratios of the APG homologues were similar, so that they migrated altogether.

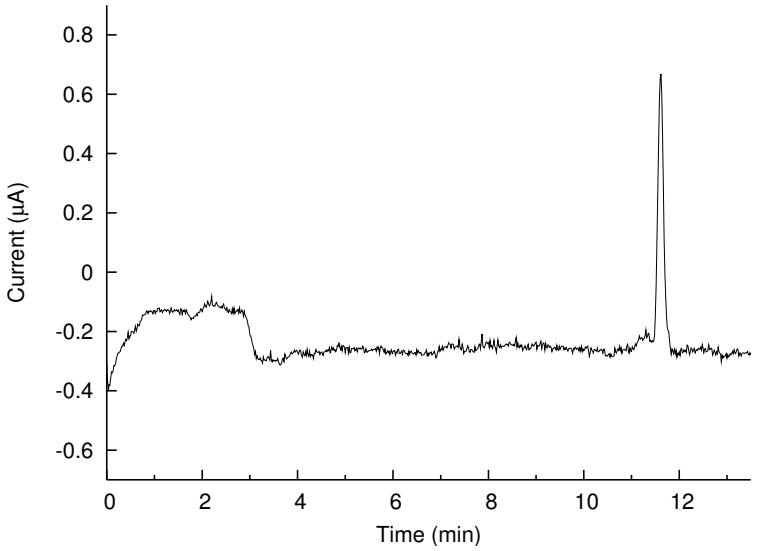

Figure 4.26: Analysis of 1.5 mM C_8-β-D-glucopyranoside; electrolyte: 0.1 M NaOH; voltage: 15 kV

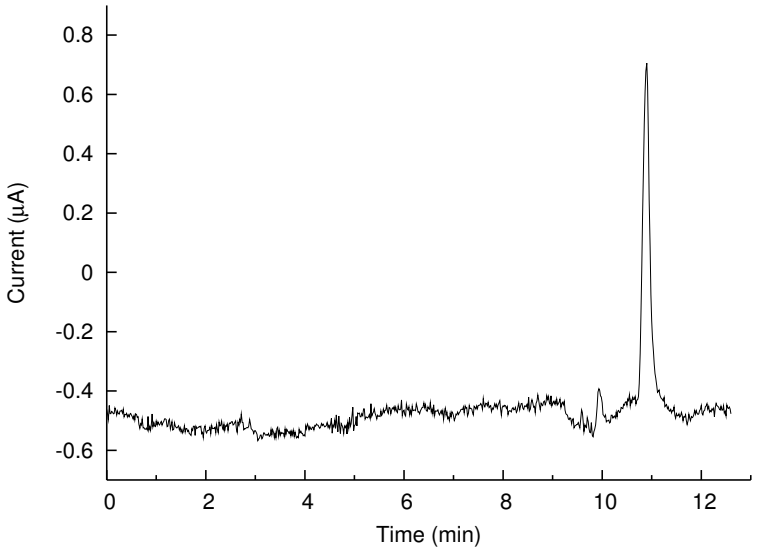

Figure 4.27: Analysis of 1.5 mM C_{10}-β-D-glucopyranoside; electrolyte: 0.1 M NaOH; voltage: 15 kV

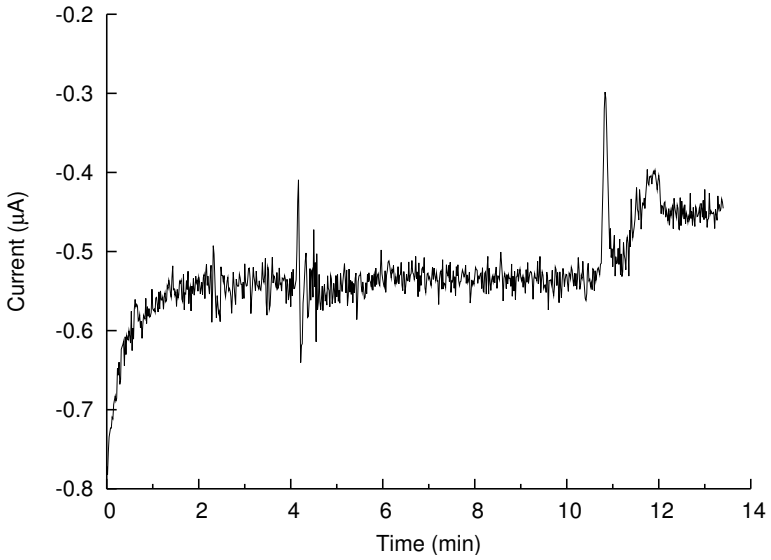

Figure 4.28: Analysis of Cognis sample 7706-1 (1.5 mM); electrolyte: 0.1 M NaOH; voltage: 15 kV

In the next part of this work, MEKC was applied to enhance the separation of APGs.

4.5.6 Separation of sugars by MEKC

In order to enhance the selectivity for APGs, micellar solutions were employed to allow separation of analytes on the basis of their partitioning into the micelles. As a first attempt, glucose was analysed with 0.1 M NaOH electrolyte containing 10 mM SDS (**Figure 4.29**).

A single signal was observed, but the baseline was very unstable. This was in accordance with literature reports that the use of SDS as surfactant in MEKC generally reduces the sensitivity of CE-PAD through electrode fouling or reduced access of the analyte to the electrode surface [112].

At high pH, the sugars as well as the APGs are dissociated. Therefore, neutral

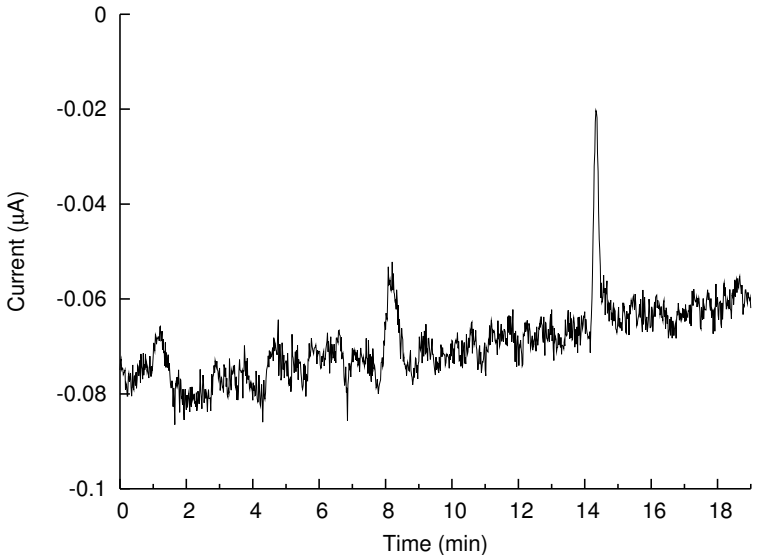

Figure 4.29: Analysis of 1.5 mM glucose; electrolyte: 10 mM SDS in 0.1 M NaOH; voltage: 15 kV

micelles formed by nonionic surfactants, such as Brij 35, could also be used for separation. This surfactant would not only serve to form micelles, but also to generate a dynamic coating on the capillary wall by binding to silanol hydrogen through hydrogen bonding [160, 161]. This in turn would reduce the electroosmotic flow.

In this expectation, Brij 35 was included in the 0.1 M NaOH electrolyte at a concentration of 2500 mg/L. This concentration was chosen on the basis of a reported separation of fatty acids with an electrolyte containing Brij 35 [66].

The disaccharides lactose, melibiose, maltose, lactulose, cellobiose, saccharose and trehalose, each 0.5 mM, were separated fairly well with this electrolyte (**Figure 4.30**).

Another mixture of mono- and disaccharides (glucose, rhamnose, lactose, saccharose, trehalose, ribose and raffinose) could also be separated well under the same conditions (**Figure 4.31**).

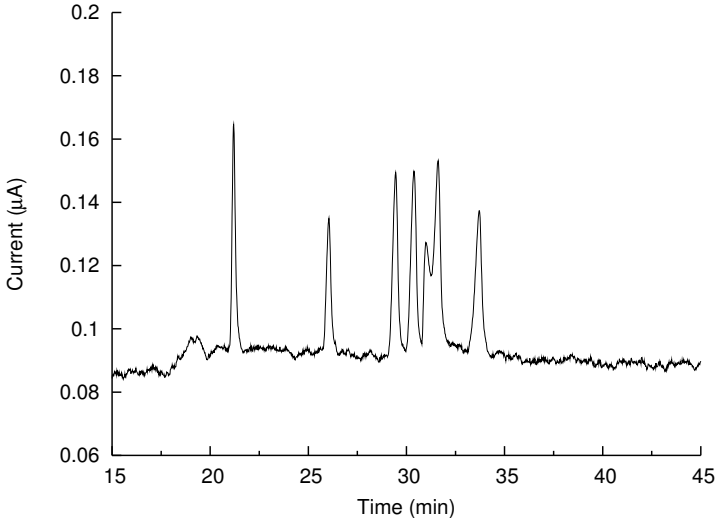

Figure 4.30: Analysis of the mixture of lactose, melibiose, maltose, lactulose, cellobiose, saccharose and trehalose, each 0.5 mM; electrolyte: 2500 mg/L Brij 35 in 0.1 M NaOH; voltage: 8 kV

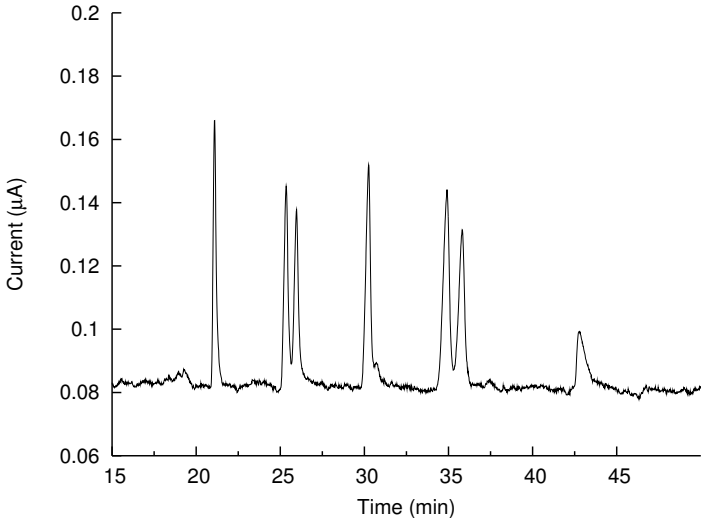

Figure 4.31: Analysis of the mixture of glucose, rhamnose, lactose, saccharose, trehalose, ribose and raffinose, each 0.5 mM; electrolyte: 2500 mg/L Brij 35 in 0.1 M NaOH; voltage: 8 kV

It is interesting that a mixture of isomeric inositols can also be partly resolved with this micelles system, as illustrated in **Figure 4.32**.

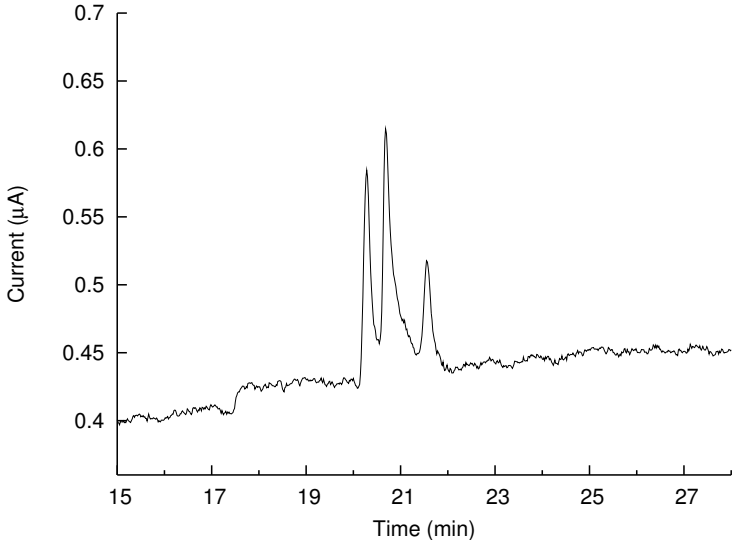

Figure 4.32: Analysis of the mixture of neo-, epi-, myo-, scyllo- and L-chiro-inositols, each 20 μM; electrolyte: 2500 mg/L Brij 35 in 0.1 M NaOH; voltage: 8 kV

4.5.7 Separation of APGs by MEKC

SDS was initially added to the electrolyte to improve the separation. C_8-β- and C_{12}-β-D-glucopyranoside were separated well. However, as in the case of glucose, an unstable baseline was also observed (**Figure 4.33**) with SDS.

With Brij 35 instead of SDS to form the pseudo-stationary phase in the electrolyte (2500 mg/L Brij 35 in 0.1 M NaOH), the C_8-α- and C_8-β-D-glucopyranosides (GP) could be resolved easily (**Figure 4.34**). In addition, 2.5 mM APG 220 (a mixture of C_8-α-, C_8-β-, C_{10}-α- and C_{10}-β-monoglucosides) was analysed satisfactorily with this buffer (**Figure 4.35**).

The order of signals in the electropherogram above was determined by the standard addition method. For example, 1.5 mM C_8-α-D-glucopyranoside was added to 2.5 mM APG 220, as in **Figure 4.36**.

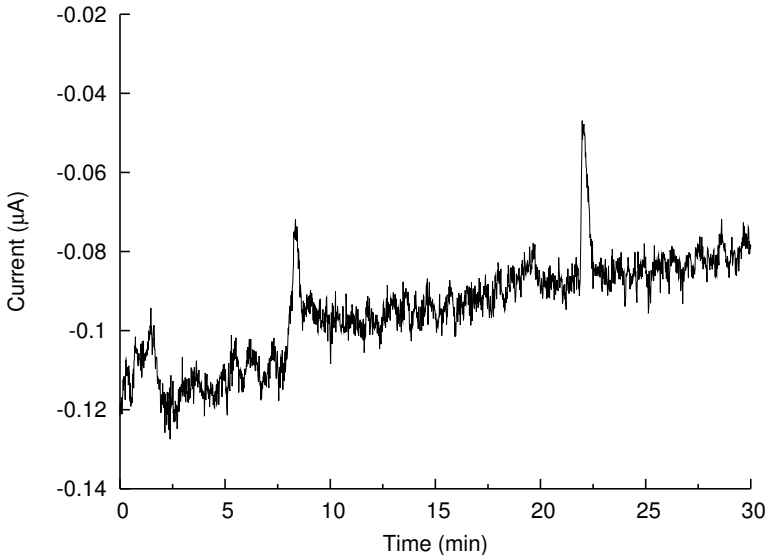

Figure 4.33: Analysis of C_8-β- and C_{12}-β-D-glucopyranoside, each 1.5 mM; electrolyte: 10 mM SDS in 0.1 M NaOH; voltage: 15 kV

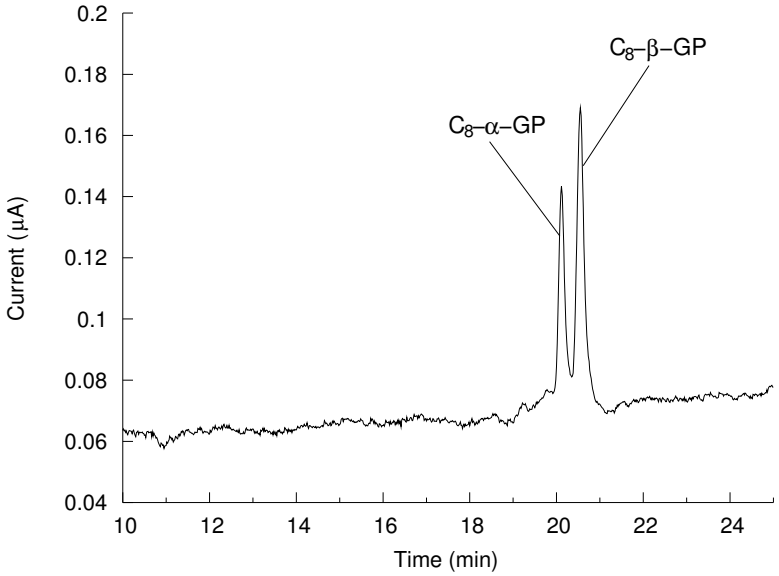

Figure 4.34: Analysis of C_8-α- and C_8-β-D-glucopyranosides, each 1.5 mM; electrolyte: 2500 mg/L Brij 35 in 0.1 M NaOH; voltage: 8 kV

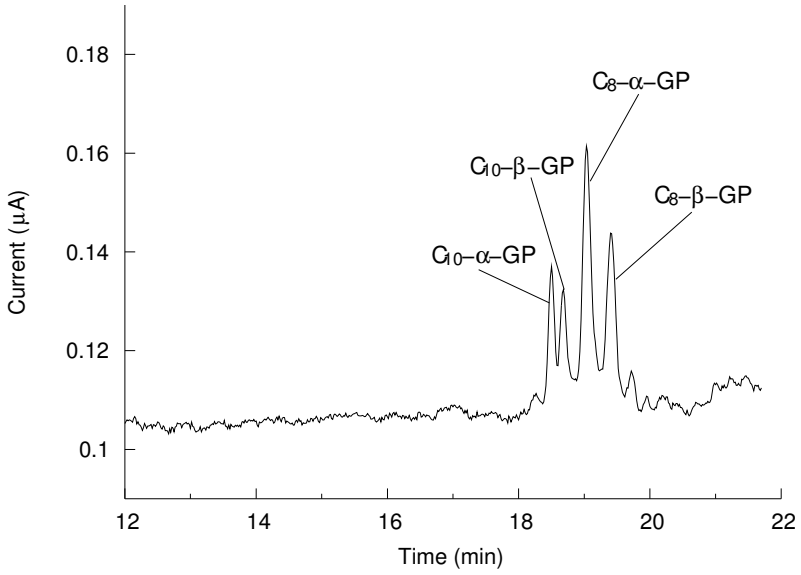

Figure 4.35: Analysis of 2.5 mM APG 220; electrolyte: 2500 mg/L Brij 35 in 0.1 M NaOH; voltage: 8 kV

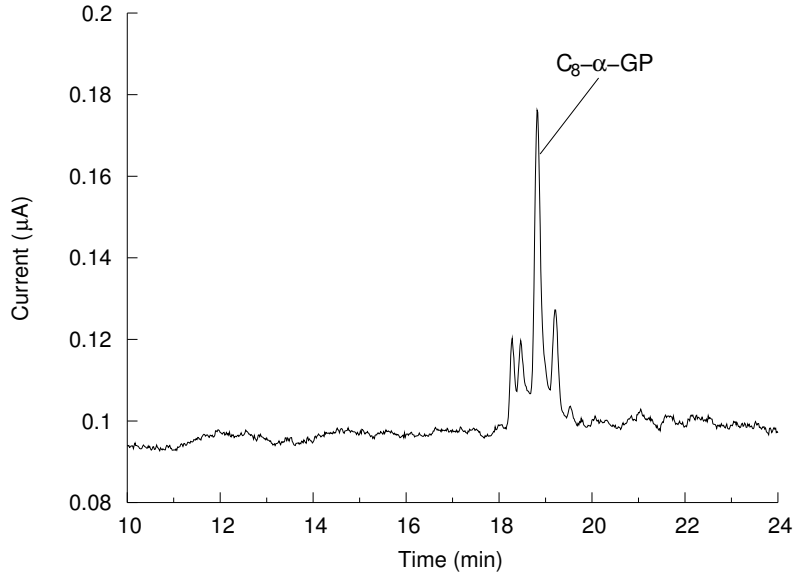

Figure 4.36: Analysis of 2.5 mM APG 220 with added 1.5 mM C_8-α-D-glucopyranoside; electrolyte: 2500 mg/L Brij 35 in 0.1 M NaOH; voltage: 8 kV

Figure 4.37 shows the nearly baseline separation of C_8-α-, C_8-β-, C_{10}-β- and C_{12}-β-D-glucopyranoside standards.

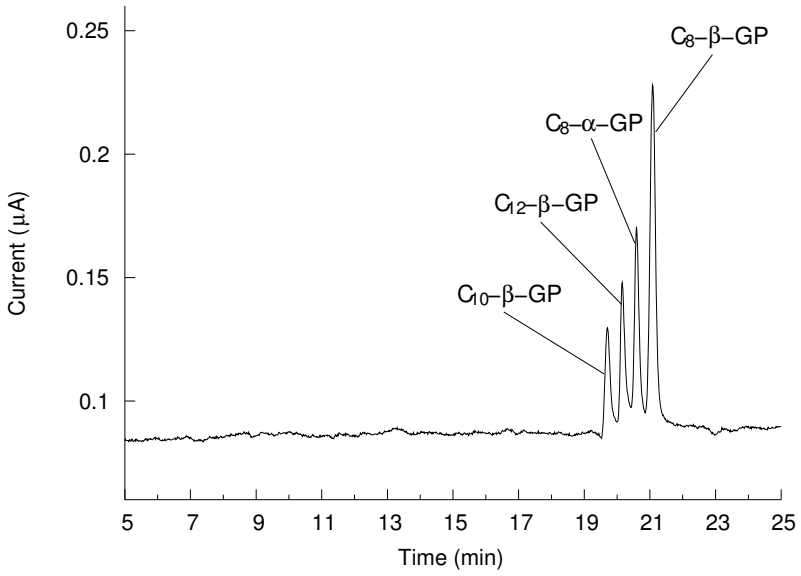

Figure 4.37: Analysis of C_8-α-, C_8-β-, C_{10}-β- and C_{12}-β-D-glucopyranosides, each 0.5 mM; electrolyte: 2500 mg/L Brij 35 in 0.1 M NaOH; voltage: 8 kV

This mixture was spiked with C_{10}-α-D-glucopyranoside, and the electropherogram in **Figure 4.38** was obtained. However, the addition of C_{12}-α-D-glucopyranoside to this spiked mixture gave no additional signal, which means that C_{12}-α- and C_{12}-β-D-glucopyranosides were not being separated.

It was observed that the sequence of signals did not follow the order of polarity of these substances. Here, C_{10} was the first compound eluted, C_8 was the last, and C_{12} was in the middle. The reason is that the separation is based not only on the difference in hydrophobicity of the analytes but also on the formation of hydrogen bonds or the dipole-dipole interactions between the oxygen atoms in the oxyethylene units of Brij 35 and the hydrogen atoms in the hydroxyl groups of APGs.

On the other hand, the mixture of C_{12}-glucopyranoside and its carboxymethyl derivative could be resolved, as shown in **Figure 4.39**.

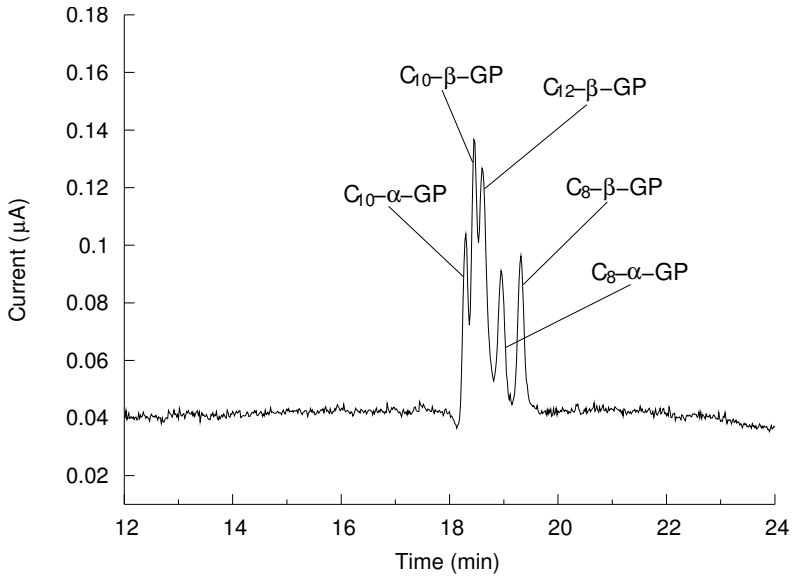

Figure 4.38: Analysis of C_8-α-, C_8-β-, C_{10}-α-, C_{10}-β- and C_{12}-β-D-glucopyranosides, each 0.5 mM; electrolyte: 2500 mg/L Brij 35 in 0.1 M NaOH; voltage: 8 kV

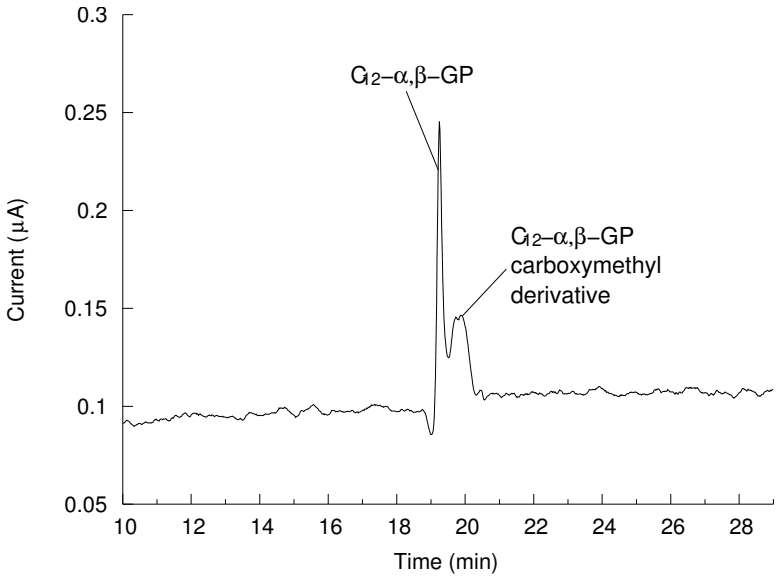

Figure 4.39: Analysis of C_{12}-glucopyranoside and its carboxymethyl derivative, each 3 mM; electrolyte: 2500 mg/L Brij 35 in 0.1 M NaOH; voltage: 8 kV

In summary, by including 2500 mg/L Brij 35 in the 0.1 M NaOH electrolyte, APGs with alkyl chain lengths of 8, 10 and 12 carbons as well as their α- and β-isomers could be resolved (except for the pair of C_{12}-α- and C_{12}-β-D-glucopyranoside). However, APGs with longer alkyl chains (C_{14}) could not be separated from C_{12}, since only a single signal instead of four was obtained from the Cognis samples APG 600 and APG 1200, which contain both C_{12} and C_{14} with α- and β-isomers .

C_{16} and C_{18} APGs were not soluble in the electrolyte used and therefore could not be analysed. However, it was supposed that these APGs would also not be separated from C_{12} and C_{14}.

In the next step, the separation as well as the detection parameters were optimised for this system.

4.5.8 Optimisation of the separation conditions

The capillary

Capillaries from CS Chromatographie Service GmbH (Langerwehe, Germany), from Beckman Coulter (Fullerton, CA, USA) and from Polymicro Technologies (Phoenix, AZ, USA) were compared with regard to their influence on the electrophoretic separation. It was found that the capillary from Polymicro Technologies performed best, so it was used, unless otherwise stated, for all of the successive experiments.

Over the course of several studies, it was observed that the best separation efficiency was obtained with new capillaries. Separation efficiencies decreased after the capillaries had been used for few days, and the peak tailing became more obvious. This may be due to either a change in the properties of the internal wall of the capillaries as a result of interaction between the analyte and the wall or to the high pH of the electrolyte.

The length of the capillary was chosen as 55 cm, which was the minimum distance from the capillary inlet to the external capillary outlet where the separation capillary met the electrodes and was held by the capillary-electrode holder. A longer

separation capillary was avoided lest it result in an unstable baseline, since the external part of the capillary was no longer surrounded by cooling liquid and would be subjected to Joule heating.

Comparison of the membrane filters

Prior to use, the electrolyte solutions were passed through a membrane filter. Two cellulose acetate membrane filters (Sartorius, Goettingen, Germany) with a diameter of 25 mm and pore sizes of 0.45 μm and 0.22 μm were tested. With the 0.45-μm membrane, the baseline was more stable and the separation was better, while with the latter a large drift was always observed. The reason for this observation has not yet been found.

The separation voltage

The mixture of C_8-β-, C_{10}-β- and C_{12}-β-D-glucopyranosides was analysed with separation voltages of 6 kV, 8 kV and 10 kV.

Overall, the baseline was somewhat less stable at the higher separation voltage, possibly because of electrical interference from the applied field. For practical applications, compromises may thus have to be sought.

Also evident from the comparison was the effect of the applied voltage on the appearance of the peaks. The peak heights increased with the applied voltage because of the decrease in diffusion, while the peak areas were identical, indicating that the electrode efficiency was constant.

It was observed that 8 kV resulted in better separation than 10 kV; with 6 kV, the separation was not improved, but the migration time was longer. Therefore, 8 kV was chosen as the most suitable separation potential.

The injection time

Hydrodynamic injection of the sample was achieved by applying 0.5 psi for 3, 5 or 10 seconds.

When the analyte was introduced into the capillary for 3 seconds, a very small signal was obtained, which had a quite low signal-to-noise ratio. This was due to the small injection volume, of ca. 3 nL, which was only 0.3 % of the total capillary volume (ca. 1080 nL for a capillary with 50 μm I.D. and 55 cm length). Therefore, the injection time of 3 seconds might not be long enough.

When an injection time of 5 seconds was used, acceptable signals and separation were observed.

However, if the injection time increased to 10 seconds, the separation was poor; the signals partly overlapped because of overloading of the sample, since the injection volume (ca. 11 nL) now occupied 1 % of the total capillary volume. This was in accordance with the report that band broadening occurs when the injected plug of analyte in the capillary is $\geq$ 1 % of its volume [49].

The separation temperature and sample storage temperature

It was observed that, the higher the temperature, the shorter the migration time. When the temperature increased from 20°C to 25°C, the separation was improved and the signals were more intense. However, at 30°C both the resolution and the baseline became worse. Therefore 25°C was chosen as the most suitable temperature for separation. This separation was also used for storage of the samples in the automatic injector.

The concentration of the NaOH solution

An approach which offers the possibility of fine-tuning the separation of APGs is using the pH of the electrophoresis medium to adjust the net charge on the very weakly acidic hydroxyl groups of the analytes.

NaOH solutions with concentrations of 0.025 M, 0.050 M, 0.075 M, 0.10 M and 0.125 M were tested with a Brij 35 concentration of 2500 mg/L.

Changing the pH of the buffer solution altered the retention times by influencing both the electroosmotic flow and the electrophoretic mobility of the dissociated APGs. The observed migration time was longer with the increased NaOH concentration because the EOF moves in the opposite direction from the analytes.

The separation improved with increasing NaOH concentrations up to 0.10 M, but was poorer again at 0.125 M. Also, with 0.125 M NaOH solution the baseline was not very stable, and the peak shape was bad. Therefore, 0.10 M appeared to be the best NaOH concentration.

The concentration of Brij 35 in NaOH solution

Brij 35 concentrations of 1000, 1500, 2000, 2500 and 3000 mg/L were screened. There was clearly an interaction between the APGs and the micelles of Brij 35, because the change in concentration of Brij influenced both the migration time and the separation of the analytes. The resolution was enhanced, and the baseline was improved with the concentration of Brij 35 up to 2500 mg/L, but was worse with 3000 mg/L.

The organic modifier

The effect of the addition of organic solvents to influence the distribution of the analytes between micelles and electrolyte was also examined. Several organic modifiers (MeOH, ACN, iso-propanol, acetone) were added to the electrolyte at various concentrations (1 % to 10 %). The baseline was very bad except with acetone, which, however, gave no improvement over the case where no modifier was added to the electrolyte.

4.5.9 Separation of APGs with mixed micelles

Other available surfactants (SDS, Tween 20, Tween 80) were screened as single micelles, as their mixture or in mixture with Brij 35.

The mixed micelles of Brij 35 and SDS were found to give the best resolution, and APGs with different alkyl chain lengths could easily be separated. **Figures 4.40** and **4.41** illustrate this. It was interesting that the migration sequence of the APGs was substantially different from that when Brij 35 was used alone. Here, C_8 was eluted first, followed by C_{10} and C_{12}. The reason was probably that the use of SDS alone leads to the separation of APGs merely according to their different hydrophobicities, whilst the interaction of APGs with Brij micelles is based additionally on the formation of hydrogen bonds or dipole-dipole interactions.

The α- and β-isomers could still not be well resolved, even though their sequence was also different from that of the previously used micelles system. With these mixed micelles, the β-isomer always reached the detector before the α-isomer.

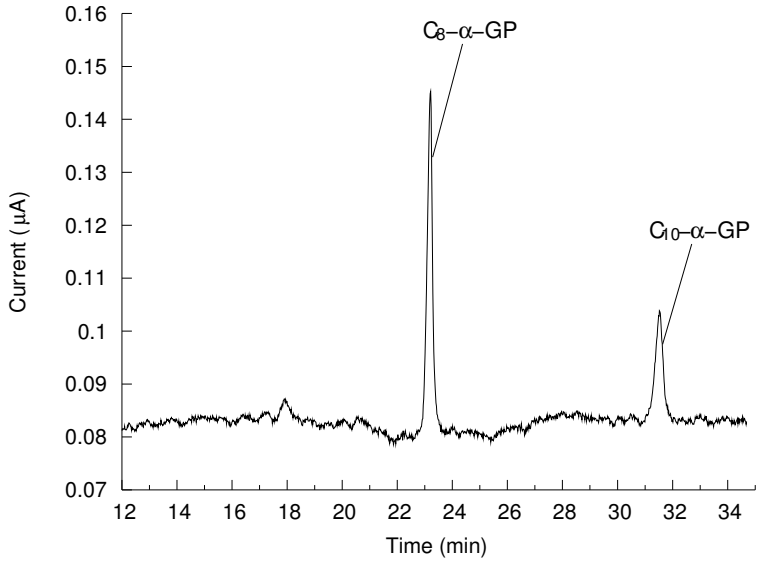

Figure 4.40: Analysis of C_8-α- and C_{10}-α-D-glucopyranoside, each 0.8 mM; electrolyte: 2500 mg/L Brij 35 and 5 mM SDS in 0.1 M NaOH; voltage: 8 kV

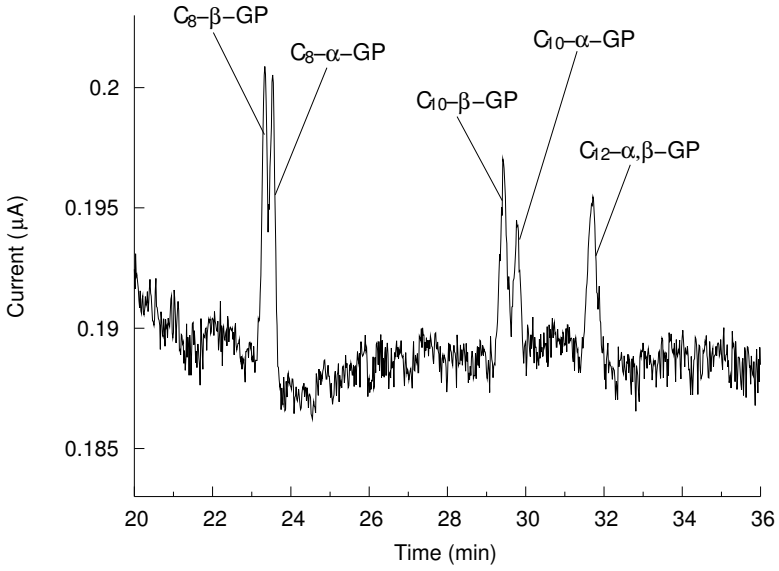

Figure 4.41: Analysis of C_8-α-, C_8-β-, C_{10}-α-, C_{10}-β-, C_{12}-α- and C_{12}-β-D-glucopyranoside, each 0.25 mM; electrolyte: 2500 mg/L Brij 35 and 5 mM SDS in 0.1 M NaOH; voltage: 8 kV

4.5.10 Screening of various micelles systems

A range of surfactants were obtained from Cognis. These all have structures close to that of Brij in containing a $C_{12/14}$ fatty alcohol attached to a number of ethylene oxide and/or propylene oxide units. However, only half of these surfactants could be studied in our system, since the others were not soluble in 0.1 M NaOH, as shown in **Table 4.5**.

The best result was found with the mixture of Dehydol LS 30 (D30) and Dehydol LS 50 (D50) at a ratio of 1:1. With D30+D50, each 1250 mg/L, in 0.1 M NaOH as electrolyte, APG 220 can be separated a bit better than with Brij 35 as micelles builder (**Figure 4.42**). The sequence of signals was the same as that from the Brij 35 micelles system.

Name	Composition	Solubility in NaOH
Dehydol LS 4N	$C_{12/14}$-fatty alcohol + $(EO)_4$	No
Dehydol LS 6	$C_{12/14}$-fatty alcohol + $(EO)_6$	Yes
Dehydol LS 10	$C_{12/14}$-fatty alcohol + $(EO)_{10}$	Yes
Dehydol LS 16	$C_{12/14}$-fatty alcohol + $(EO)_{16}$	Yes
Dehydol LS 30	$C_{12/14}$-fatty alcohol + $(EO)_{30}$	Yes
Dehydol LS 50	$C_{12/14}$-fatty alcohol + $(EO)_{50}$	Yes
Dehypon LS 36	$C_{12/14}$-fatty alcohol + $(EO)_3$ + $(PO)_6$	No
Dehypon LS 45	$C_{12/14}$-fatty alcohol + $(EO)_4$ + $(PO)_5$	No
Dehypon LS 54	$C_{12/14}$-fatty alcohol + $(EO)_5$ + $(PO)_4$	No
Lorol $C_{12/14}$ 10-PO	$C_{12/14}$-fatty alcohol + $(PO)_{10}$	No

EO : ethylene oxide

PO : propylene oxide

e.g. Dehypon LS 36 :

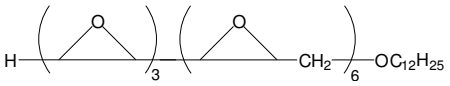

Table 4.5: The new surfactants from Cognis

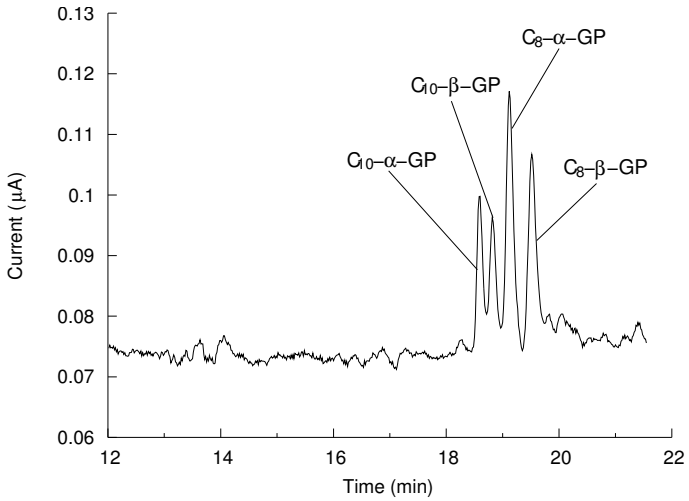

Figure 4.42: Analysis of 2.5 mM APG 220; electrolyte: Dehydol LS 30 and Dehydol LS 50, each 1250 mg/L in 0.1 M NaOH; voltage: 8 kV

With a capillary of smaller I.D. (25 μm), the baseline was more stable, but no improvement in the separation was obtained (**Figure 4.43**).

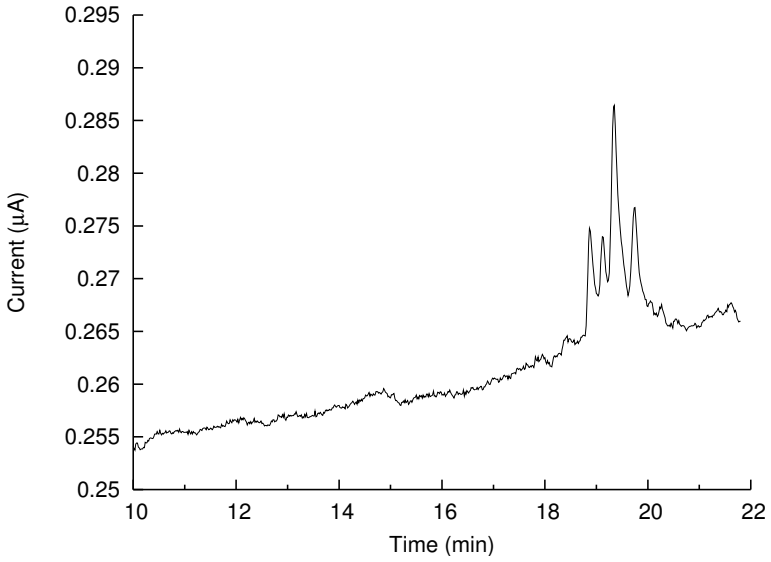

Figure 4.43: Analysis of 2.5 mM APG 220; electrolyte: Dehydol LS 30 and Dehydol LS 50, each 1250 mg/L in 0.1 M NaOH; 25-μm-ID capillary; voltage: 8 kV

With this mixed-micelles system, C_{12}-glucopyranoside and its carboxymethyl derivative could also be separated (**Figure 4.44**).

In addition, the mixture of C_8-α-, C_8-β-, C_{10}-α-, C_{10}-β-, C_{12}-α- and C_{12}-β-D-glucopyranoside could be resolved better than they were with Brij 35 alone (**Figure 4.45**). However, even here C_{12}-α- and C_{12}-β-D-glucopyranoside could still not be separated.

Since the mixture of D30 and D50 (1:1) gave the most successful separation, we predicted that D40, with intermediate properties, would also give satisfactory separation and an even more stable baseline, because of the simpler micelles system. Therefore, Cognis produced D40 to meet our special requirement.

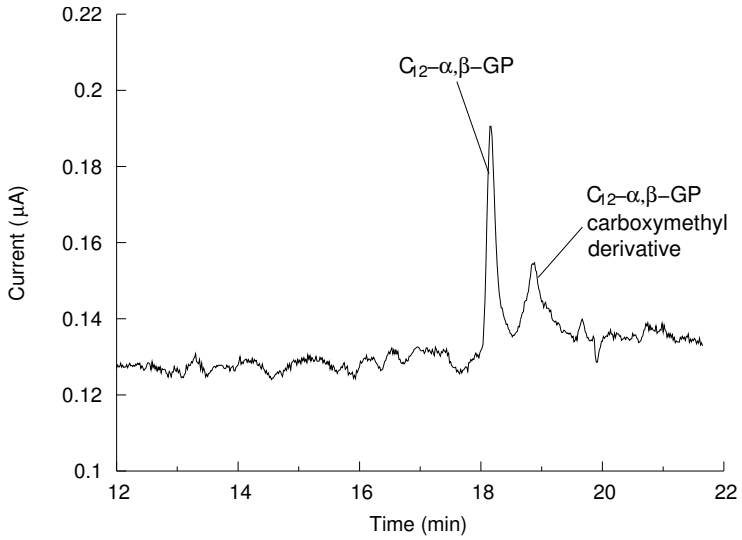

Figure 4.44: Analysis of C_{12}-glucopyranoside and its carboxymethyl derivative, each 1.5 mM; electrolyte: Dehydol LS 30 and Dehydol LS 50, each 1250 mg/L in 0.1 M NaOH; voltage: 8 kV

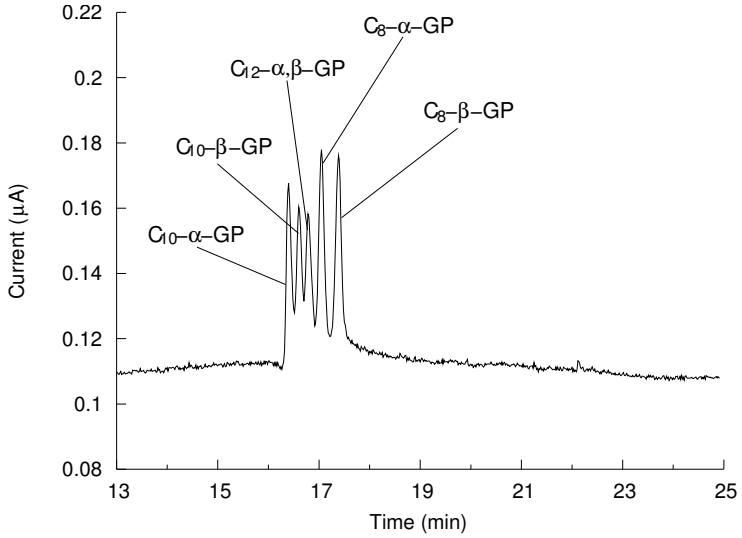

Figure 4.45: Analysis of C_8-α-, C_8-β-, C_{10}-α-, C_{10}-β-, C_{12}-α- and C_{12}-β-D-glucopyranoside, each 0.5 mM; electrolyte: Dehydol LS 30 and Dehydol LS 50, each 1250 mg/L in 0.1 M NaOH; voltage: 8 kV

As a result, separation of C_8-α-, C_8-β-, C_{10}-α-, C_{10}-β-, C_{12}-α- and C_{12}-β-D-glucopyra-noside was indeed improved (better resolution and more stable baseline), even though the analysis time was longer (**Figure 4.46**). This system, however, still failed to separate C_{12}-α- and C_{12}-β-D-glucopyranoside.

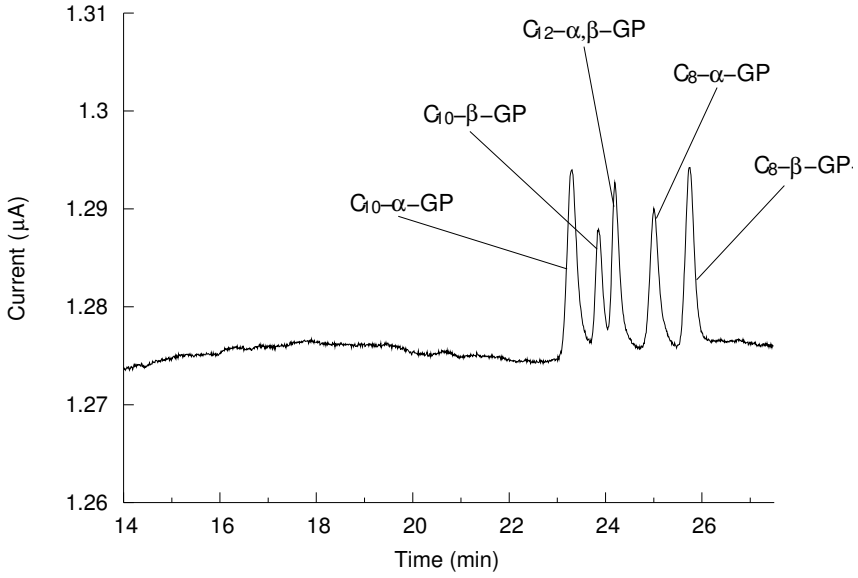

Figure 4.46: Analysis of C_8-α-, C_8-β-, C_{10}-α-, C_{10}-β-, C_{12}-α- and C_{12}-β-D-glucopyranoside, each 0.25 mM; electrolyte: Dehydol LS 40 2500 mg/L in 0.1 M NaOH; voltage: 8 kV

Furthermore, various concentrations of NaOH (0.05 M, 0.15 M and 0.2 M) in the new electrolyte were again compared to see their influence on the separation as well as on the migration time of analytes. The observations are shown in **Figures 4.47** and **4.48**. It was clear that higher concentrations of base improved resolution and also increased the migration time. However, Joule heating was a problem at higher concentrations of the electrolyte (0.2 M); this resulted in a very unstable baseline and poor efficiency because of band broadening.

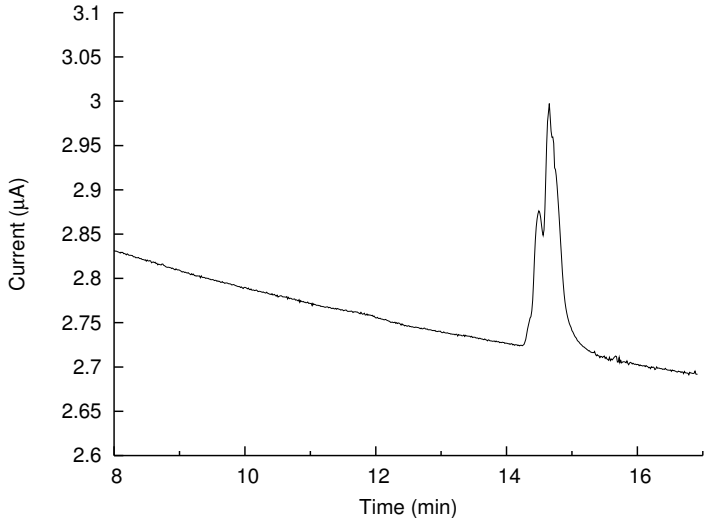

Figure 4.47: Analysis of C_8-α-, C_8-β-, C_{10}-α-, C_{10}-β-, C_{12}-α- and C_{12}-β-D-glucopyranoside, each 0.25 mM; electrolyte: Dehydol LS 40 2500 mg/L in 0.05 M NaOH; voltage: 8 kV

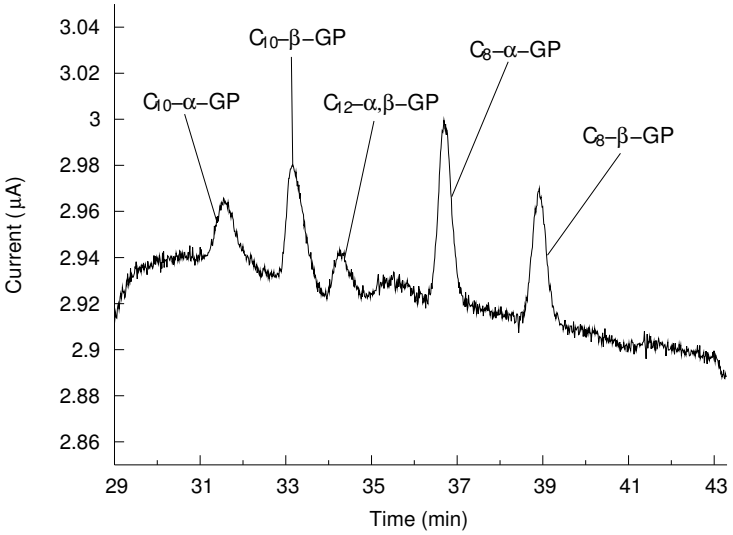

Figure 4.48: Analysis of C_8-α-, C_8-β-, C_{10}-α-, C_{10}-β-, C_{12}-α- and C_{12}-β-D-glucopyranoside, each 0.25 mM; electrolyte: Dehydol LS 40 2500 mg/L in 0.2 M NaOH; voltage: 8 kV

4.5.11 Optimisation of the detection parameters

Optimisation of E_{det}, t_{del} and t_{int} in the PAD waveform

The potential applied to the working electrode is the most important parameter in PAD. It can be compared to setting the detector wavelength in a UV detector. Determination of the optimum potential is normally carried out with an electrochemical technique called hydrodynamic voltammetry. This technique is performed by continuously moving a solution containing the analyte and supporting electrolyte past the surface of the working electrode in an amperometry cell. The measured current is plotted versus potential. Voltammetry can be accomplished in a standard beaker-type cell with a rotating disk electrode. This kind of electrode was, however, not available. Therefore, the plot of peak height versus potential was obtained by the alternative approach of making multiple injections of APGs and increasing the potential after each injection. This was done after the separation conditions had been optimised.

By varying the potential at the working electrode (E_{det}) from -600 to 300 mV in increments of 50 mV and keeping the potential-time waveform as $t_{del} = 400\ ms$, $t_{int} = 200\ ms$, $E_{oxd} = 800mV$ ($t_{oxd} = 100\ ms$) and $E_{red} = -600mV$ ($t_{red} = 100\ ms$), it was shown that the response increased as the potential increased up to 200 mV. However, no further increase in response was obtained on going to 250 mV at the working electrode, and when 300 mV was applied no signal at all was obtained.

It appears that, between the potentials of 150 and 200 mV, 100 % of the analyte reaching the surface of the working electrode is oxidised, so that the current in that range is no longer a linear function of the potential. Increasing the potential beyond this value can increase only the noise and not the signal and must also decrease the selectivity by allowing more species to be oxidised.

Fine tuning from 140 to 210 mV in 10 mV increments gave a maximum signal-to-noise ratio (S/N) at 170 mV. This potential probably gives maximum response for APGs and minimum noise (little or no O_2 reduction or oxide formation). This potential was then chosen as the optimum value for further detection of APGs.

Typically, PAD waveforms have a frequency (f) of ca. 1 Hz [162]

$$f = \frac{1}{t_{del} + t_{int} + t_{oxd} + t_{red}}$$

where f is the frequency, t_{del} the delay time, t_{int} the integration time, t_{oxd} the oxidative cleaning time and t_{red} the reductive reactivation time.

The optimum value of t_{del} was determined by making repeated injections while increasing the delay time from 0 ms to 600 ms. For any value $t_{del} > 20$ ms, a significant response was obtained. Of more importance was the observation that the S/N has a maximum value at $t_{del} = 400$ ms, both the background noise and baseline drift being worse for the shorter value of t_{del}. The delay time of $t_{del} = 400$ ms was thought to be sufficient to allow the charging current to diminish toward zero.

To discriminate against the high-frequency noise originating from the alternating-current (a.c.) power supply (which operates at 50 Hz in Europe and at 60 Hz in the US), values of t_{int} should be chosen to correspond to an integer multiple (n) of 20 ms (1/50 Hz^{-1}) or of 16.7 ms (1/60 Hz^{-1}) [163]. Therefore, the t_{int} values of 200, 400, 600 and 800 ms were tested. Despite the fact that PAD sensitivity increased with increasing t_{int} [101], no further increase in S/N was observed with t_{int} longer than 200 ms. This was probably the result of electrode fouling that can occur for large t_{int} in conjunction with insufficient oxidative cleaning. However, we did not want to increase both t_{int} and t_{oxd} because the resulting decrease in frequency f decreases the definition of very sharp CE peaks [101]. Hence, the t_{int} value of 200 ms was also chosen as optimal in our case.

Optimisation of E_{oxd} and t_{oxd}

The potential $E_{oxd} = 300$ mV was indicated by LaCourse and Johnson [162] as sufficient to evoke oxidative cleaning of the gold electrode surface. At lower potential, the once-clean electrode becomes progressively fouled by the detection products because there is no surface oxide formed while the PAD waveform is being applied.

The rate of oxidative surface cleaning might be accelerated at large values of E_{oxd} where vigorous evolution of O_2 can occur [164]. The value $E_{oxd} > 800$ mV, however, may result in formation of O_2 bubbles which can adhere to the electrode surface and thereby interfere with the transport of analyte to the electrode [162]. $E_{oxd} = 800\ mV$ was thus chosen as optimal potential for oxidative cleaning.

The oxidative cleaning time (t_{oxd}) was scanned from 10 to 400 ms. The S/N increased with the t_{oxd} up to 100 ms, but no further improvement was observed with longer cleaning time. Therefore, 100 ms was sufficient for efficient oxidative cleaning of the electrode surface.

Optimisation of the E_{red} and t_{red}

The surface oxide formed during application of E_{oxd} in the PAD waveform quickly results in loss of electrode response for APGs. Hence, it is essential that the values of E_{red} and t_{red} be chosen to achieve complete reductive dissolution of the surface oxide.

The response was constant for $E_{red} = -800$ to $100\ mV$; therefore, any value in this range was sufficient to dissolve the surface oxide formed at E_{oxd}. At $E_{red} \geq 200\ mV$, reductive dissolution of the surface oxide did not occur, and APG response was terminated. The choice of $E_{red} = -600\ mV$ was based on published kinetic data indicating this potential to be sufficient for rapid oxide reduction [165].

The dependence of peak signals on the variation of t_{red} over the range $50 - 450\ ms$ was investigated. It was apparent that an appreciable increase in the signal occurred as t_{red} increased from 50 to $100\ ms$; however, the change in peak signal was more gradual when t_{red} increased to values $> 100\ ms$. Whereas increases in t_{red} give greater assurance that the surface oxide is being reduced during reductive surface reactivation, the longer delay period can also increase peak signals by allowing more time for the diffusion layer to be replenished with analyte from the bulk solution, which increases the electrode current during the subsequent detection period. On the basis of these data, the optimal minimal value for t_{red} was chosen as $100\ ms$.

Comparison of gold working electrodes of two dimensions

The 300 μm disk electrode performed stably.

When the 25-μm electrode was tested, almost no signal was obtained. It is possible that the position of such a small electrode is simply too difficult to adjust.

4.5.12 Optimal conditions

Analyses were best with 55-cm lengths of fused-silica capillaries (Polymicro Technologies) of 50 μm I.D. and 360 μm O.D. and with an applied voltage of 8 kV. Both the separation temperature and the sample storage temperature were 25°C. The best electrophoresis medium was 0.1 M NaOH containing 2500 mg/L Dehydol LS 40. Sample injection was carried out hydrodynamically at 0.5 psi for 5 seconds. All solutions introduced into the reservoirs were filtered through a 0.45-μm membrane.

Detection was achieved with the PAD waveform designated as $E_{det} = 170\ mV$ ($t_{del} = 400\ ms$, $t_{int} = 200\ ms$), $E_{oxd} = 800\ mV$ ($t_{oxd} = 100\ ms$) and $E_{red} = -600\ mV$ ($t_{red} = 100\ ms$).

4.5.13 Quantitative analysis

Calibration line

The calibration lines of C_8-α-, C_8-β- and C_{10}-β-D-glucopyranoside were established with five concentrations. For all three standards, the peak area was linearly proportional to concentrations from 0.3 mM up to 1.5 mM, as shown in **Figure 4.49**. The correlation coefficients (R^2) all are larger than 0.99, which is sometimes considered an indication of acceptable fit of the data to the regression line [166].

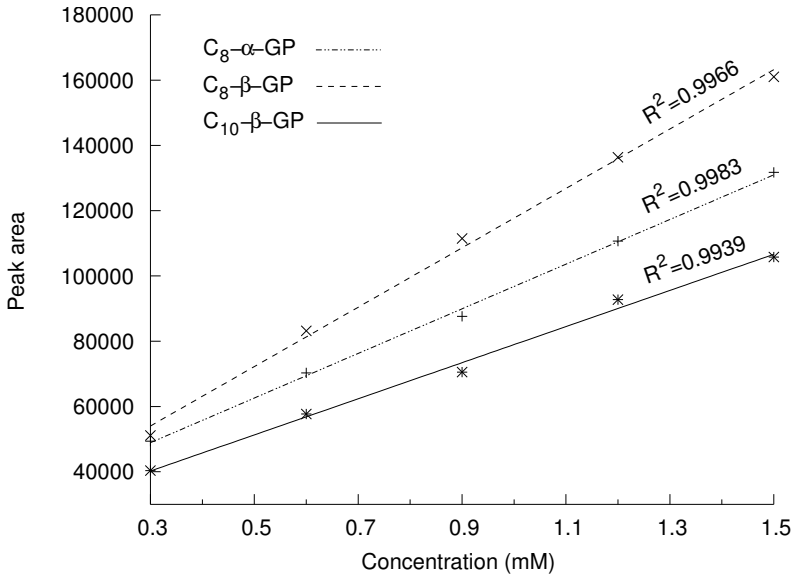

Figure 4.49: Calibration lines of C_8-α-, C_8-β- and C_{10}-β-D-glucopyranoside

Furthermore, the quality coefficient (QC), which characterises the quality of the fit of the data to the straight line calibration model, was calculated as [166]:

$$QC = \sqrt{\frac{\sum \left(\frac{\widehat{y}_i - y_i}{\bar{y}}\right)^2}{n-1}} \times 100\ \%$$

where $\widehat{y}_i$ represents the response for standard i predicted by the model, y_i the response measured for standard i, $\bar{y}$ the mean of the measured responses and n the number of data points.

The smaller the quality coefficient, the better the experimental points fit the line [166]. The quality coefficients for C_8-α-, C_8-β- and C_{10}-β-D-glucopyranoside were found to be 1.5 %, 2.3 % and 2.8 %, respectively. These values can be considered acceptable with all three standards.

Standard addition method

The amount of each component in the sample APG 220 was determined in two spiked samples, with different concentrations of C_8-α-, C_8-β-, C_{10}-α- and C_{10}-β-D-glucopyranoside (0.5 mM and 1 mM) being added to the 2 mM APG 220 sample. Both the fortified samples and the sample APG 220 itself were analysed in triplicate.

The amount of each component was calculated as [167]:

$$C_X = \frac{A_1 C_S V_S}{A_2 (V_S + V_X) - A_1 V_X}$$

where C_X represents the unknown amount of that component in the initial sample (g), V_X and A_1 the volume (mL) and peak area of this sample, respectively, C_S the amount of standard spiked to the initial sample (g), V_S the volume of the added standard solution (mL) and A_2 the peak area obtained from the fortified sample.

The percentages of C_8-α-, C_8-β-, C_{10}-α- and C_{10}-β-D-glucopyranoside in sample APG 220 were found to be 26.6 %, 15.0 %, 13.6 % and 10.8 %, respectively. This was in accordance with the results found by Cognis by gas chromatography-mass spectroscopy (GC-MS) [168].

4.6 Analysis of a commercial product

The baby-shampoo "Sanft" (Siegelsbach, Germany) could be analysed without any derivatisation prior to injection. Instead, 10 mg shampoo was simply diluted in 1.5 mL of 0.1 M NaOH solution. This shampoo could be partially separated, as shown in **Figure 4.50**. The sequence of signals from C_8-β-, C_{10}-α- and C_{10}-β-D-glucopyranoside was determined by the standard-addition method. The APGs with longer alkyl chains, from C_{12} to C_{16}, were all eluted together at around 31 minutes. The signal at 35.2 minutes has not yet been assigned.

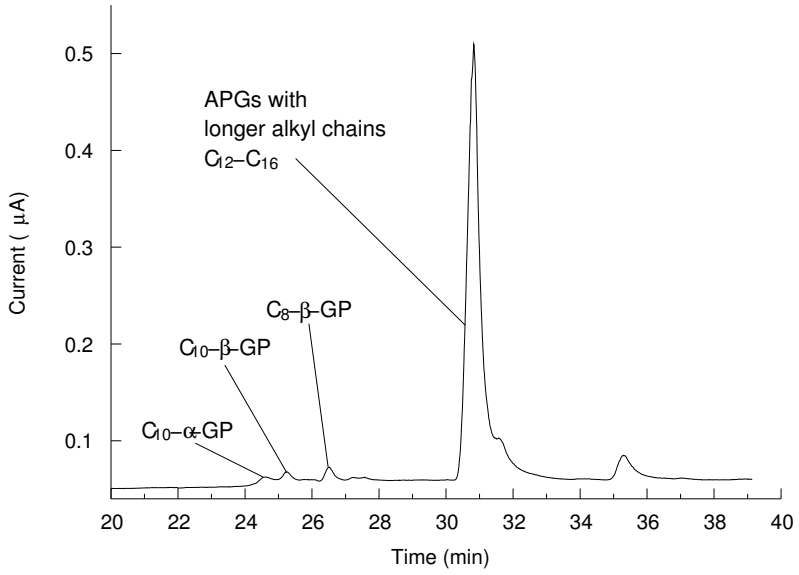

Figure 4.50: Analysis of baby-shampoo "Sanft", 10 mg diluted in 1.5 mL of 0.1 M NaOH solution; electrolyte: Dehydol LS 40 2500 mg/L in 0.1 M NaOH; voltage: 8 kV

4.7 Another application

The determination of noradrenaline, L-dopa and ascorbic acid by amperometric detection at constant potential with platinum as working electrode [169] was carried out on our system. This was to test whether our detection cell is stable and applicable for analysis of various electro-active compounds other than sugars and APGs. Such compounds may, for example, require the use of other materials for the working electrode.

Separations were performed on 55-cm fused-silica capillaries (Polymicro Technologies) with 50 μm I.D. and 360 μm O.D and with an applied voltage of 12 kV. The buffer was 20 mM borate at pH 9.3. Electrophoretic injection of the sample was carried out at a voltage of 10 kV for 10 seconds. The microcylindrical platinum working electrode was fabricated in the same manner as the gold electrode, and the 250-μm platinum wire was also sealed into the borosilicate glass tubes. The constant potential applied at this working electrode was 1 V.

In the separation buffer used, noradrenaline was cationic, L-dopa was neutral and ascorbic acid was anionic [169]. This resulted in excellent separation, as shown in **Figure 4.51**. The very stable baseline indicated that the detection system hardly disturbed by the surrounding electronic devices.

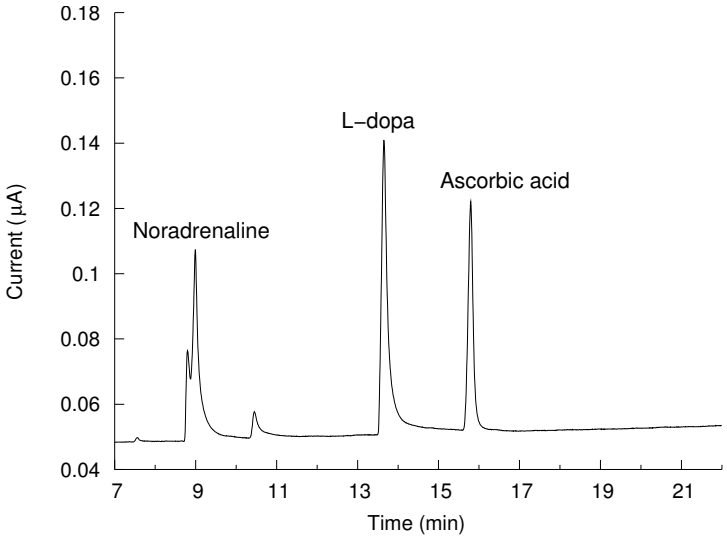

Figure 4.51: Analysis of 1 mM noradrenaline, 2 mM L-dopa and 5 mM ascorbic acid; electrolyte: 20 mM borate, pH 9.3; voltage: 12 kV

The calibration lines of these analytes were constructed. The peak area was found to be linear in the concentration range of 0.2 to 5 mM for noradrenaline ($R^2 = 0.9998$), 1.2 to 10 mM for L-dopa ($R^2 = 0.999$) and 3 to 25 mM for ascorbic acid ($R^2 = 0.9927$). These are illustrated in **Figures C.1, C.2** and **C.3** (see Appendix). The quality coefficient values were found to be 1.4 %, 3.2 % and 11.3 %, respectively. The last one was considerably higher than the others because of the broader concentration range, but these values could still be considered acceptable [166].

Chapter 5

Summary

In this work, a CE method was developed for analysis of APGs. Two detection methods were examined, namely UV and amperometric detection.

First, indirect UV detection was applied with the addition of micelles or charged cyclodextrins or with the use of highly alkaline electrolyte to make it possible to separate the APGs. Then the direct detection approach was tested, with the formation of borate complexes with the APGs; such negatively charged complexes not only allow direct UV detection but can also migrate electrophoretically and thus be separated from the neutral components. However, unsatisfactory results were obtained with both direct and indirect UV detection.

Secondly, pulsed amperometric detection (PAD) following micellar electrokinetic chromatography (MEKC) was applied successfully to the direct detection of APGs without prior conversion to highly absorbent or fluorescent derivatives.

A highly alkaline electrolyte, an 0.1 M NaOH solution, was used to ionise the hydroxyl groups of these compounds. The resulting negatively charged species are necessary for sensitive detection as well as for differential electromigration of these analytes. The separation was enhanced by the inclusion of Dehydol® LS 40 (polyethylene glycol ether from Cognis Deutschland GmbH) as surfactant in the background electrolyte in order to form micelles. The analytes were then separated on the basis of the differences in both electrophoretic mobility and phase distribution.

The main problems associated with the combination of electrochemical detection and CE are the need for isolating the electrochemical detector from the voltage source used in the CE separation and the difficulty of aligning the working electrode with the end of the capillary. To overcome these problems, a simple capillary-electrode holder was constructed in this work. The electrical grounding of this holder decouples the CE and PAD systems and thus precludes the requirement for incorporating an opening in the capillary prior to the PAD. This holder also automatically aligns the capillary and the electrode in a wall-jet configuration without the aid of micropositioners. The design facilitates the exchange of electrodes and capillaries without reconstruction of the entire capillary-electrode setup.

Special microcylindrical gold electrodes were produced by sealing 300-μm-diameter gold wires into borosilicate-glass tubes. To avoid poisoning of the gold working electrode by oxidation of the APGs in the amperometric detection at constant potential (ADCP) mode, the PAD technique was used. With PAD, the applied potential is accompanied by pulsed steps at extreme positive and negative potentials to clean the electrode and activate its surface.

Both the separation and the detection parameters were optimised. The optimal conditions were as follow:

- Separation is carried out with 55-cm lengths of fused-silica capillaries (Polymicro Technologies) of 50 μm I.D. and 360 μm O.D. and at an applied voltage of 8 kV; both the separation temperature and the sample storage temperature are 25°C; the electrophoresis medium is 0.1 M NaOH containing 2500 mg/L Dehydol® LS 40; samples are injected hydrodynamically at 0.5 psi for 5 seconds; all solutions introduced into the reservoirs are filtered through a 0.45-μm membrane.
- Detection is achieved with the PAD waveform designated as $E_{det} = 170\ mV$ ($t_{del} = 400\ ms$, $t_{int} = 200\ ms$), $E_{oxd} = 800\ mV$ ($t_{oxd} = 100\ ms$) and $E_{red} = -600\ mV$ ($t_{red} = 100\ ms$). The potential applied at the working electrode is referenced to that of an Ag/AgCl electrode.

Under these conditions, APGs with different alkyl chain lengths C_8, C_{10} and C_{12}, including α- and β-isomers, could be baseline separated. Calibration lines of C_8-α-, C_8-β- and C_{10}-β-D-glucopyranoside were established. For all three standards, the peak area was linearly proportional to concentrations from 0.3 mM up to 1.5 mM.

Chapter 6

Experimental

6.1 Apparatus

The CE-EC system is shown in **Figure 6.1**.

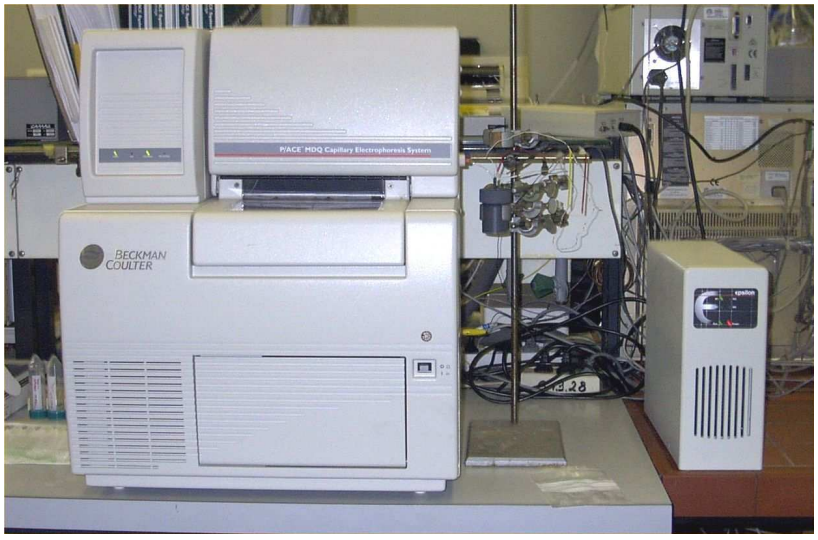

Figure 6.1: The CE-EC system

Between the CE system (left side) and the electrochemical detector (right side) is the home-made detection cell mounted on a stand. The cell is magnified in **Figure 6.2**.

Figure 6.2: The detection cell

The following instruments and materials were used in this work

Electrophoresis system	P/ACE^{TM} MDQ capillary electrophoresis system, Beckman Coulter, München; Diode array detector; 32 Karat^{TM} software, version 5.0 (2002), Beckman Coulter, München
Fused-silica capillaries	CS Chromatographie Service GmbH, Langerwehe Polymicro Technologies (Phoenix, AZ, USA) Beckman Coulter, (Fullerton, CA, USA)

Amperometric detector	Epsilon^{TM}, Bioanalytical Systems, Inc., Warwickshire, UK ChromGraph software
Gold wire 99.99 % insulated by PTFE	Goodfellow, Huntingdon, UK
Platinum wire 99.998 %	Goodfellow, Huntingdon, UK
Reference electrode	RE-6, Bioanalytical Systems, Inc.
Auxiliary electrode	MW-4130, Bioanalytical Systems, Inc.
NMR-instrument	Bruker AR 400 ^{1}H-NMR 400 MHz ^{13}C-NMR 100 MHz
Alumina and diamond paste	Leco, St. Joseph, MI, USA
Polishing cloth red	Heraeus Kulzer, Wehrheim/Ts.
Borosilicate glass tubes	Hilgenberg, Malsfeld
Microtorch	Kager GB-2001
RP-18 F_{254s} TLC plates	Merck, Darmstadt
Silica-gel F_{254} TLC plates	Merck, Darmstadt
Vortexer	REAX 2000, Heidolph, Schwabach
Analytical balance	M2P, Sartorius, Göttingen
Transferpetten®	Brand, Wertheim
pH-Meter	Beckman ϕ350, Beckman Coulter, München
pH-Standard electrode	511275-AB, Beckman Coulter, München

6.2 Chemical list

(-)-Adenosine 5'-monophosphate monohydrate	Sigma, Steinheim
2-Hydroxy-3-trimethylammonoiapropyl-β-cyclodextrin	Wacker-Chemie, München
4-Octylbenzenesulfonic acid, sodium salt	Aldrich, Steinheim
Acetone	Carl Roth, Karlsruhe
Acetonitrile, HPLC gradient grade	Acros organics, Geel, Belgium
Boric acid	Merck, Darmstadt
Brij 35 (Polyoxyethylenlaurylether)	Merck, Darmstadt
Carboxymethyl β-cyclodextrin	In house
Cholic acid sodium salt	Acros organics, Geel, Belgium
Conjugated linoleic acid	Sigma, Steinheim
D-Trehalose	Serva, Heidelberg
D-Xylose	Serva, Heidelberg
D(-)-Fructose	Merck, Darmstadt
D(-)-Ribose	Merck, Darmstadt
D(+)-Cellobiose	Fluka, Buchs
D(+)-Galactose	Fluka, Buchs
D(+)-Glucose anhydrous	Merck, Darmstadt
D(+)-Lactose monohydrate	Fluka, Buchs
D(+)-Maltose monohydrate	Fluka, Buchs
D(+)-Mannose	Fluka, Buchs
D(+)-Melibiose	Fluka, Buchs

D(+)-Raffinose pentahydrate	Fluka, Buchs
di-Sodium hydrogen phosphate	Merck, Darmstadt
di-Sodium tetraborate decahydrate	Merck, Darmstadt
Dodecylbenzenesulfonic acid, sodium salt	Aldrich, Steinheim
Ethyl p-aminobenzoate	Sigma, Steinheim
Fluorescein, sodium salt	Fluka, Buchs
Glycine benzyl ester toluene-4-sulfonate	Fluka, Buchs
Highly sulfated α-cyclodextrins	Beckman Coulter, CA, USA
Highly sulfated β-cyclodextrins	Beckman Coulter, CA, USA
Hydrochloric acid 37 %	Merck, Darmstadt
neo-, epi-, myo-, scyllo-, L-chiro-Inositols	Department of Biochemistry
L-Ascorbic acid, sodium salt	Aldrich, Steinheim
L-Dopa	Fluka, Buchs
L-Noradrenaline	Fluka, Buchs
L(+)-Rhamnose monohydrate	Fluka, Buchs
Lactulose	Fluka, Buchs
Methanol-d_4 (CD_3OD)	Merck, Darmstadt
Methanol, HPLC grade	Carl Roth, Karlsruhe
n-Decyl α-D-glucopyranoside	Sigma, Steinheim
n-Decyl β-D-glucopyranoside	Sigma, Steinheim
n-Dodecyl α-D-glucopyranoside	Sigma, Steinheim
n-Dodecyl β-D-glucopyranoside	Sigma, Steinheim
n-Dodecyl β-D-maltoside	Sigma, Steinheim
n-Octyl α-D-glucopyranoside	Sigma, Steinheim
n-Octyl β-D-glucopyranoside	Sigma, Steinheim

n-Tetradecyl β-D-maltoside	Sigma, Steinheim
Potassium hydroxide pellets	Merck, Darmstadt
Propanol-2	Fisher Chemicals, Leics, UK
Saccharose	Merck, Darmstadt
Sodium chloride	Carl Roth, Karlsruhe
Sodium dihydrogen phosphate dihydrate	Merck, Darmstadt
Sodium hydroxide pellets	Merck, Darmstadt
Sodiumdodecyl sulfate	Merck, Darmstadt
Sorbic acid	Sigma, Steinheim
Sulfuric acid	Merck, Darmstadt
Taurocholic acid sodium salt hydrate	Fluka, Buchs
Trichloromethane	Carl Roth, Karlsruhe
Tridest. water	BU Wuppertal
Tris(hydroxymethyl)aminomethane hydrochloride	Fluka, Buchs
Tween® 20	Fluka, Buchs
Tween® 80	Fluka, Buchs

6.3 Preparation of solutions

6.3.1 Phosphate solution

The phosphate buffer at a concentration of 10 mM, pH 6.8, was made by first preparing 10 mM NaH_2PO_4 and 10 mM Na_2HPO_4. Then, one solution was slowly added to the other until the desired pH is reached, as determined by a pH meter.

6.3.2 APG solution

The mixture of APGs was dissolved in ca. 200 μL methanol in a 1.5-mL Eppendorf cap. An N_2 jet was used to evaporate the methanol, leaving a precipitate on the wall of the cap. The precipitate was then dissolved in an appropriate electrolyte prior to injection. Without being dissolved first in methanol, mixtures of APGs can not be dissolved directly in the aqueous electrolyte. A clear solution could not be obtained if only one APG was dissolved in methanol; at least two APGs should be used. The reason for this observation could be the formation of mixed micelles between APGs to enable them to dissolve in the electrolyte; or it could be the superiority in solubility of mixtures relative to the pure compound because of the difficulty of the former in forming crystals.

6.3.3 NaOH solution

The NaOH solution must be prepared fresh each day, since this solution quickly absorbs CO_2 from the air.

6.4 Nuclear magnetic resonance spectroscopy

Since C_{12}-β-D-glucopyranoside is soluble in MeOH but not in H_2O, CD_3OD was used instead of D_2O; 50 mg C_{12}-β-D-glucopyranoside were dissolved in 1.5 mL CD_3OD.

The basic solution of C_{12}-β-D-glucopyranoside was prepared by dissolving 50 mg of this analyte in 1.5 mL of 1 M NaOH in CD_3OD.

6.5 The electrodes

6.5.1 Reference electrode

The RE-6 reference electrode from BAS (Bioanalytical Systems, Inc., Warwickshire, UK) was used. This compact electrode has a 6-mm-OD glass body and a length of 30 mm. It uses a ceramic frit as porous junction and consists of a silver wire coated with silver chloride and immersed in a 3 M NaCl gel. The silver wire terminates in a 1.524-mm OD gold-plated connecting pin mounted on the end of a length of flexible plastic-coated wire. Connection to this electrode was made with a 1.524-mm gold-plated female connector.

At the end of each day, the electrode was stored by immersing the porous tip in a 3 M NaCl solution (a solution with the same chloride concentration as the filling solution) to extend its lifetime. Once wet, the tip must remain so, to prevent damage to the frit.

6.5.2 Auxiliary electrode

The MW-4130 auxiliary electrode from BAS (Bioanalytical Systems, Inc., Warwickshire, UK) was used. It comprises a 0.5-mm-diameter platinum wire with a length of 60 mm. The platinum wire terminates in a gold-plated brass connector. Electrical connection to this pin was made by a 1.016-mm gold-plated connector.

6.5.3 Ground

The ground initially used was simply a copper wire with 1-mm O.D., covered by an insulated layer.
Whenever bubbles were observed in the detection cell, the baseline was very unstable. A closer look at all the electrodes revealed that the gas originated at this

ground. This means that the copper wire was also taking part in the electrochemical reaction.

For this reason, for the rest of the analyses, 0.5-mm-O.D. platinum wire was used instead. This gave a more stable baseline and no bubbles in the detection cell.

6.6 Separation conditions

6.6.1 Experiments with a UV detector

Experiments were performed with 50-μm-I.D., 360-μm-O.D. fused-silica capillaries (CS Chromatographie Service GmbH, Langerwehe, Germany) with a total length of 60 cm and a length to the detector of 50 cm. Injections were performed hydrodynamically by applying 0.5 psi for 5 seconds (2.5 psi×s). Both sample storage and separation temperature were 25°C. The separation voltage was 25 kV. The buffers were filtered through a 0.45 μm porous filter before use.

New capillaries were conditioned by first rinsing with 1 M NaOH for 15 minutes followed by 1 M HCl, again 1 M NaOH, each for 15 minutes, then distilled water for 5 minutes and buffer for 10 minutes. Finally, the separation voltage of 8 kV was applied for 2 minutes with both inlet and outlet reservoirs containing run buffer. Afterward, the capillary was ready for use.

6.6.2 Experiments with a PAD detector

The hydrodynamic injection was 2.5 psi×s, the temperature was 25°C and the separation voltage was 8 kV.

Separations were performed on fused-silica capillaries from CS Chromatographie Service GmbH (Langerwehe, Germany), from Beckman Coulter (Fullerton, CA, USA) and from Polymicro Technologies (Phoenix, AZ, USA). They all had I.D. of 50 μm,

O.D. of 360 μm and lengths of 55 cm. The capillary was cut to the desired length and to as high a degree of flatness as possible with a capillary cutter.

The electrolyte solutions were passed through a membrane filter of 0.45-μm pore size. Before use, the filtered solutions were degassed by sonication in an ultrasonic bath.

Newly installed capillaries were initially flushed with 0.1 M NaOH for 30 minutes, followed by water and run buffer for 10 minutes each. On subsequent days, capillaries were flushed 10 minutes each with NaOH, water, and run buffer. After capillary flushing, the cell reservoirs were rinsed with water, and the working electrode was installed through the detection end to form a capillary-wall-jet configuration.

6.7 Troubleshooting

It should be noted that the detector sometimes shut down automatically. There were several possible reasons for this problem:

- The buffer was not well filtered.
- The capillary was blocked or its end was damaged by the long-time-storage in NaOH solution.
- The working electrode was not well polished.
- The auxiliary electrode was oxidised, so that the platinum wire became black.
- The ground was not well connected.
- The reference electrode was damaged by long storage in NaOH solution, which gave rise to an incorrect potential applied to this electrode. If this potential was too high, the platinum wires used as ground and auxiliary electrode would take part in the electrochemical reaction. This reaction released oxygen, and as a result bubbles were formed in the detection cell. This led to an unstable baseline.

- The ChromGraph software still had some bugs: some methods altered automatically and a new method had to be written.

Bibliography

[1] K. Hill, W. Rybinski, and G. Stoll, editors, *Alkyl Polyglycosides: Technology, Properties and Applications*, VCH Verlagsgesellschaft mbH, Weinheim, Germany, 1997.

[2] D. Balzer and H. Lüders, editors, *Nonionic surfactants: Alkyl Polyglucosides*, Marcel Dekker, Inc., New York, USA, 2000.

[3] R. Spilker, B. Menzebach, U. Schneider, and I. Venn, Analytik von Alkylpolyglucosiden, *Tenside Surf. Det.* **33 (1)** (1996) 21-25.

[4] N. Buschman and S. Wodarczak, Analytical methods for alkylpolyglucosides. Part I: Colorimetric determination, *Tenside Surf. Det.* **32 (4)** (1995) 336-339.

[5] H. S. Klaffke, T. Neubert, and L. W. Kroh, Analysis of alkyl polyglycosides using liquid chromatographic methods, *Tenside Surf. Det.* **35 (2)** (1998) 108-111.

[6] P. Billian, W. Hock, R. Doetzer, H. J. Stan, and W. Dreher, Isolation of n-decyl-$\alpha(1\rightarrow6)$ isomaltoside from a technical APG mixture and its identification by the parallel use of LC-MS and NMR spectroscopy, *Anal. Chem.* **72** (2000) 4973-4978.

[7] P. Eichhorn and T. P. Knepper, Investigations on the metabolism of alkyl polyglucosides and their occurrence in waste water by means of LC-ES-MS, *J. Chromatogr. A* **854** (1999) 221-232.

[8] B. Capon, Mechanism in carbohydrate chemistry, *Chem. Rev.* **69 (4)** (1969) 407-498.

[9] C. T. Bishop and F. P. Cooper, Glycosidation of sugars. II. Methanolysis of D-xylose, D-arabinose, D-lyxose, and D-ribose, *Can. J. Chem.* **41** (1963) 2743-2758.

[10] V. Smirnyagin and C. T. Bishop, Glycosidation of sugars. IV. Methanolysis of D-glucose, D-galactose, and D-mannose, *Can. J. Chem.* **46** (1968) 3085-3090.

[11] H. Paulsen, Advances in selective chemical syntheses of complex oligosaccharides, *Angew. Chem. Int. Ed. Engl.* **21** (1982) 155-224.

[12] R. R. Schmidt, New methods for the synthesis of glycosides and oligosaccharides - Are there alternatives to the Koenigs-Knorr method?, *Angew. Chem. Int. Ed. Engl.* **25** (1986) 212-235.

[13] W. J. De Grip and P. H. M. Bovee-Geurts, Synthesis and properties of alkylglucosides with mild detergent action: improved synthesis and purification of β-1-octyl-, -nonyl-, and -decyl-glucose. Synthesis of β-1-undecylglucose and β-1-dodecylmaltose., *Chem. Phys. Lipids* **23** (1979) 321-325.

[14] P. Rosevear, T. VanAken, J. Baxter, and S. Ferguson-Miller, Alkyl glycoside detergents: a simpler synthesis and their effects on kinetic and physical properties of cytochrome C oxidase, *Biochemistry* **19** (1980) 4108-4115.

[15] P. Landauer, K.-P. Ruess, and M. Liefländer, Modulation of acetylcholinesterase activity by glycoside-detergents and their solubilization efficiency for neuronal membranes from bovine nucleus caudatus, *Biochem. Biophys. Res. Commun.* **106** (1982) 848-855.

[16] D. E. Koeltzow, Improved yields in the synthesis of alkyl glycosides, *J. Carbohydr. Chem.* **4** (1985) 125-128.

[17] J. F. W. Keana and R. B. Roman, Improved synthesis of n-octyl-beta-D-glucoside: a nonionic detergent of considerable potential in membrane biochemistry, *Membr. Biochem.* **1** (1978) 323-327.

[18] N. Weber and H. Benning, Synthesis of alkyl β-glycosides, *Chem. Phys. Lipids* **31** (1982) 325-329.

[19] V. Vill, Th. Böcker, J. Thiem, and F. Fischer, Studies on liquid-crystalline glycosides, *Liq. Cryst.* **6** (1989) 349-356.

[20] J. Banoub and D. R. Bundle, Stannic tetrachloride catalysed glycosylation of 8-ethoxycarbonyloctanol by cellobiose, lactose, and maltose octaacetates; synthesis of α- and β-glycosidic linkages, *Can. J. Chem.* **57** (1979) 2085-2090.

[21] Z.-J. Li, L.-N. Cai, and M.-S. Cai, Studies on glycosides. X. An alternate method for highly stereoselective synthesis of alkyl-β-D-glucopyranosides, *Synth. Commun.* **22** (1992) 2121-2124.

[22] B. Focher, G. Savelli, and G. Torri, Neutral and ionic alkylglucopyranosides. Synthesis, characterization and properties, *Chem. Phys. Lipids* **53** (1990) 141-155.

[23] W. Klotz and R. R. Schmidt, Anomeric *O*-alkylation of *O*-unprotected hexoses and pentoses - Convenient synthesis of decyl, benzyl, and allyl glycosides, *Liebigs Ann. Chem.* (1993) 683-690.

[24] R. R. Schmidt, A. Oftring, G. Oetter, W. Klotz, and C. Schmidt, Neue Typen oberflächenaktiver Substanzen durch direkte anomere O-Alkylierung, in *Proc. 4th World Surfact. Congr. in Barcelona*, volume 1, pages 593–604, Royal Society of Chemistry, Cambridge, U.K., 1996.

[25] G. Wolf, A. Oftring, G. Oetter, R. R. Schmidt, and W. Klotz, PCT Int. WO 93/21197 to BASF AG, 1993.

[26] E. N. Vulfson, R. Patel, and B. A. Law, Alkyl-β-glucoside synthesis in a water-organic two-phase system, *Biotechnol. Lett.* **12** (1990) 397-402.

[27] Z. Chahid, D. Montet, M. Pina, and J. Graille, Effect of water activity on enzymatic synthesis of alkylglycosides, *Biotechnol. Lett.* **14** (1992) 281-284.

[28] H. Shinoyama, K. Takei, A. Ando, T. Fujii, M. Sasaki, Y. Doi and T. Yasui, Enzymatic synthesis of useful alkyl β-glucosides, *Agric. Biol. Chem.* **55** (1991) 1679-1681.

[29] P. T. Schulz, Principles of technical synthesis of alkyl glucosides, in *Proc. BACS Symp.*, volume 91, pages 33–37, Satton, England, 1991.

[30] M. Biermann, K. Schmid, and P. Schulz, Alkylpolyglucoside - Technologie und Eigenschaften, *Starch/Stärke* **45** (1993) 281-288.

[31] K. Hill and M. Weuthen, Alkylglucoside - Tenside aus Zucker und Pflanzenöl, *Spektrum der Wissenschaft* **Juni** (1994) 113-114.

[32] C. D. Roth, K. B. Moser, and W. A. Bomball, Eur. Patent EP 35.589 to A. E. Staley Mfg. Co., 1980.

[33] H. Lüder, Eur. Patent EP 253.996 to Hüls AG, 1987.

[34] P. M. McCurry, Henkel Corporation, unpublished results.

[35] L. F. Tietze, K. Böge, and V. Vill, Liquid-crystalline D-glucose dialkyl acetals and dodecyl D-glucofuranosides, *Chem. Ber.* **127** (1994) 1065-1068.

[36] S. Matsumura, K. Imai, S. Yoshikawa, K. Kawada, and T. Uchibori, Surface activities, biodegradability and antimicrobial properties of n-alkyl glucosides, mannosides and galactosides, *J. Am. Oil Chem. Soc.* **67 (12)** (1990) 996-1001.

[37] A. J. J. Straathof, H. van Bekkum, and A. P. G. Kieboom, Efficient preparation of octyl α-D-glucopyranoside monohydrate: a recirculation procedure involving water removal by product crystallisation, *Starch/Stärke* **40 (6)** (1988) 229-234.

[38] A. J. J. Straathof, J. Romein, F. van Rantwijk, A. P. G. Kieboom, and H. van Bekkum, Preparation of long-chain alkyl D-glucosides by alcoholysis of 1,2:5,6-di-O-isopropylidene-α-D-glucofuranose, *Starch/Stärke* **39 (10)** (1987) 362-368.

[39] M. Biermann, K. Hill, W. Wüst, R. Eskuchen, J. Wollmann, A. Bruns, G. Hellmann, K.-H. Ott, W. Winkle and K. Wollmann, Ger. Patent DE 3.723.826 to Henkel KGaA, 1989.

[40] K. Hill and M. Biermann, Ger. Patent DE 3.842.541 to Henkel KGaA, 1990.

[41] J. Gruetzke and S. Schmidt, Ger. Patent DE 4.431.856 to Hüls AG, 1996.

[42] J. Kahre and H. Tesmann, Alkylpolyglycoside - Ein neues Konzept für Pflege und Verträglichkeit in der Kosmetik, *Seifen, Öle, Fette, Wachse Journal* **8** (1995) 598-611.

[43] W. Ruback and S. Schmidt, *Carbohydrates as Organic Raw Materials III*, page 231, VCH Verlagsgesellschaft mbH, Weinheim, Germany, 1996.

[44] Th. Böcker and J. Thiem, Synthese und Eigenschaften von Kohlenhydrattensiden, *Tenside Surf. Det.* **26 (5)** (1989) 318-324.

[45] J. F. W. Keana, A. P. Guzikowski, C. Morat, and J. J. Volwerk, Detergents containing a 1,3-diene group in the hydrophobic segment. Facile chemical modification by a Diels-Alder reaction with hydrophilic dienophiles in aqueous solution, *J. Org. Chem.* **48** (1983) 2661-2666.

[46] K. R. Holme and L. D. Hall, Chitosan derivatives bearing C_{10}-alkyl glycoside branches: a temperature-induced gelling polysaccharide, *Macromolecules* **24** (1991) 3828-3833.

[47] J. Greiner, A. Milius, and J. G. Riess, The abnormal issue of the Koenigs-Knorr reaction with perfluoroalkylated alcohols, *Tetrahedron Lett.* **29 (18)** (1988) 2193-2194.

[48] A. Milius, J. Greiner, and J. G. Riess, Synthesis of f-alkylated glycosides as surfactants for in vivo uses. Effects of the length of the hydrocarbonated spacer in the aglycone on Koenigs-Knorr reaction, surface activity and biological properties, *New J. Chem.* **15** (1991) 337-344.

[49] H. Engelhardt, W. Beck, and T. Schmitt, *Kapillarelektrophorese: Methoden und Möglichkeiten*, Friedr. Vieweg & Sohn Verlagsgesellschaft mbH, Braunschweig/Wiesbaden, Germany, 1994.

[50] W. Kok, Capillary electrophoresis: instrumentation and operation, *Chromatographia* **51** (2000) S1-S89.

[51] R. Kuhn and S. Hoffstetter-Kuhn, *Capillary Electrophoresis: Principles and Practice*, Springer-Verlag, Berlin Heidelberg, Germany, 1993.

[52] F. Foret, L. Křivánková, and P. Boček, *Capillary Zone Electrophoresis*, VCH Verlagsgesellschaft mbH, Weinheim, Germany, 1993.

[53] R. Weinberger, *Practical Capillary Electrophoresis*, Academic Press, Inc., San Diego, CA, USA, 1993.

[54] J. W. Jorgenson and K. D. Lukacs, High resolution separations based on electrophoresis and electroosmosis, *J. Chromatogr.* **218** (1981) 209-216.

[55] J. W. Jorgenson and K. D. Lukacs, Zone electrophoresis in open-tubular glass capillaries, *Anal. Chem.* **53** (1981) 1298-1302.

[56] J. W. Jorgenson and K. D. Lukacs, Capillary zone electrophoresis, *Science* **222** (1983) 266-272.

[57] K. D. Altria, Overview of capillary electrophoresis and capillary electrochromatography, *J. Chromatogr. A* **856** (1999) 443-463.

[58] R. A. Frazier, J. M. Ames, H. E. Nursten, and J. M. Nursten, *Capillary Electrophoresis for Food Analysis: Method Development*, Royal Society of Chemistry, Cambridge, UK, 2001.

[59] S. Terabe, K. Otsuka, K. Ichikawa, A. Tsuchiya, and T. Ando, Electrokinetic separations with micellar solutions and open-tubular capillaries, *Anal. Chem.* **56** (1984) 111-113.

[60] S. Terabe, K. Otsuka, and T. Ando, Electrokinetic chromatography with micellar solution and open-tubular capillary, *Anal. Chem.* **57** (1985) 834-841.

[61] J. Vindevogel and P. Sandra, *Introduction to Micellar Electrokinetic Chromatography*, Hthig, Heidelberg, Germany, 1992.

[62] G. M. Janini and H. J. Issaq, Micellar electrokinetic capillary chromatography: basic considerations and current trends, *J. Liq. Chromatogr.* **15** (1992) 927-960.

[63] S. Terabe, *Capillary Electrophoresis Technology*, volume 64 of *Chromatographic Science Series*, chapter Micellar Electrokinetic Chromatography, pages 65–87, Marcel Dekker, New York, 1993.

[64] M. G. Khaledi, Micelles as separation media in high-performance liquid chromatography and high-performance capillary electrophoresis: overview and perspective, *J. Chromatogr. A* **780** (1997) 3-40.

[65] Z. E. Rassi, *Carbohydrate Analysis: High Performance Liquid Chromatography and Capillary Electrophoresis*, Elsevier, Amsterdam, The Netherlands, 1995.

[66] O. Schmitz, *Entwicklung kapillarelektrophoretischer Methoden zur Analyse von Fettsurehydroperoxiden*, Ph.D. thesis, Department of Chemistry, Bergische Universität-Gesamthochschule Wuppertal, 1997.

[67] H. Corstjens, H. A. H. Billiet, J. Frank, and K. Ch. A. M. Luyben, Optimisation of selectivity in capillary electrophoresis with emphasis on micellar electrokinetic capillary chromatography, *J. Chromatogr. A* **715** (1995) 1-11.

[68] S. Hjertén et al., Carrier-free zone electrophoresis, displacement electrophoresis and isoelectric focusing in a high-performance electrophoresis apparatus, *J. Chromatogr.* **403** (1987) 47-61.

[69] E. S. Yeung, Indirect detection methods: looking for what is not there, *Acc. Chem. Res.* **22** (1989) 125-130.

[70] R. A. Wallingford and A. G. Ewing, Capillary zone electrophoresis with electrochemical detection, *Anal. Chem.* **59** (1987) 1762-1766.

[71] R. D. Rocklin, *A Practical Guide to HPLC Detection*, Academic Press, Inc., New York, USA, 1993, page 145.

[72] C. Harber, *Handbook of Capillary Electrophoresis*, CRC Press, Boca Raton, Finland, 1997, page 425.

[73] J. Ye and R. P. Baldwin, Amperometric detection in capillary electrophoresis with normal size electrodes, *Anal. Chem.* **65** (1993) 3525-3527.

[74] J. Ye and R. P. Baldwin, Determination of carbohydrates, sugar acids, alditols by capillary electrophoresis and electrochemical detection at a copper electrode, *J. Chromatogr. A* **687** (1994) 141-148.

[75] T. J. O'Shea, S. M. Lunte, and W. R. LaCourse, Detection of carbohydrates by capillary electrophoresis with pulsed amperometric detection, *Anal. Chem.* **65** (1993) 948-951.

[76] W. Lu and R. M. Cassidy, Pulsed amperometric detection of carbohydrates separated by capillary electrophoresis, *Anal. Chem.* **65** (1993) 2878-2881.

[77] P. Weber, T. Kornfelt, N. K. Klausen, and S. M. Lunte, Characterization of glycopeptides from recombinant coagulation factor VIIa by high-performance liquid chromatography and capillary zone electrophoresis using ultraviolet and pulsed electrochemical detection, *Anal. Biochem.* **225** (1995) 135-142.

[78] W. R. LaCourse and G. S. Owens, Pulsed electrochemical detection of nonchromophoric compounds following capillary electrophoresis, *Electrophoresis* **17** (1996) 310-318.

[79] G. S. Owens and W. R. LaCourse, Pulsed electrochemical detection of thiols and disulfides following capillary electrophoresis, *J. Chromatogr. B* **695** (1997) 15-25.

[80] J. Zhou and S. M. Lunte, Direct determination of amino acids by capillary electrophoresis/electrochemistry using a copper microelectrode and zwitterionic buffers, *Electrophoresis* **16** (1995) 498-503.

[81] P. D. Voegel, W. Zhou, and R. P. Baldwin, Integrated capillary electrophoresis/electrochemical detection with metal film electrodes directly deposited onto the capillary tip, *Anal. Chem.* **69** (1997) 951-957.

[82] J. Zhou and S. M. Lunte, Membrane-based on-column mixer for capillary electrophoresis/electrochemistry, *Anal. Chem.* **67** (1995) 13-18.

[83] M. Zhong and S. M. Lunte, Integrated on-capillary electrochemical detector for capillary electrophoresis, *Anal. Chem.* **68 (15)** (1996) 2488-2493.

[84] P. L. Weber and S. M. Lunte, Capillary electrophoresis with pulsed amperometric detection of carbohydrates and glycopeptides, *Electrophoresis* **17** (1996) 302-309.

[85] F. D. Swanek, G. Chen, and A. G. Ewing, Identification of multiple compartments of dopamine in a single cell by CE with scanning electrochemical detection, *Anal. Chem.* **68** (1996) 3912-3916.

[86] A. M. Fermier, M. L. Gostkowski, and L. A. Colón, Rudimentary capillary-electrode alignment for capillary electrophoresis with electrochemical detection, *Anal. Chem.* **68** (1996) 1661-1664.

[87] M. Zhong, J. Zhou, S. M. Lunte, G. Zhao, D. M. Giolando, and J. R. Kirchhoff, Dual-electrode detection for capillary electrophoresis/electrochemistry, *Anal. Chem.* **68** (1996) 203-207.

[88] S. Park and C. E. Lunte, A perfluorosulfonated ionomer end-column electrical decoupler for capillary electrophoresis/electrochemical detection, *Anal. Chem.* **67 (23)** (1995) 4366-4370.

[89] S. Park, S. M. Lunte, and C. E. Lunte, A perfluorosulfonated ionomer joint for capillary electrophoresis with on-column electrochemical detection, *Anal. Chem.* **67** (1995) 911-918.

[90] F. M. Matysik and U. Backofen, Capillary electrophoresis and capillary flow injection analysis with electrochemical detection, *Fresenius J. Anal. Chem.* **356** (1996) 169-172.

[91] M. A. Malone, H. Zuo, S. M. Lunte, and M. R. Smyth, Determination of tryptophan and kynurenine in brain microdialysis samples by capillary electrophoresis with electrochemical detection, *J. Chromatogr. A* **700** (1995) 73-80.

[92] M. E. Hadwiger, S. R. Torchia, S. Park, M. E. Biggin, and C. E. Lunte, Optimization of the separation and detection of the enantiomers of isoproterenol in microdialysis samples by cyclodextrin-modified capillary electrophoresis using electrochemical detection, *J. Chromatogr. B* **681** (1996) 241-249.

[93] D.-K. Xu, L. Hua, and H.-Y. Chen, Determination of purine bases by capillary zone electrophoresis with wall-jet amperometric detection, *Anal. Chim. Acta* **335** (1996) 95-101.

[94] M. E. Hadwiger, S. Park, S. R. Torchia, and C. E. Lunte, Simultaneous determination of the elimination profiles of the individual enantiomers of racemic isoproterenol using capillary electrophoresis and microdialysis sampling, *J. Pharm. Biomed. Anal.* **15** (1997) 621-629.

[95] S. Hu, Z.-L. Wang, P.-B. Li, and J.-K.Cheng, Amperometric detection in capillary electrophoresis with an etched joint, *Anal. Chem.* **69** (1997) 264-267.

[96] M.-C. Chen and H.-J. Huang, An electrochemical cell for end-column amperometric detection in capillary electrophoresis, *Anal. Chem.* **67** (1995) 4010-4014.

[97] L. Hua, D.-K. Xu, and H.-Y. Chen, Simultaneous determination of purine bases, ribonucleosides and ribonucleotides by capillary electrophoresis-electrochemistry with a copper electrode, *J. Chromatogr. A* **760** (1997) 227-233.

[98] A. M. Fermier and L. A. Colón, Capillary electrophoresis with constant potential amperometric detection using a nickel microelectrode for detection of carbohydrates, *J. High Resol. Chromatogr.* **19** (1996) 613-616.

[99] X. J. Huang and W. Th. Kok, Determination of thiols by capillary electrophoresis with electrochemical detection using a palladium field-decoupler and chemically modified electrodes, *J. Chromatogr. A* **716** (1995) 347-353.

[100] W. Zhou and R. P. Baldwin, Capillary electrophoresis and electrochemical detection of underivatized oligo- and polysaccharides with surfactant-controlled electroosmotic flow, *Electrophoresis* **17** (1996) 319-324.

[101] R. E. Roberts and D. C. Johnson, Variation in PED response at a gold microelectrode as a function of waveform parameters when applied to alditols and carbohydrates separated by capillary electrophoresis, *Electroanalysis* **7 (11)** (1995) 1015-1019.

[102] M.-C. Chen and H.-J. Huang, Application of a nickel-microelectrode-incorporated end-column detector for capillary electrophoretic determination of alditols and alcohols, *Anal. Chim. Acta* **341** (1997) 83-90.

[103] X. J. Huang and W. Th. Kok, Determination of sugars by capillary electrophoresis with electrochemical detection using cuprous oxide modified electrodes, *J. Chromatogr. A* **707** (1995) 335-342.

[104] J. Liu, W. Zhou, T. You, F. Li, E. Wang, and S. Dong, Detection of hydrazine, methylhydrazine, and isoniazid by capillary electrophoresis with a palladium-modified microdisk array electrode, *Anal. Chem.* **68** (1996) 3350-3353.

[105] F. M. Matysik, A. Meister, and G. Werner, Electrochemical detection with microelectrodes in capillary flow systems, *Anal. Chim. Acta* **305** (1995) 114-120.

[106] H. Salimi-Moosavi and R. M. Cassidy, Capillary electrophoresis of inorganic anions in nonaqueous media with electrochemical and indirect UV detection, *Anal. Chem.* **67** (1995) 1067-1073.

[107] F.-M. Matysik, Experimental characterization of end-column electrochemical detection in conjunction with nonaqueous capillary electrophoresis, *Anal. Chem.* **72** (2000) 2581-2586.

[108] F.-M. Matysik, L. Nyholm, and K. E. Markides, Comparison of μm and mm sized disk electrodes for end-column electrochemical detection in capillary electrophoresis, *Fresenius J. Anal. Chem.* **363** (1999) 231-235.

[109] F.-M. Matysik, Non-aqueous capillary electrophoresis with electrochemical detection, *J. Chromatogr. A* **802** (1998) 349-354.

[110] F.-M. Matysik, Application of non-aqueous capillary electrophoresis with electrochemical detection to the determination of nicotine in tobacco, *J. Chromatogr. A* **853** (1999) 27-34.

[111] J. H. T. Luong, A. Hilmi, and A.-L. Nguyen, Nonaqueous capillary electrophoresis equipped with amperometric detection for analysis of chlorinated phenolic compounds, *J. Chromatogr. A* **864** (1999) 323-333.

[112] R. A. Wallingford and A. G. Ewing, Amperometric detection of catechols in capillary zone electrophoresis with normal and micellar solutions, *Anal. Chem.* **60** (1988) 258-263.

[113] S. Park, M. J. McGrath, M. R. Smyth, D. Diamond, and C. E. Lunte, Voltammetric detection for capillary electrophoresis, *Anal. Chem.* **69** (1997) 2994-3001.

[114] J. C. Olsson, P. E. Andersson, B. Karlberg, and A.-C. Nordström, Determination of plant indoles by capillary electrophoresis with amperometric detection, *J. Chromatogr. A* **755** (1996) 289-298.

[115] J. Wen and R. M. Cassidy, Anodic and cathodic pulse amperometric detection of metal ions separated by capillary electrophoresis, *Anal. Chem.* **68** (1996) 1047-1053.

[116] D. Müller, I. Jelínek, F. Opekar, and K. Štulík, A conductometric detector for capillary separations, *Electroanalysis* **8** (1996) 722-725.

[117] T. R. I. Cataldi, I. G. Casella, E. Desimoni, and T. Rotunno, Cobalt-based glassy carbon chemically modified electrode for constant-potential amperometric detection of carbohydrates in flow-injection analysis and liquid chromatography, *Anal. Chim. Acta* **270** (1992) 161-171.

[118] T. R. I. Cataldi, A. Guerrieri, I. G. Casella, and E. Desimoni, Study of cobalt-based surface modified glassy carbon electrode: electrocatalytic oxidation of sugars and alditols, *Electroanalysis* **7** (1995) 305-311.

[119] J. Wang and Z. Taha, Catalytic oxidation and flow detection of carbohydrates at ruthenium dioxide modified electrodes, *Anal. Chem.* **62** (1990) 1413-1416.

[120] R. P. Baldwin, Electrochemical determination of carbohydrates: Enzyme electrodes and amperometric detection in liquid chromatography and capillaries electrophoresis, *J. Pharm. Biomed. Anal.* **19** (1999) 69-81.

[121] L. A. Woods and A. G. Ewing, Etched electrochemical detection for electrophoresis in nanometer inner diameter capillaries, *Chemphyschem* **4** (2003) 207-211.

[122] J. Hong and R. P. Baldwin, Profiling clinically important metabolites in human urine by capillary electrophoresis and electrochemical detection, *J. Cap. Elec.* **4** (1997) 65-71.

[123] X. Fang, J. Ye, and Y. Fang, Determination of polyhydroxy antibiotics by capillary zone electrophoresis with amperometric detection at a nickel electrode, *Anal. Chim. Acta* **329** (1996) 49-55.

[124] P. D. Voegel and R. P. Baldwin, Evaluation of copper-based electrodes for the analysis of aminoglycoside antibiotics by CEEC, *Electroanalysis* **9** (1997) 1145-1151.

[125] W. R. Everett, C. Bohs, and M. I. Davies, Use of a new interface cell for off-column CE-EC determination of catecholamine neurotransmitters, *Curr. Sep.* **19 (1)** (2000) 25-28.

[126] W. Zhou, J. Liu, and E. Wang, Determination of aminopyrine and its metabolite by capillary electrophoresis-electrochemical detection, *J. Chromatogr.* **715** (1995) 355-360.

[127] L. A. Colón, R. Dadoo, and R. N. Zare, Determination of carbohydrates by capillary zone electrophoresis with amperometric detection at a copper microelectrode, *Anal. Chem.* **65** (1993) 476-481.

[128] H. Waldhoff, J. Scherler, M. Schmitt, and J. R. Varvil, *Alkyl Polyglucosides: Technology, Properties and Applications*, page 23, VCH Verlagsgesellschaft mbH, Weinheim, Germany.

[129] N. Buschmann, L. Merschel, and S. Wodarczak, Analytical methods for alkyl polyglucosides. Part II: Qualitative determination using thin layer chromatography and identification by means of in-situ secondary ion mass spectrometry, *Tenside Surf. Det.* **33** (1996) 16-20.

[130] N. Buschmann and S. Wodarczak, Analytical methods for carbohydrate surfactants, *Jorn. Com. Esp. Deterg.* **25** (1994) 203-207.

[131] N. Buschmann, F. Hülskötter, A. Kruse, and S. Wodarczak, Analytical methods for the determination of alkylpolyglucosides, *Fett/Lipid* **98** (1996) 399-402.

[132] S. Wodarczak and N. Buschmann, Analytische Verfahren für Alkylpolyglucoside, *GIT Fachz. Lab* **5** (1995) 410-412.

[133] N. Buschmann, *Nonionic surfactants: Alkyl Polyglucosides*, page 279, Marcel Dekker, Inc., New York, USA, 2000.

[134] P. Billian and H.-J. Stan, Gas chromatography/mass spectrometry of alkyl polyglucosides as their trimethylsilylethers, *Tenside Surf. Det.* **35** (1998) 181-184.

[135] M. Krämer and H. Engelhardt, Analysis of carbohydrates by HPLC with post-column derivatization, *J. High Resolut. Chromatogr.* **15** (1992) 24-29.

[136] A. Bruns, H. Waldhoff, and W. Winkle, Applications of HPLC with evaporative light scattering detection in fat and carbohydrate chemistry, *Chromatographia* **27** (1989) 340-342.

[137] A. Kruse and N. Buschmann, Separation and detection of alkylpolyglucosides in HPLC, *Jorn. Com. Esp. Deterg.* **26** (1995) 209-213.

[138] P. Chaimbault, C. Elfakir, M. Lafosse, F. Blanchard, and I. Marc, HPLC control of an alkyl glycoside synthesis, *J. High Resol. Chromatogr.* **22** (1999) 188-190.

[139] N. Buschmann and F. Hülskötter, Potentiometric titration of carbohydrate surfactants: alkylpolyglucosides, N-acylglucamides, sorbitanesters, *Jorn. Com. Esp. Deterg.* **27** (1997) 419-425.

[140] M. T. García, I. Ribosa, E. Campos, and J. Sanchez Leal, Ecological properties of alkylglucosides, *Chemosphere* **35** (1997) 545-556.

[141] L. W. Kroh, T. Neubert, E. Raabe, and H. Waldhoff, Enzymatic analysis of alkyl polyglycosides, *Tenside Surf. Det.* **36** (1999) 19-21.

[142] R. Bastl-Borrmann and L. W. Kroh, Novel enzymatic assay for determination of alkyl polyglycosides with short chain fatty alcohols, *Fresenius J. Anal. Chem.* **371** (2001) 939-943.

[143] H. F. Schröder, Alkylpolyglucosides in the biological waste water treatment process. Pursuit of their degradation behaviour by LC/MS and FIA/MS, in *Proc. 4th World Surfact. Congr. in Barcelona*, volume 3, pages 121–135, Royal Society of Chemistry, Cambridge, U.K., 1996.

[144] H. Waldhoff, D. Scherler, and L. Bütfering, *Analytiker Taschenbuch* **20** (1999) 251.

[145] D. O. Hummel, *Analysis of Surfactants. Atlas of FTIR Spectra with Interpretations*, Hanser Verlag, München, 1996.

[146] T. M. Schmitt, *Analysis of Surfactants*, volume 96 of *Surfactant Science Series*, Marcel Dekker, New York, second edition, 2001.

[147] G. Rauscher, *Nonionic Surfactants: Chemical Analysis*, Marcel Dekker, New York, 1987.

[148] A. B. Foster, Zone electrophoresis of carbohydrates, *Adv. Carbohydr. Chem.* **12** (1957) 81-116.

[149] S. Hofstetter-Kuhn, A. Paulus, E. Gassmann, and H. M. Widmer, Influence of borate complexation on the electrophoretic behaviour of carbohydrates in capillary electrophoresis, *Anal. Chem.* **63** (1991) 1541-1547.

[150] S. Honda, K. Yamamoto, S. Suzuki, M. Ueda, and K. Kakehi, High-performance capillary zone electrophoresis of carbohydrates in the presence of alkaline earth metal ions, *J. Chromatogr.* **588** (1991) 327-333.

[151] J. A. Rendleman, Ionization of carbohydrates in the presence of metal hydroxides and oxides, *Adv. Chem. Ser* **117** (1971) 51-69.

[152] A. E. Vorndran, P. J. Oefner, H. Scherz, and G. K. Bonn, Indirect UV detection of carbohydrates in capillary zone electrophoresis, *Chromatographia* **33** (1992) 163-168.

[153] P. J. Oefner, A. E. Vorndran, E. Grill, C. Huber, and G. K. Bonn, Capillary zone electrophoretic analysis of carbohydrates by direct and indirect UV detection, *Chromatographia* **34** (1992) 308-316.

[154] X. Xu, W. T. Kok, and H. Poppe, Sensitive determination of sugars by capillary zone electrophoresis with indirect UV detection under highly alkaline conditions, *J. Chromatogr. A* **716** (1995) 231-240.

[155] T. Tsuda, K. Nomura, and G. Nakagawa, Open-tubular microcapillary liquid chromatography with electro-osmosis flow using a UV detector, *J. Chromatogr.* **248** (1982) 241-247.

[156] K. Kakehi, S. Suzuki, S. Honda, and Y. C. Lee, Precolumn labeling of reducing carbohydrates with 1-(p-methoxy)phenyl-3-methyl-5-pyrazolone: analysis of neutral and sialic acid-containing oligosaccharides found in glycoproteins, *Anal. Biochem.* **199** (1991) 256-268.

[157] M. van Duin, J. A. Peters, A. P. G. Kieboom, and H. van Bekkum, Studies on borate esters II, *Tetrahedron* **41** (1985) 3411-3421.

[158] M. A. Schwarz, B. Galliker, K. Fluri, T. Kappes, and P. C. Hauser, A two-electrode configuration for simplified amperometric detection in a microfabricated electrophoretic separation device, *Analyst* **126** (2001) 147-151.

[159] S. Hughes and D. C. Johnson, Amperometric detection of simple carbohydrates at platinum electrodes in alkaline solutions by application of a triple-pulse potential waveform, *Anal. Chim. Acta* **132** (1981) 11-22.

[160] N. Iki and E. S. Yeung, Non-bonded poly(ethylen oxide) polymer-coated column for protein separation by capillary electrophoresis, *J. Chromatogr. A* **731** (1996) 273-282.

[161] J. K. Towns and F. E. Regnier, Capillary electrophoretic separations of proteins using nonionic surfactant coatings, *Anal. Chem.* **63** (1991) 1126-1132.

[162] W. R. LaCourse and D. C. Johnson, Optimization of waveforms for pulsed amperometric detection of carbohydrates based on pulsed voltammetry, *Anal. Chem.* **65** (1993) 50-55.

[163] G. G. Neuburger and D. C. Johnson, Pulsed coulometric detection of carbohydrates at a constant detection potential at gold electrodes in alkaline media, *Anal. Chim. Acta* **192** (1987) 205-213.

[164] D. C. Johnson, J. A. Polta, T. Z. Polta, G. G. Neuburger, J. Johnson, A. P.-C. Tang, I.-H. Yeo and J. Baur, Anodic detection in flow-through cells, *J. Chem. Soc., Faraday Trans. 1* **82** (1986) 1081-1098.

[165] R. Roberts and D. C. Johnson, Fast pulsed amperometric detection at noble metal electrodes: a study of oxide formation and dissolution kinetics at gold in 0.1 M NaOH, *Electroanal.* **4** (1992) 741-749.

[166] D. L. Massart, B. G. M. Vandeginste, L. M. C. Buydens, S. De Jong, P. J. Lewi and J. Smeyers-Verbeke, *Handbook of Chemometrics and Qualimetrics: Part A* , Elsevier, Amsterdam, 1997.

[167] D. A. Skoog, editor, D. M. West, F. J. Holler, and S. R. Crouch, *Fundamentals of Analytical Chemistry*, Brooks Cole, Belmont, CA, USA, 8th edition, 2004, p. 795.

[168] Personal document obtained from Dr. H. W. Kling, Cognis Deutschland GmbH&Co.KG.

[169] U. Backofen, F.-M. Matysik, and C. E. Lunte, A chip-based electrophoresis system with electrochemical detection and hydrodynamic injection, *Anal. Chem.* **74** (2002) 4054-4059.

Appendix A

Nuclear magnetic resonance spectroscopy

^{13}C-spectra of C_{12}-β-D-glucopyranoside before and after exposure to 1 M NaOH solution are shown in **Figures A.1** and **A.2**, respectively.

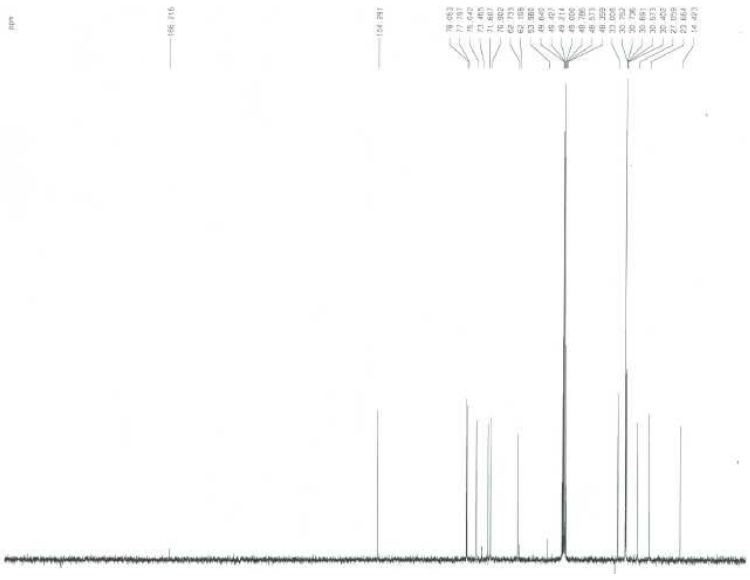

Figure A.1: ^{13}C-NMR spectrum of C_{12}-β-D-glucopyranoside in CD_3OD

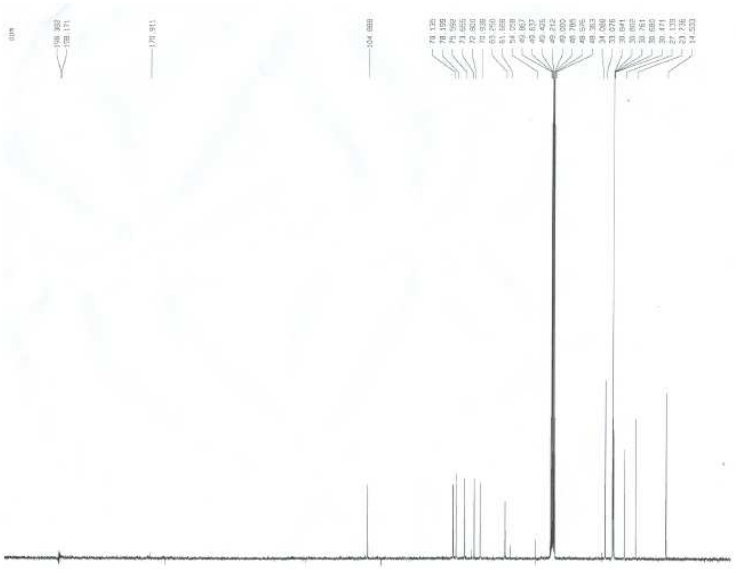

Figure A.2: ^{13}C-NMR spectrum of C_{12}-β-D-glucopyranoside in 1 M NaOH in CD_3OD

Appendix B

Separation of sugars by CZE

The mixture of glucose and ribose was injected. The separation voltage of 10 kV was applied (**Figure B.1**). The simultaneous application of both pressure and voltage for CE separation was also tested, as shown in **Figure B.2**.

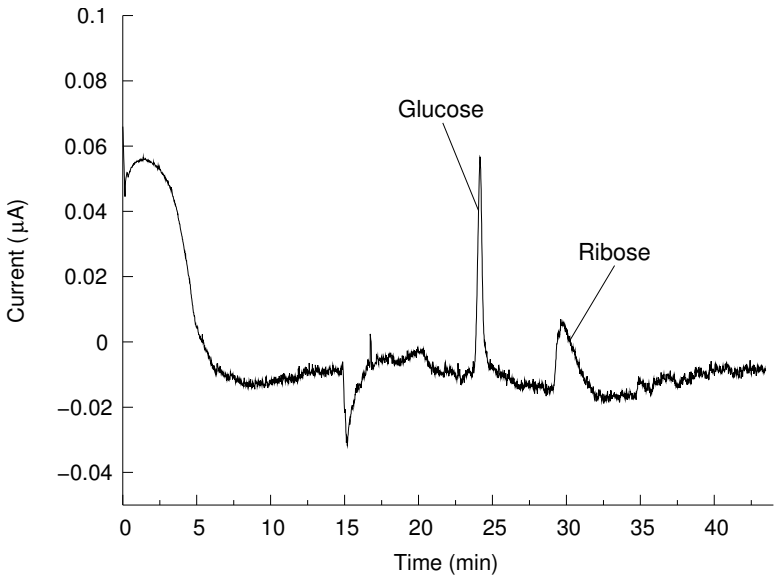

Figure B.1: Analysis of glucose and ribose, each 1.5 mM; electrolyte: 0.1 M NaOH; voltage: 10 kV

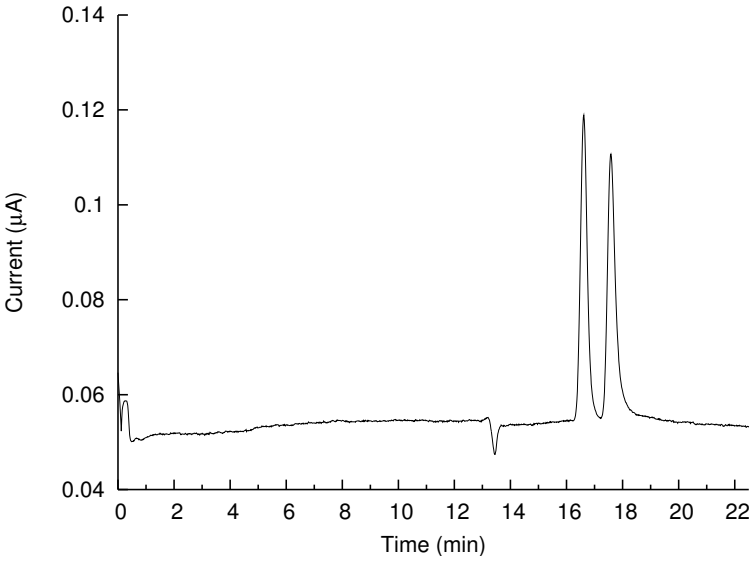

Figure B.2: Analysis of glucose and ribose, each 1.5 mM; electrolyte: 0.1 M NaOH; application of both pressure and voltage: 0.5 psi and 5 kV

Appendix C

Linearity of the response to noradrenaline, L-dopa and ascorbic acid

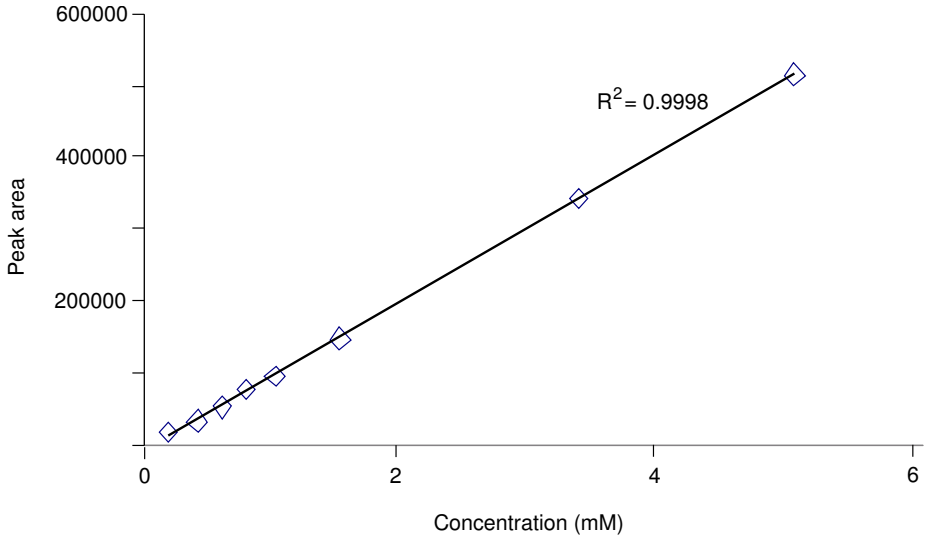

Figure C.1: Calibration line of noradrenaline

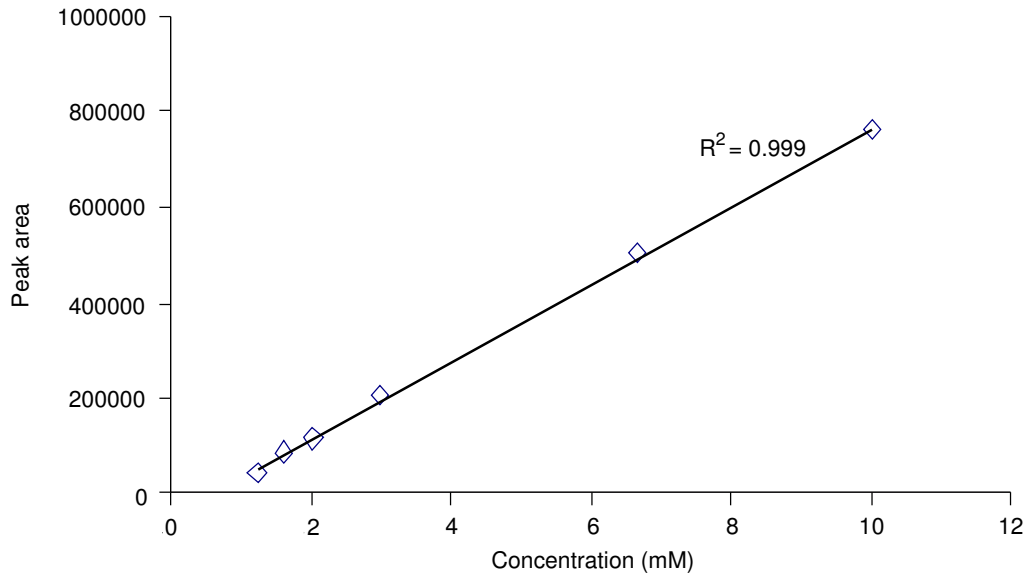

Figure C.2: Calibration line of L-dopa

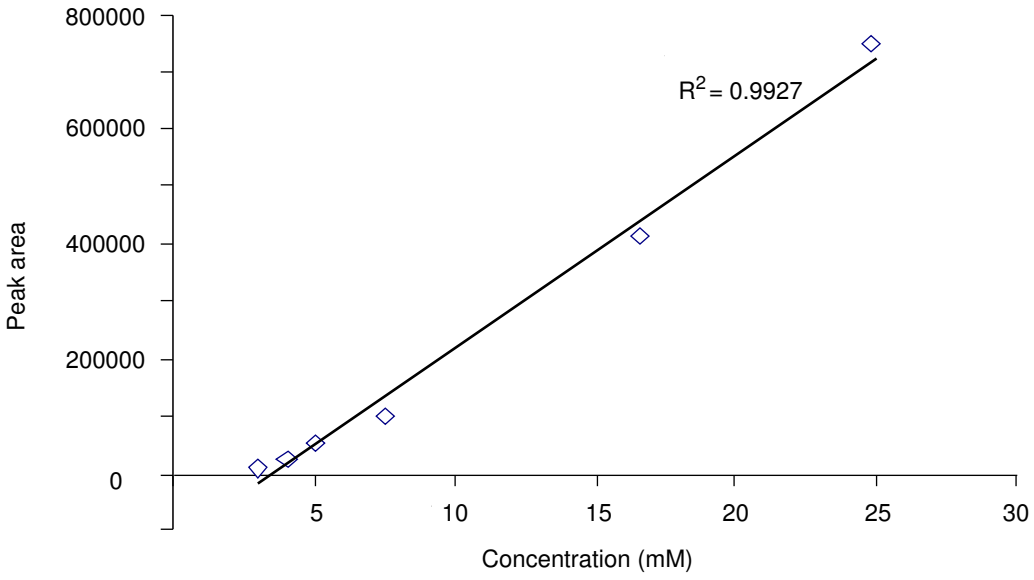

Figure C.3: Calibration line of ascorbic acid